Technical Report

TR-06-31

Groundwater chemistry around a repository for spent nuclear fuel over a glacial cycle

Evaluation for SR-Can

L F Auqué, M J Gimeno, J B Gómez
University of Zaragoza, Spain

I Puigdomenech, Svensk Kärnbränslehantering AB

J Smellie, Conterra AB

E-L Tullborg, Terralogica AB

December 2006

Svensk Kärnbränslehantering AB
Swedish Nuclear Fuel
and Waste Management Co
Box 5864
SE-102 40 Stockholm Sweden
Tel 08-459 84 00
+46 8 459 84 00
Fax 08-661 57 19
+46 8 661 57 19

Groundwater chemistry around a repository for spent nuclear fuel over a glacial cycle

Evaluation for SR-Can

L F Auqué, M J Gimeno, J B Gómez
University of Zaragoza, Spain

I Puigdomenech, Svensk Kärnbränslehantering AB

J Smellie, Conterra AB

E-L Tullborg, Terralogica AB

December 2006

Abstract

The chemical composition of groundwater in the rock volume surrounding a spent nuclear fuel repository is of importance to many factors that affect repository performance. The geochemical characteristics of present-day Swedish groundwater systems are governed by successive mixing events of several waters during the post-glacial evolution of the sites. The expected development of groundwaters at two Swedish sites – Forsmark and Laxemar – during a glacial cycle has been evaluated within the SR-Can project, and the results are presented in this report.

For the temperate period following repository closure, an approach is proposed here to investigate the spatial and temporal evolution of groundwater geochemistry by coupling hydrogeological and geochemical models in a sequential way. The procedure combines hydrogeological results obtained with CONNECTFLOW within the SR-Can project with a mixing and reaction-path simulation using PHREEQC. The hydrological results contain mixing proportions of four component waters (a deep brine, glacial meltwater, marine water, and meteoric infiltration) at each time step and at every node of the 3D regional model domain. In this work the mixing fractions are fed into PHREEQC using software developed to build formatted input files and to extract the information from output files for subsequent plotting and analysis. The geochemical calculations included both chemical mixing and equilibrium reactions with selected minerals: calcite, chalcedony and an Fe(III) oxy-hydroxide. Results for the Forsmark and Laxemar sites are graphically presented as histograms and box-and-whisker plots. Cross sections, where each node is colour-coded with respect to an important variable (pH, Eh or concentrations of main elements), are used to visualize the future evolution of the site. Sensitivity analyses are made to evaluate the effects of the different reactions and/or assumptions. The results reflect the progressive inflow of meteoric waters into the sites, and indicate that far-field groundwaters during the temperate period will not affect negatively the performance of the safety functions of the repository.

For the permafrost and glacial periods, groundwater compositions are proposed based on the results from hydrological evaluations performed within the SR-Can project. It is concluded that for permafrost conditions groundwaters in the rock volume surrounding a repository will not affect negatively its performance. However, under glacial conditions meltwaters are expected to penetrate deep into the bedrock and, on the whole, groundwaters would then have such low salinities that it would affect negatively the stability of the bentonite buffer surrounding the canisters in the repository.

An analysis of the possibility of penetration of O_2-rich meltwaters down to repository depths during glacial periods is made based on studies performed within the SR-Can project and elsewhere. It is concluded the inflow of oxygen in single fractures is neutralised by the process of matrix diffusion and dissolution of Fe(II) minerals in the rock matrix. For fracture zones, with water advective times down to repository depths of only a few years, advancement of O_2-rich waters to repository depth does not occur if variables are cautiously selected. For extreme situations, and given our present understanding of fracture zones, the occurrence of oxidizing conditions at repository depths within large fracture zones can not at present be completely ruled out, but at least they can be avoided in the repository design.

Contents

1 Introduction

1.1 Background

This report describes the chemical compositions for groundwaters in the rock volume around a final repository for spent nuclear fuel in Sweden based in the KBS-3 concept. The aim is to provide geochemistry data for the safety report SR-Can /SKB 2006g/ in the form of boundary conditions for calculations of bentonite porewaters, and as conditions determining radionuclide speciation, solubility and sorption.

Because the barrier functions of a spent nuclear repository will be required for periods of time of at least 100,000 years, changes in groundwater chemistry over at least one glacial cycle are evaluated.

Two sites in Sweden are being characterised as possible candidates for hosting the proposed repository: Forsmark and Laxemar in the municipalities of Östhammar and Oskarshamn, respectively. Another site in the Oskarshamn municipality, Simpevarp, was previously investigated as a potential site, but only Forsmark and Laxemar are considered in SR-Can. Groundwater chemical data are provided in this report for these two sites.

SR-Can is based on the site description models (SDM) version 1.2 /SKB 2005b, 2006h/, and this report describes groundwater chemistries and their variations with time for the Forsmark and Laxemar sites, based on data and evidence gathered before the data-freezes corresponding to the models version 1.2.

Part of the text and some of the figures in this report are also presented in SR-Can's main report /SKB 2006g/ although more details are given here. In addition, the data from this report is also cited in SR-Can's data report /SKB 2006c/.

1.2 Groundwater requirements from a KBS-3 repository

The primary safety function of the KBS-3 concept is to completely isolate the spent nuclear fuel within copper canisters over the entire assessment period, which is one million years in SR-Can. Should a canister be damaged, the secondary safety function is to retard any releases from the canisters. The two issues of isolation and retardation are thus of primary importance throughout the assessment.

In order to break down the problem and to evaluate and understand in a more detailed and quantitative manner the two safety functions, measurable or calculable quantities or barrier conditions are introduced in SR-Can /SKB 2006g/. Factors like the thickness of the copper canister, or the buffer density are referred to as *function indicators*. The quantitative criteria that imply whether the desired function is provided or not are called *function indicator criteria*.

For the part of the geosphere surrounding the repository, most of the function indicators concern the composition of groundwaters in the fracture network; several of the groundwater characteristics are essential for providing a chemically favourable environment for the repository. The related function indicators for groundwater are described below. The text, with minor modifications, has been copied from /SKB 2006g/.

Reducing conditions

A fundamental requirement is that of reducing conditions. A necessary condition is the absence of dissolved oxygen, because any evidence of its presence would indicate oxidizing conditions. The presence of reducing agents that react quickly with O_2, such as Fe(II) and sulphide is sufficient to indicate reducing conditions. Other indicators of redox conditions, such as negative redox potential, Eh, are not always well defined or easily measured and thus less practical as a basis. Nevertheless, the redox potential is useful as a measure of the availability of all kinetically active oxidizing species in a groundwater.

This requirement ensures that canister corrosion due to oxygen dissolved in the groundwater is avoided. Furthermore, should a canister be penetrated, reducing conditions are essential to ensure a low dissolution rate of the fuel matrix, to ensure favourable solubilities of several radioelements and, for some elements, also redox states favourable for sorption in buffer, backfill and host rock.

In addition to dissolved O_2, other oxidized groundwater components could be considered, for example nitrate and sulphate. However, while dissolved oxygen may react directly e.g. with the copper canister or the spent fuel, nitrate and sulphate can only be reactive by the intervention of microbes, which require both nutrients and reduced species such as dissolved hydrogen, methane or organic matter in order to be able to reduce nitrate or sulphate.

Ionic strength, salinity

The salinity of the groundwater should neither be too high, nor too low. The total concentration of divalent cations should exceed 1 mM in order to avoid chemical erosion of buffer and backfill, hence /SKB 2006a/:

$$\sum [M^{2+}] \geq 10^{-3} \text{ M}$$

Groundwaters of high ionic strengths would have a negative impact on the buffer and backfill properties, in particular on the backfill swelling pressure and hydraulic conductivity. In general, ionic strengths corresponding to NaCl concentrations of approximately 70 g/L (1.2 M NaCl) are a safe limit for maintaining backfill properties, whereas the corresponding limit for the buffer is around 100 g/L (1.7 M). The limit of tolerable ionic strength is however highly dependent on the material properties of these components, and since, in particular for the backfill, alternative materials are to be evaluated in the assessment, no specific criterion is given in SR-Can /SKB 2006g/.

Colloid concentrations

The concentration of natural colloids should be low to avoid transport of radionuclides mediated by colloids. The stability of colloids is largely decreased if the concentration of divalent cations exceeds 1 mM, a condition that, as discussed above, is also required for the stability of the buffer and backfill.

Concentrations of detrimental agents

Regarding canister corrosion, there should be low groundwater concentrations of canister corroding agents in the rock volume surrounding the deposition holes, in particular sulphide, HS^-. For sulphide to pose a problem, considerably higher concentrations than have ever been observed in Swedish groundwaters would be required. The quantitative extent of such corrosion also depends on the groundwater flow around the deposition hole and on the transport properties of fractures intersecting the hole.

Furthermore, it is desirable to have low groundwater concentrations of agents detrimental to long-term stability of the buffer and backfill, in particular potassium and iron /SKB 2006a/.

pH

Regarding pH, a criterion can be formulated from the point of view of buffer and backfill stability /SKB 2006a/:

$pH \leq 11$

This is fulfilled for any natural groundwater in Sweden. However, construction and stray materials in the repository, in particular concrete, could contaminate the groundwater such that high pH values are reached.

Other requirements

A further requirement is that the combination of low pH values and high chloride concentrations should be avoided in order to exclude chloride corrosion of the canister. In quantitative terms, in SR-Can the requirement is assigned a preliminary criterion:

$pH > 4$ or $[Cl^-] < 3M$

1.3 Evaluation of the geochemical conditions in SR-Can

From the function indicator criteria listed in the previous subsection, it is clear that groundwater chemical conditions are quite important when evaluating the performance of a spent nuclear fuel repository based on the KBS-3 concept. Furthermore, the expected evolution with time of groundwater properties must be considered. In the reference evolution of the repository in SR-Can two variants are evaluated. In the first one the external conditions during the first 120,000 year glacial cycle are assumed to be similar to those experienced during the most recent glacial cycle, the Weichselian. Thereafter, seven repetitions of that cycle are assumed to cover the entire 1,000,000 year assessment period. For the greenhouse variant of the reference evolution it is assumed that future climate and hence external conditions will be substantially influenced by increased human-induced greenhouse gas emissions. Detailed descriptions of the base and greenhouse variants of the main scenario in SR-Can are reported in /SKB 2006b/. Figure 1-1 and Figure 1-2 illustrate the evolution of climate-related variables that affect groundwater composition for the base variant of the main scenario at Forsmark and Laxemar, respectively.

The geochemical conditions in SR-Can are evaluated in three periods:

- The excavation and operation phases of the repository.
- The initial period of temperate climate after repository closure.
- The remaining part of the reference glacial cycle, with emphasis on permafrost and glacial conditions.

In addition, the possible impact of the greenhouse variant on groundwater geochemistry is qualitatively evaluated.

The general strategy to evaluate groundwater compositions in SR-Can is by combining the results of hydrogeological models with chemical mixing and reaction models. However, the extent of the chemical modelling differs for the different periods evaluated. Detailed calculations have been performed for the temperate period after repository closure, while generic calculations and specific models have been applied for the other time periods.

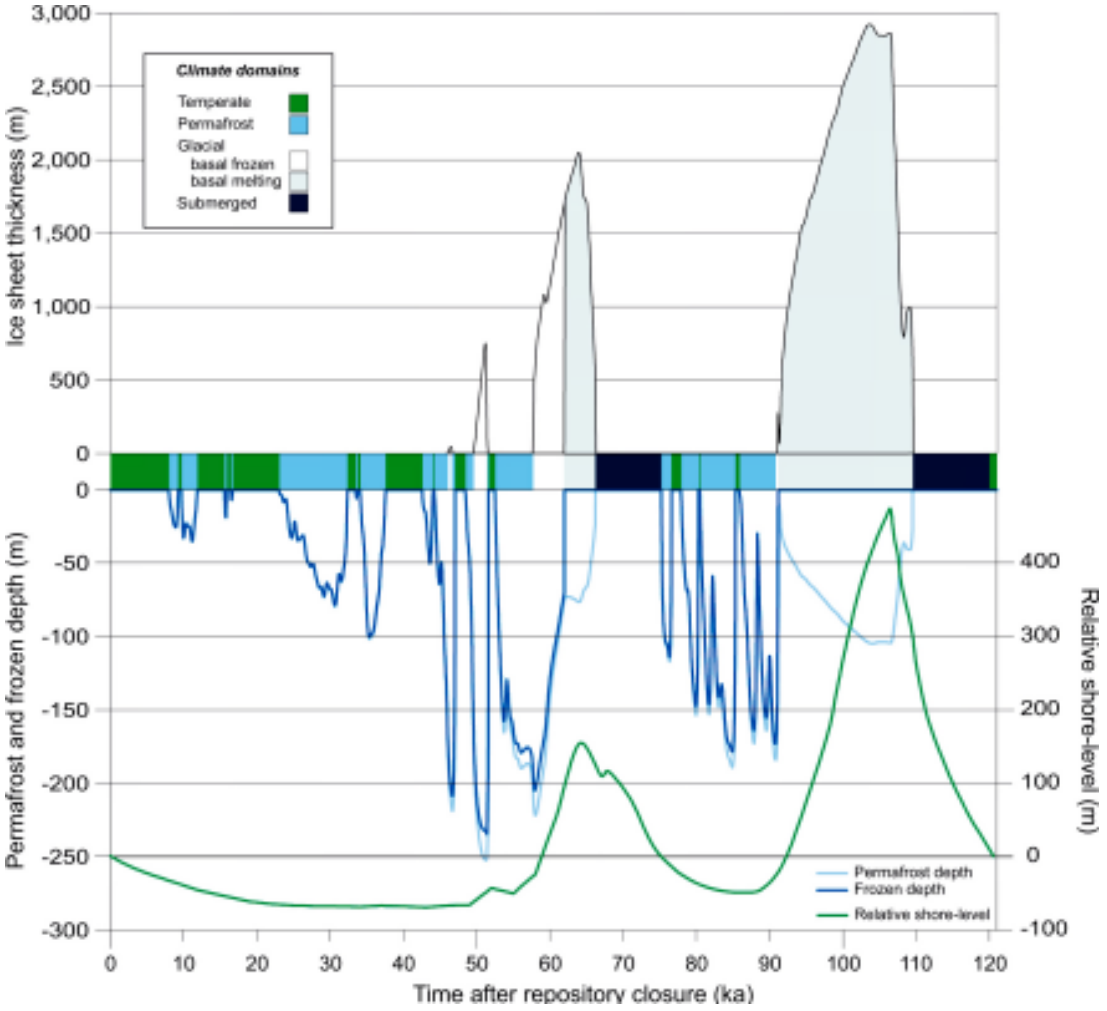

Figure 1-1. *Evolution of important climate-related variables at Forsmark for the base variant of the main scenario in SR-Can. From /SKB 2006b/.*

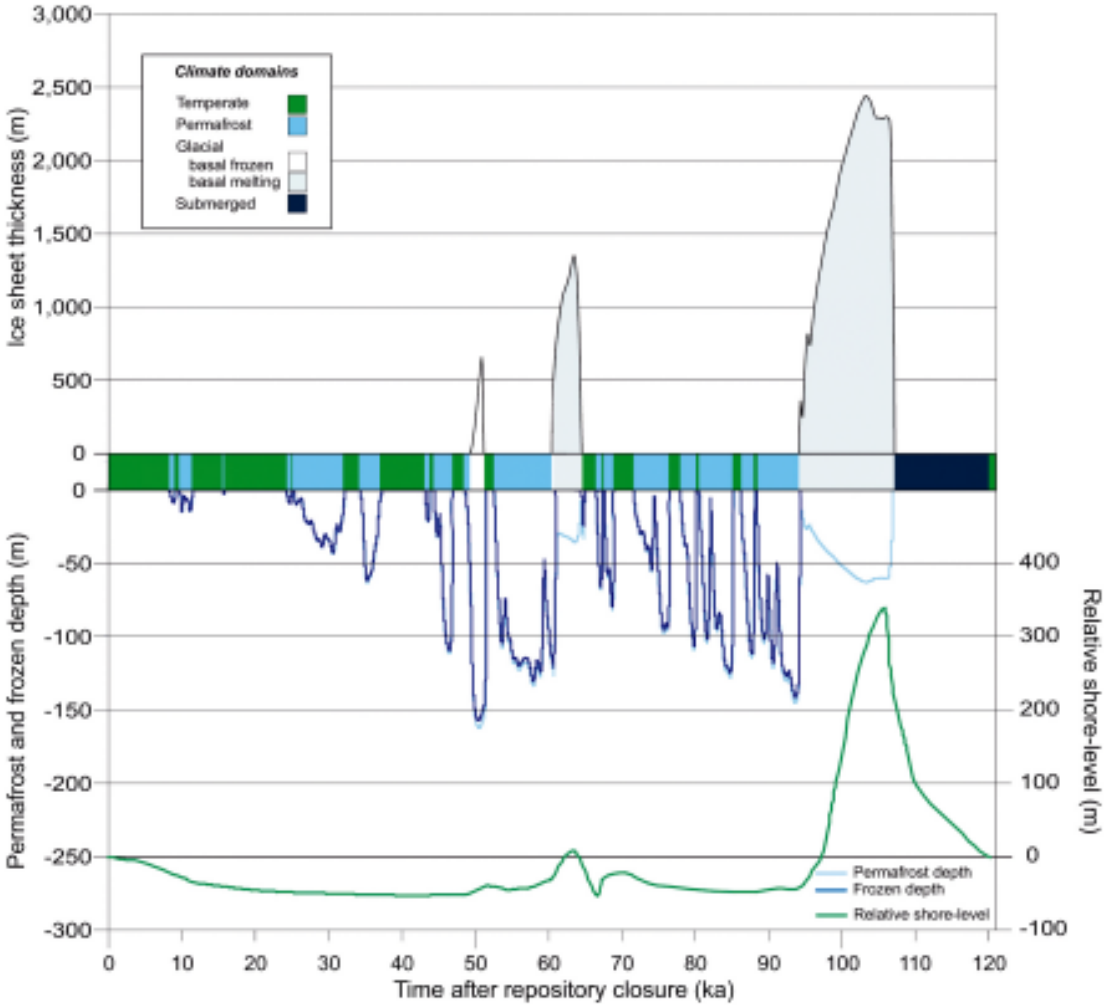

Figure 1-2. *Evolution of important climate-related variables at Laxemar for the base variant of the main scenario in SR-Can. From /SKB 2006b/.*

2 The excavation and operation phases

2.1 Background

The geochemical analysis for the excavation and operation phases of the repository has focused mainly on disturbances of the hydrological and chemical conditions induced by the excavation/operational activities.

The duration of this stage can be assumed to be several tens up to a hundred years, depending on the progress of the excavation/operational activities and the total number of canisters to be disposed.

During this period hydraulic conditions will change as described in /Svensson 2005, 2006/. Some of these changes will be induced by the presence of the repository, but also shore-level displacements and climatic variations may cause more limited alterations. The models show that the salinity in some parts of the repository may decrease due to an increased infiltration of diluted waters of meteoric origin, whereas in other regions upconing might instead induce an increase in salinity.

In addition to the groundwater changes caused by hydrological processes, other chemical aspects need to be considered during this period. It is to be expected that the excavation will be accompanied by grouting, and the chemical influence of grout on groundwater must be considered. In general, cementitious grouts will increase the pH of the water. During the operational phase, the role of stray materials must be assessed, as well as that of any other process that could possibly change the chemical conditions in the repository, such as the precipitation of minerals as waters emerge in the tunnels. These processes might, for example, affect the generation of colloids and the sorption properties of minerals.

When deposition tunnels are backfilled and plugged, air will be trapped in the porous buffer and backfill, and processes consuming oxygen must be evaluated. Air will also cause some initial corrosion of the copper canisters until anoxic conditions are reached.

2.2 Natural groundwater conditions at the sites

The chemical characteristics of groundwater at Forsmark and Laxemar prior to the construction of the repository are set out in detail in their corresponding SDM 1.2 /SKB 2005a, 2006e/. Typical groundwater compositions near repository depth are listed in Table 2-1, which also contains the compositions of other reference waters useful when discussing the evolution of a repository during a glacial cycle.

Table 2-1. Examples of groundwater compositions in mol/L (except TDS). All concentrations except pH are total concentrations.

	Forsmark	Laxemar	Äspö	Finnsjön	Gideå	Grimsel: interacted glacial meltwater	"Most saline" groundwater at Laxemar	"Most saline" groundwater at Olkiluoto	Cement pore water	Baltic seawater	Ocean water	Maximum salinity from glacial upconing
pH	7.2	7.9	7.7	7.9	9.3	9.6	7.9	7.0	12.5	7.9	8.15	7.9
Na	0.089	0.034	0.091	0.012	0.0046	0.00069	0.349	0.415	0.002	0.089	0.469	0.25
Ca	0.023	0.0058	0.047	0.0035	0.00052	0.00014	0.464	0.449	0.018	0.0024	0.0103	0.27
Mg	0.0093	0.00044	0.0017	0.0007	0.000045	0.0000006	0.0001	0.0053	< 0.0001	0.010	0.053	0.0001
K	0.0009	0.00014	0.0002	0.00005	0.00005	0.000005	0.0007	0.0007	0.0057	0.002	0.01	0.0005
Fe	33×10^{-6}	8×10^{-6}	4×10^{-6}	32×10^{-6}	0.9×10^{-6}	0.003×10^{-6}	8×10^{-6}	60×10^{-6}	$\leq 10\times10^{-6}$	0.3×10^{-6}	0.04×10^{-6}	2×10^{-6}
HCO_3^-	0.0022	0.0031	0.00016	0.0046	0.00023	0.00045	0.00010	0.00014	≈ 0	0.0016	0.0021	0.00015
Cl^-	0.153	0.039	0.181	0.0157	0.0050	0.00016	1.283	1.275	≈ 0	0.106	0.546	0.82
SO_4^{2-}	0.0052	0.0013	0.0058	0.00051	0.000001	0.00006	0.009	0.00009	≈ 0	0.0051	0.0282	0.01
HS^-	≈ 0	3×10^{-7}	5×10^{-6}	–	$< 3\times10^{-7}$	–	$< 3\times10^{-7}$	$< 1.6\times10^{-7}$	≈ 0	–	–	$< 3\times10^{-7}$
O_2 fugacity (bar)	$<< 10^{-20}$	$<< 10^{-20}$	$<< 10^{-20}$	$<< 10^{-20}$	$<< 10^{-20}$	$< 10^{-0.17}$ (a)	$<< 10^{-20}$	$<< 10^{-20}$	$\approx 10^{-20}$	$10^{-0.7}$	$10^{-0.7}$	$<< 10^{-20}$
Ionic strength (mol/L)	0.19	0.053	0.24	0.025	0.006	0.0013	1.75	1.76	0.057	0.13	0.65	1.09
TDS (g/L)	9.32	2.78	11.1	1.33	0.33	0.08	73.7	73.4	1.63	6.81	35.1	47.2
Reference	/1/	/2/	/3/	/3/	/3/	/4/	/5/	/6/	/7/	/2/	/8/	/2/
Notes	Borehole KFM02A, 512 m depth	Borehole KLX03, 380 m depth	Repository depth	Repository depth	Repository depth	Max. O_2 fugacity in glacial meltwaters	Depth ≈ 1,500 m.	See also /Pitkänen et al. 1999/ depth = 863 m, sample 42		Sampled at Simpevarp		Laxemar water at 1,350 m

Notes: (a) Oxygen fugacity for glacial conditions: The maximum content is estimated to be 1.4×10^{-3}M for glacial meltwater at 0°C /Ahonen and Vieno 1994/. The corresponding maximum fugacity at 0°C is 0.67 bar. In Grimsel the O_2 content is less than 3×10^{-8} M.

References: /1/ SKB 2005a, /2/ SKB 2006e, /3/ Laaksoharju et al. 1998, /4/ Hoehn et al. 1998, /5/ Laaksoharju et al. 1995, /6/ Pitkänen et al. 2004, /7/ Berner 1987, Engkvist et al. 1996, /8/ Stumm and Morgan 1996.

2.2.1 Correlations between main groundwater components

Chloride is the main anion in the groundwaters at the Forsmark and Laxemar sites. This is evidenced in Figure 2-1 which shows that there is a strong correlation between chloride concentrations and groundwater salinity expressed as *total dissolved solids*, TDS. This correlation may be used to estimate approximate values for chloride concentrations if TDS is known, and *vice-versa*. This is useful when evaluating the groundwater salinities obtained as a result of the hydrological models described in Chapter 4.

It will be seen later in Section 3.3 that there are strong correlations between the concentrations of those groundwater components that are mainly controlled by mixing. This is seen both in the Laxemar and Forsmark areas, for example in the correlation between calcium and chloride on p. 169 in /SKB 2004/ and on p. 276 in /SKB 2005a/. Figure 2-2 shows the relationships between calcium and sodium with chloride in the groundwaters at the sites. Plots displaying the variation of concentrations with depth in the granitic rocks at the sites seldom show so clear trends, e.g. Figure 4-8 on p. 170 of /SKB 2005a/ because the hydraulic conditions of the different fractures influence the mixing between waters of different origins.

2.3 Salinity

Upconing may occur as a consequence of the groundwater inflow into open tunnel sections. This phenomenon has been observed for example in some boreholes at Äspö. In extreme cases, high salinities in the groundwaters might decrease the swelling pressure of the backfill. It is to be expected that groundwater conditions will return to normal after the repository has been backfilled and closed, and that saline groundwaters that had moved upwards will then sink due to their higher density. Diffusion into the rock matrix and mixing with groundwaters in fractures which are relatively stagnant might retain a certain amount of salts at repository depth, but the excavation and operation phases are too short for the diffusion process to be of importance.

The inflow to the tunnels will be reduced by injecting grout into the surrounding fractures. This decreases the depression of groundwater levels near the ground surface as well as the upconing of saline waters.

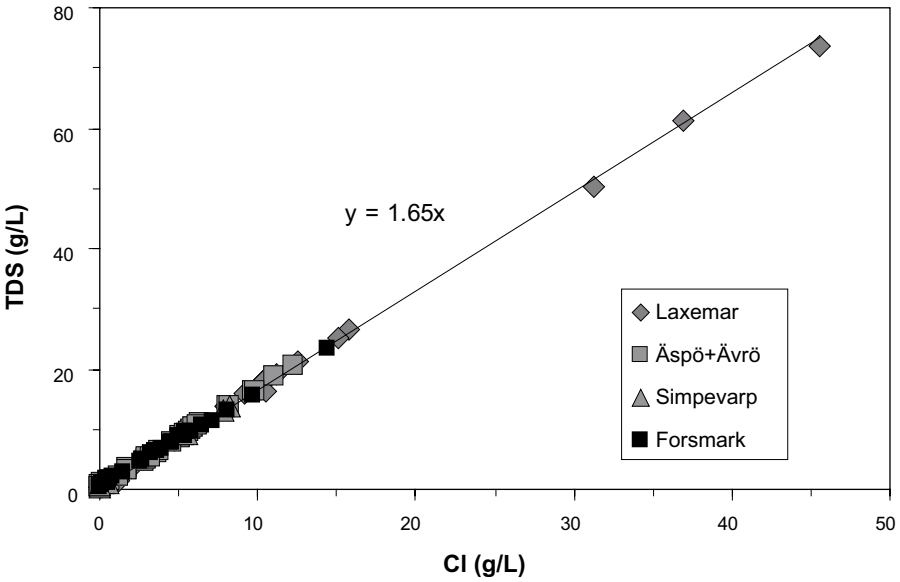

Figure 2-1. *Correlation between chloride concentrations and salinity for selected groundwaters.*

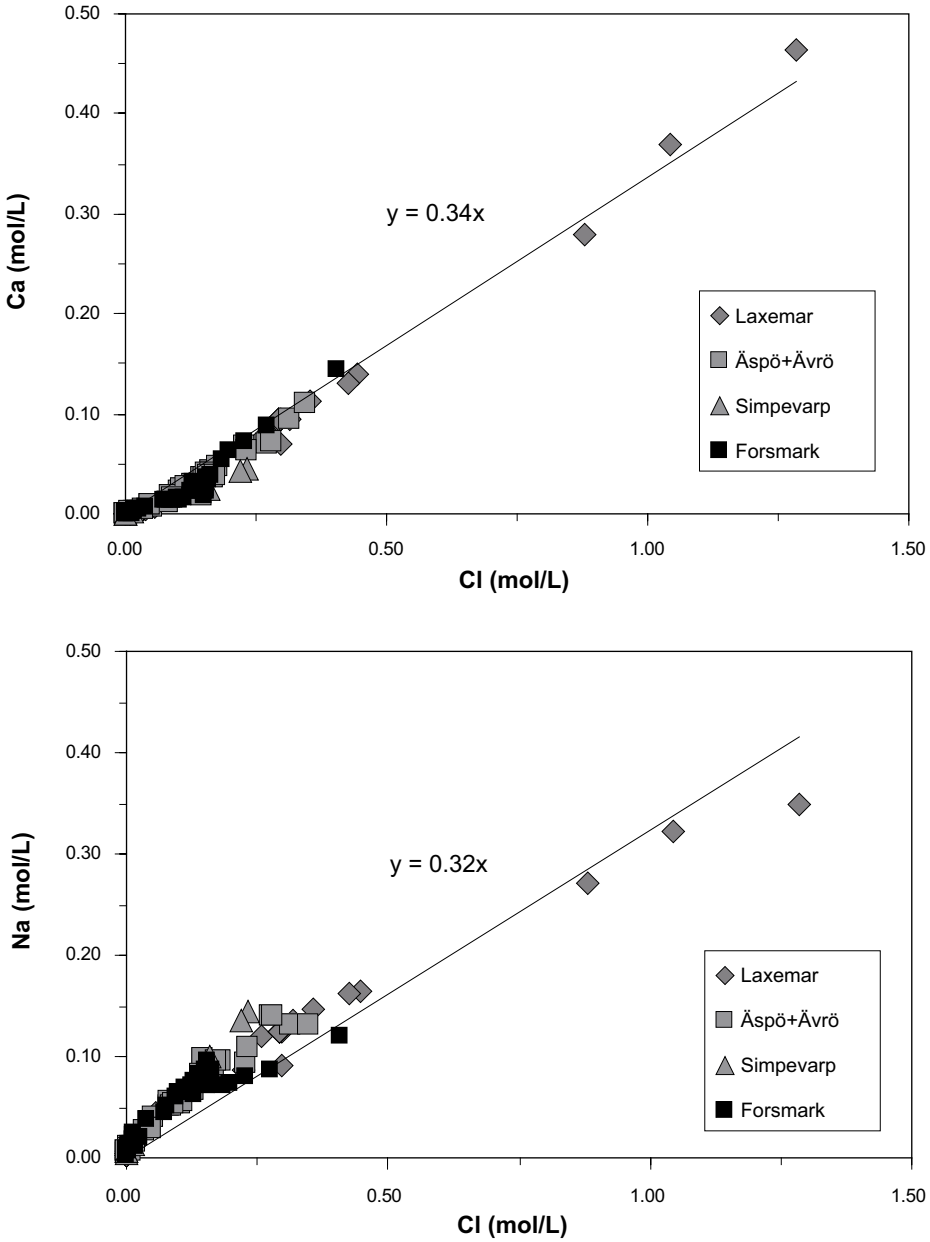

Figure 2-2. *Relationships between chloride concentrations and calcium (upper diagram) and sodium (lower diagram) for selected groundwaters. The correlations indicated in the figures should only be used for qualitative purposes.*

The hydrological consequences of grouting have been modelled for both sites /Svensson 2005, 2006/. The results using the code DarcyTools indicate that for both Forsmark and Laxemar very little upconing of saline groundwaters is to be expected during construction and operation of a repository located at these sites. It is concluded from these studies that the changes in groundwater salinities are small. It should be noted that the Laxemar site is for the moment less well characterised and that the hydrological modelling for this site is preliminary.

2.4 Redox conditions

Even with moderate amounts of inflow into the open tunnels, large amounts of superficial waters are predicted to percolate when considering the whole period of repository operation. Infiltrating waters will be originally equilibrated with oxygen in the atmosphere, whether they are of marine, lake, stream or meteoric origin. It could be contended that the redox stability of the rock volume on top of the repository area might be challenged by the large amounts of infiltrating O_2-rich waters.

However, microbial oxygen consumption takes place already in the overburden and in the first few metres of rock, and therefore infiltrating waters are free of dissolved O_2. Oxygen consumption in saturated soils is well documented, see for example /Drew 1983, Silver et al. 1999, Pedersen 2006/. The Äspö Redox Zone experiment /Banwart 1999, Molinero-Huguet et al. 2004/ also showed that microbial respiration in the upper metres of a fracture zone effectively consume the oxygen in infiltrating waters. This is confirmed by the fact that samples from either Äspö or Stripa are always found to contain dissolved Fe(II) /Wikberg et al. 1988, Nordstrom et al. 1989/ indicating that groundwaters remain reducing even after prolonged periods of inflow into the tunnels.

In conclusion, the reducing capacity of transmissive fracture zones is not affected during the excavation and operation periods, because microbial consumption of oxygen in infiltrating waters takes place already in soils, sediments as well as in the upper metres of fractures.

2.5 Effects of grout, shotcrete and concrete on pH

Injection of grout into fractures surrounding the repository tunnels might be necessary to decrease the inflow of groundwater. Traditionally, cement-based grout is used when excavating tunnels. Standard Portland cement paste has porewater which is highly alkaline (pH ≈ 12.5) for long periods of time. In order to avoid detrimental effects from porewater diffusing out of the cement matrix, cement recipes with porewaters having pH ≤ 11 are planned to be used in the repository. Such materials are being developed and tested.

Grout could have a large impact on the geosphere conditions, as it is widely and diffusely distributed in the fracture system. Grouting is, however, necessary to avoid a large groundwater drawdown (increased meteoric water influx) and the upconing of saline waters. Grouting is also needed for construction purposes; the ingress of water needs to be limited for the engineering installation and for worker safety. Two types of grout are envisaged for the final repository /SKB 2006f/: low-pH cement based grouts and suspensions of nano-sized silica particles (Silica Sol). The solidified Silica Sol grout is similar in its properties to the silica present in large quantities in the rock and fracture fillings, and may, therefore, be ignored in a long-term safety context. Cement-based grouts on the other hand have chemical properties quite different from the surrounding rock, and their effects have to be studied.

Boreholes crossing grouted fractures at Olkiluoto have yielded waters with high pH values since sampling started /Ahokas et al. 2006/. The more limited experience from Äspö shows that a pulse of alkaline solutions may be detected in the immediate vicinity of the grouted fractures. This pulse of alkaline waters is believed to be due to two factors: pore water released while the liquid grout solidifies; and erosion and dilution of grout by flowing groundwater in the outer edge of the grouted volume. These effects in the non-grouted fractures at Äspö were transitory, and after a few days the chemical composition of the groundwater returned to its original state. The pH values were sufficiently low as to indicate that substantial dilution had occurred. The data from Olkiluoto indicates that the intensity of this short alkaline pulse will be decreased by the use of “low-pH” grout /Ahokas et al. 2006/. Because of its short duration and its low intensity, its effects are negligible.

At Forsmark, it is expected that only deformation zones will require grouting to avoid the inflow of groundwater into the tunnels during repository operation. These zones, however, may have a large role in model simulations of radionuclide transport. In deposition tunnels, the average amount of grout in rock fractures is expected to be less than 20 kg per metre of tunnel /SKB 2006f/, while shotcrete will only be used in transport tunnels and other cavities in which deposition does not occur. The values for Laxemar are more uncertain, but they might be in the range 69 to 110 kg per metre of tunnel /SKB 2006f/. It must be noted that grouting will be concentrated to a few locations in each deposition tunnel and that therefore grout will be unevenly distributed.

After repository closure grout will start to react with circulating groundwater, and a slightly alkaline plume will develop downstream in the grouted fractures. A generic model has been used to illustrate this process /Luna et al. 2006/. The results show that a moderately high pH plume (pH ≈ 9) can develop in grouted fractures intersected by the deposition tunnel and to a minor extent also in the backfill material. The leaching of grout material also leads to the precipitation of CSH phases (calcium silicate hydrates) and calcite ($CaCO_3$) in the fracture.

A consequence of this process is that some of the transport pathways for potentially released radionuclides will include groundwaters that have circulated through a grouting zone and have been modified to higher pH (≈ 9) and lower carbonate (due to increased calcium concentrations and consequent calcite precipitation). This could affect the retention properties of the transport pathways affected. The model mentioned above does not take into account changes of porosity in the fracture when CSH phases and calcite are precipitated. Experience from the HPF experiment in Grimsel /Mäder et al. 2004/ shows that this could be an important factor in reducing the transport of alkaline fluids, although the HPF experiment was conducted with solutions simulating standard cement (pH ≈ 12.5). The groundwater sampled in grouted fractures at Onkalo show high pH values /Ahokas et al. 2006/, but the time span for these measurements is too short (some months) for conclusions to be drawn relevant to the longer timescale addressed here. There is, therefore, no experimental evidence to indicate that the model results are pessimistic.

It may be concluded that the effect of grout in fractures will be to increase the pH in deformation zones to values ≈ 9 for relatively long periods of time, probably lasting throughout the first glacial cycle (≈ 120,000 years). pH values ≈ 9 are, however, within the criterion for the safety function indicator in Section 1.2 (i.e. that pH should be ≤ 11). Radionuclide sorption data /SKB 2006c/ have been selected in SR-Can for the pH range 7 to 9, and are therefore adequate as long as "low" pH materials are used for grouting.

2.6 Precipitation/dissolution of minerals

During the operational phase, inflow of groundwater into the tunnel and mixing of groundwaters of different origin within rock fractures will probably result in precipitation or dissolution of minerals. This process may be observed at the Äspö HRL where it is believed to cause the observed decrease in the overall water inflow at Äspö by ≈ 4% each year. However, the process is expected to only indirectly affect the safety function indicators listed in Section 1.2. Numerical simulations have been performed to confirm that they do not influence the performance of the repository negatively /Domènech et al. 2006/. The results show that calcite and iron(III) oxy-hydroxide are expected to precipitate at the tunnel/backfill boundary. The conclusions of that study are that, as expected, the precipitation of these minerals has no significant chemical effect on the performance of the repository, and that the precipitation of secondary minerals during the operational stage of the repository does not significantly affect the porosity of the area surrounding the tunnels.

2.7 Effects of organic materials and microbial processes

Organic materials (including microbial biofilms, tobacco, plastics, cellulose, hydraulic oil, surfactants and cement additives) may be decomposed through microbiologically mediated reactions, and because of this they increase the reducing capacity of the near-field of the repository. However, these materials might also be detrimental during later periods in enhancing the potential for radionuclide transport in groundwater after repository closure, for example by the formation of organic colloids.

An inventory of organic materials and an assessment of their impact on microbial processes has been prepared /Hallbeck et al. 2006/. This study concluded that it is to be expected that microbial degradation of organic materials can have the following consequences: a) contribution to a quick consumption of any oxygen left in the repository; and b) by a combination of processes, involving anaerobic degradation and sulphate reduction, sulphide could be produced in the vicinity of the deposition holes. Some of the sulphide could diffuse to the canister where corrosion would take place. The maximum amount of sulphide that can be generated microbially is ~ 10 moles for each deposition hole /Hallbeck et al. 2006/, which, if it was able to react completely with the canister, would be equivalent to a corrosion of less than 10 μm if distributed evenly. It is, however, to be expected that most of the sulphide produced will either react with iron(II) in the groundwater or diffuse away from the canister, and, therefore, the sulphide thus produced will have a negligible impact on the copper coverage of the canisters.

2.8 Colloid formation

During the excavation and operation phases, substantial amounts of colloids may be formed due to microbial activities, bentonite erosion by fresh waters, precipitation of amorphous Fe(III) hydroxides, etc. These colloids are expected to be short-lived, mainly because colloids will aggregate and sediment in moderately saline waters, see for example /Degueldre et al. 1996/.

Other processes contributing to the elimination of colloids are microbial decomposition of organics, and the re-crystallization and sedimentation of amorphous materials.

In conclusion, an increased formation of colloids during the excavation and operational phases is not expected to affect the performance of the repository in the long-term, because the colloid concentrations will quickly resume the natural values.

2.9 Conclusions for the excavation and operation phase

During the excavation/operation phase, chemical disturbances to the natural conditions are mainly caused by the presence of the open repository.

- For both sites the effects on salinity from upconing and groundwater drawdown are assessed to be negligible.
- A short alkaline pulse in the groundwater from low-pH cement, shotcrete and concrete is likely to form, but its effects will be negligible.
- An increased precipitation of calcite and iron(III) oxy-hydroxides will occur at the tunnel wall during operations, but this process is evaluated as being of no consequence for the performance of the repository.
- Organic stray materials will be consumed by microbes, with the main effects being an increased rate of oxygen consumption and possibly also of sulphate reduction; the latter may at most contribute to an average depth of canister corrosion of about 10 μm, whereas any O_2 consumption will be favourable.
- An increased formation of colloids during the excavation and operation phases will not affect the performance of the repository in the long-term, because the colloid concentrations will quickly resume the natural values.

3 The initial period of temperate climate after repository closure

3.1 Conceptual models

As mentioned in the Introduction, the general strategy to evaluate groundwater compositions in SR-Can is by combining the results of hydrological models with chemical mixing and reaction models. It should be noted that hydrological models have been adjusted to represent as well as possible the present-day groundwater data for non-reactive chemical components in boreholes, as described in Section 3.1.2 below. In SR-Can the results from these calibrated hydrological models are used as input for geochemical reaction and mixing calculations.

3.1.1 Available data

The conceptualisation of the groundwater in the Forsmark and Laxemar sites in SR-Can is based on the all existing information about these sites within the site description models version 1.2. This includes the following:

- Bed rock properties:
  - Porosity available for diffusion of solutes.
  - Flow wetted surface area of fractures.
  - Mineralogy and chemical composition of rock and fracture filling minerals.
- The fracture network:
  - Large fractures and fracture zones estimated from surface and borehole observations. These are normally referred to as “deterministic” fracture zones.
  - A stochastic discrete fracture network (DFN) estimated from the frequency of observed fracture types in cored boreholes.
- Boundary conditions:
  - Topography.
  - The geometry of the water catchments.
- Time conditions:
  - The known past history of the site: a) changes in the elevation with respect to the sea level, and the consequent displacements of the shore line; b) the salinity of the surface waters as a function of time.
  - The estimated future evolution of the site. The reference evolution in SR-Can includes climate changes that are modelled assuming a repetition of the last glacial cycle, the Weichselian.
- “Initial” conditions, present-day data:
  - The water table: measured groundwater heads at the sites.
  - The groundwater compositions: analysed groundwater samples before the data freeze corresponding to model versions 1.2. These samples correspond to a few depths where water conducting fractures are encountered in the boreholes available. Information from pore water compositions obtained by diffusion of specially sampled drill cores is also useful if available. The reliable groundwater samples collected at depths between 300 and 600 m depth are reported in /SKB 2005a, 2006e/. Table 2-1 shows typical groundwater compositions at repository depths for the two sites, as well as other waters that can be used as reference when discussing their evolution.

In addition to the evidence listed above, models and assumptions are needed to understand and envisage the possible future evolution of groundwater at the sites. The hydrological and geochemical properties of the groundwaters are interrelated. It is however practical to discuss them separately, emphasising relevant coupling points between the two descriptions.

3.1.2 Hydrogeochemical model concepts

The granitic bedrock at the sites considered (Laxemar and Forsmark areas, situated close to the Baltic coast of Sweden) is quite old, of the order of 1,800 million years or more. Most of the time the rock has been saturated by groundwater, and the small degree of alteration of the rock suggests that either chemical reactions between the rock minerals and the circulating groundwater is a slow process, or that the groundwater is in equilibrium with the bedrock minerals, at least in some volumes.

The chemical characteristics of these groundwaters are the result of a complex mixing process driven by the input of different recharge waters during the palaeogeographic history of the sites since the last glaciation /Laaksoharju and Wallin 1997, Laaksoharju et al. 1999b, SKB 2005a/. The successive penetration at different depths of dilute glacial melt-waters and Littorina Sea marine waters has triggered complex, density and hydraulically driven flows that have mixed them with long residence time highly saline waters (brines) present in the fractures and the rock matrix. The recent infiltration of meteoric and Baltic Sea marine waters has only affected the shallowest part of the aquifer system, about $\leq$ 200 m depth.

The geochemical study of the Forsmark and Laxemar groundwaters, using either simple conservative elements /Smellie et al. 1995, Laaksoharju and Wallin 1997, SKB 2005a, 2006e/ or more refined isotopic techniques /Louvat et al. 1999, Peterman and Wallin 1999, Négrel and Casanova 2005/ has confirmed the existence of at least four component waters: an old brine, a marine (ancient Littorina Sea), a modern meteoric water, and an old glacial meltwater. As a result, from a purely geochemical viewpoint, mixing can be considered the prime irreversible process responsible for the chemical evolution of the Forsmark and Laxemar groundwater systems. The successive disequilibrium states resulting from mixing conditioned the subsequent water-rock interaction processes and hence the re-equilibration pathways of the mixed groundwaters.

The development of the M3 computer tool using principal component analysis techniques /Laaksoharju et al. 1999a, Gómez et al. 2006a/ has greatly facilitated the interpretation of the groundwater compositions using mixing of reference waters (end-members). Mixing provides a satisfactory interpretation for several of the groundwater components partly because the rates of reaction between the rock and the circulating groundwater are relatively slow, as mentioned above. Besides, an important aspect is that there are large differences in concentrations between the mixing components, e.g. between the meteoric infiltrating waters and the brine found at the deepest parts of the sites. Under such circumstances, the relative effects of water-rock interactions on the concentrations of main groundwater components are small when compared with the large effects caused by mixing.

3.1.3 Hydrogeological model concepts

The hydrogeological model may be summarised as follows:

- A mathematical conceptual model describing groundwater flow and solute transport. For the granitic rocks of the sites under consideration, the model must include density-driven flow, flow in different types of fractures and matrix diffusion. In SR-Can an equivalent continuum porous medium (EPM) model has been used.
- The site data described above in Section 3.1.1. For example: the geometry and characteristics of the fracture zones, statistics and correlations for different types of fractures, etc.
- A simple relationship between groundwater salinity (total dissolve solids, TDS) and groundwater density.

- An assumed initial spatial distribution of salinity in the two sites. For the temperate domain simulations, the time for the last ice-sheet retreat. This initial distribution of salts corresponds to given proportions of glacial meltwater as a function of depth for each site.
- Transport of component waters of different origin (deep brine, glacial meltwater, marine water, meteoric water). This allows the calculation of groundwater salinity and density as a result of the hydrological mixing processes.

When modelling the spatial and time distribution of salt and of the component waters it is found that additional constrains are needed to obtain results that agree with the available hydrological and geochemical data. The geochemical parameters that should be well modelled are those not participating extensively in chemical reactions, such as salinity, $\delta^{18}O$, tritium, chloride, etc. In the site descriptive model version 1.2 /Follin et al. 2005, 2006, Hartley et al. 2005, 2006c/ some effort was put into calibrating the hydrogeological models against the data mentioned above as well as against the calculated mixing fractions of reference waters reported in /SKB 2005a, 2006e/, obtained using the M3 code /Laaksoharju et al. 1999a, Gómez et al. 2006a/.

In order to obtain a "best" representation of all the pertinent hydrological and geochemical data only a few hydrological parameters are normally adjusted, namely:

- Transmissivity-length relationship for fractures.
- Minimum length for a fracture to be included in the numerical model.
- Permeability of different rock volumes.

3.2 Geochemical calculations methodology

3.2.1 General procedure

The main aim of the geochemical calculations during this period is to evaluate a detailed evolution of groundwater compositions for both sites. The simulations use the hydrogeological results as initial data. Calculations performed with PhreeqC /Parkhurst and Appelo 1999/ achieve the coupling of the results obtained with the hydrogeological model (discretised for specific time intervals over a regional site model) with a set of chemical processes (chemical mixing, aqueous equilibrium and mineral reactions). The kind of data supplied by the hydrogeologists (mixing proportions of four component waters) constrains the coupling methodology used in SR-Can.

Hydrogeological results

The Forsmark and Laxemar sites have been described hydrogeologically in the context of the site description model version 1.2 /Follin et al. 2005, 2006, Hartley et al. 2005, 2006c/. The main objectives of these simulations were to develop a present-day description of the sites, i.e. to assess the initial hydrological conditions for a possible repository of spent nuclear fuel. Palaeohydrogeology aspects were fundamental to gain understanding of the system and credibility for the results. It should be noted that these hydrogeological site models were calibrated by comparing the calculated mixing proportions, salinities and $\delta^{18}O$ values with the corresponding data measured at the sites /SKB 2005a, 2006e/, i.e. with the corresponding measured salinities and $\delta^{18}O$ data as well as with the mixing proportions calculated with the M3 code /Laaksoharju et al. 1999a, Gómez et al. 2006a/.

The site hydrogeological models obtained in this way were then used in the evaluation of hydrogeological changes within the SR-Can project /Hartley et al. 2006a, 2006b/. Expected displacements of the Baltic shore line and changes in annual precipitation are included as processes that influence the future hydrological evolution of the sites.

One of the processes modelled in these hydrogeological models is the transport of fractions of selected component waters (rain, marine, glacial and brine) as a method to handle variable density flow. The modelled proportions of component waters (i.e. mixing proportions) at each spatial coordinate (X,Y,Z) and time step may be used to calculate the groundwater salinity and density. The results are illustrated in Figure 3-1.

Results for SR-Can from the hydrogeological models are available at specific times: 2,020, 3,000, 4,000, 5,000, 6,000, 7,000, 8,000 and 9,000 AD for Forsmark /Hartley et al. 2006a/, and 2,020, 4,000, 6,000, 8,000, 10,000, 12,000, 14,000, 16,000, 20,000 AD for Laxemar

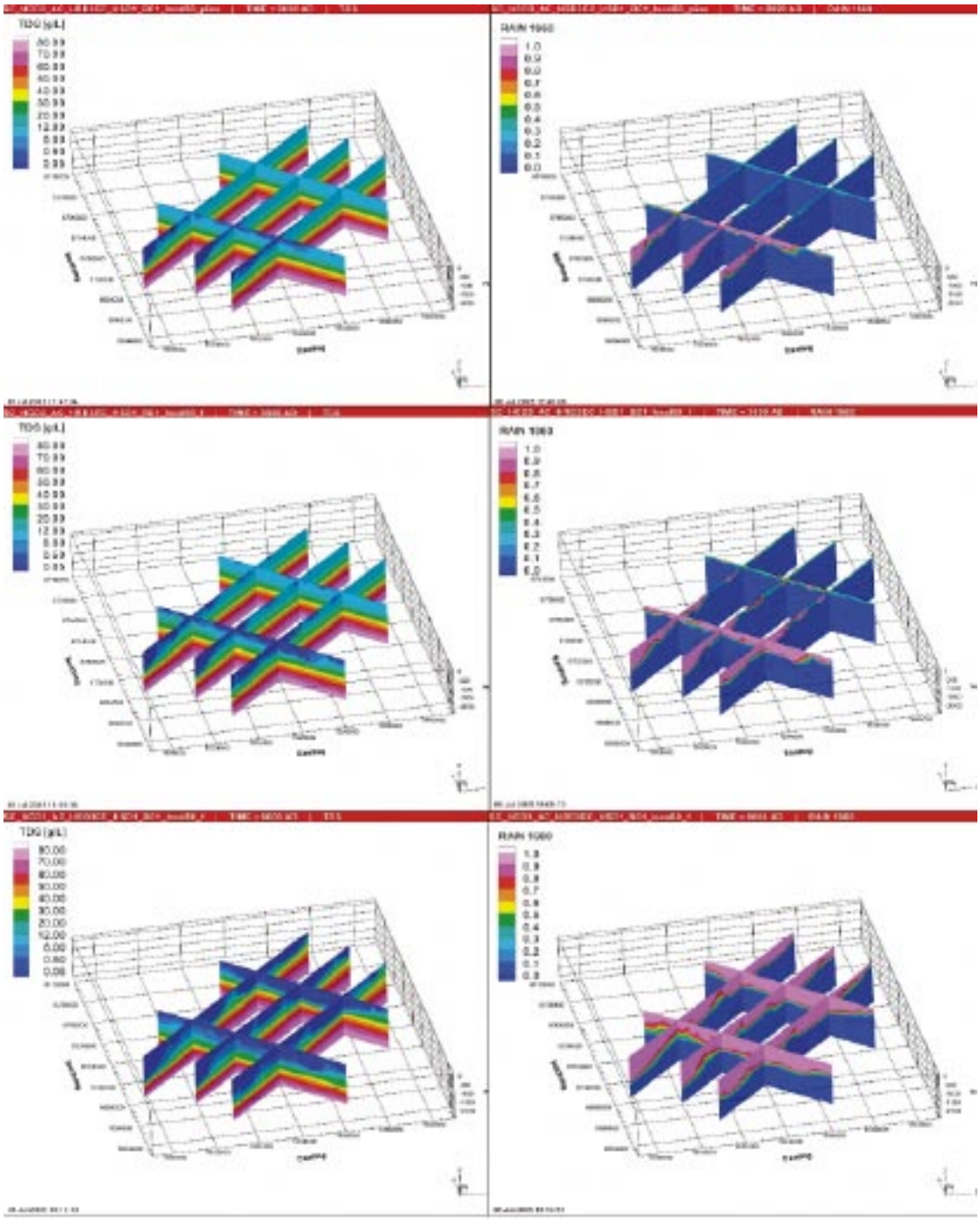

Figure 3-1. *Distribution of TDS (total dissolved solids, g/L, left) and Rain fraction (right) for Forsmark in vertical slices at times equal to (from top to bottom) 2,020 AD, 3,000 AD and 9,000 AD. From /Hartley et al. 2006a/. The figure shows the gradual inflow of rain water, and the corresponding decrease in TDS as the shore line is gradually displaced towards the upper-right corner of the modelled domain.*

/Hartley et al. 2006b/. Given the grid size of the models, 50 m in the repository area and 100 m elsewhere, the data file describing each year included around one million positions in the rock volume (958,484 for Forsmark and 1,446,196 for Laxemar). These points represent the whole regional area of Forsmark and Laxemar up to 2.3 km depth. Figure 3-1 illustrates the nature of the hydrogeological results. For each year, X, Y and Z coordinates together with the mixing proportions of the four component waters (Brine, Marine, Meteoric and Glacial) for the groundwater, both in the fractures and in the rock matrix, are given for each point in the hydrogeological files, which had the following names:

- "SC_HCD3_AC_HRD3A2_T_HSD1_BC1_local50_ZZZZ.txt" and
- "SC_HCD1P3_HRD3a_ddKhalf_ani_HSD1_BC3_MD1_IC1_2_ZZZZ.txt"

for Forsmark and Laxemar, respectively, and where "ZZZZ" is one of the years indicated above (2,020, 3,000, etc).

From each of the original data files three data subsets were extracted:

- All data at repository depth (400 ± 10 m at Forsmark and 500 ± 10 m at Laxemar) for the regional scale models.
- A subset of the above including only the data within the repository candidate areas.
- Vertical cuts approximately perpendicular and parallel to the general coast trend.

  Forsmark:
  - A section approximately parallel to the coast going through the KFM01 borehole. All nodes separated by less than 60 m from the line defined by the following two coordinate points (in km): [1628.519; 6702.421] and [1636.272; 6694.615].
  - A transversal section approximately perpendicular to the coast going through the KFM01 borehole. All nodes separated by less than 40 m from the line defined by the following two coordinate points (in km): [1628.243; 6696.449] and [1638.848; 6707.021].

  Laxemar:
  - A section approximately parallel to the coast and going through the KLX06, KLX04, KLX08, HLX30, KLX18A and KLX03 boreholes. All nodes separated by less than 60 m from the line defined by the following two coordinate points (in km): [1544.606; 6360.000] – [1550.501; 6371.701].
  - A transversal section approximately perpendicular to the coast and passing through the KLX13A, HLX34, KLX04, KLX08 and KLX02 boreholes. All nodes separated by less than 60 m from the line defined by the following two coordinate points (in km): [1540.508; 6369.415] – [1560.000; 6363.512].

  Figure 3-2 shows maps of elevation data for both Forsmark and Laxemar. The repository candidate areas are indicated as well as the lines defining the vertical cuts described above.

PhreeqC calculations

The planar data subsets defined above, including the mixing proportions for each point, were extracted into separate files and they were then used to create input files for the PhreeqC code in order to "translate" these mixing proportions into chemical compositions for each point. The procedure involved combining the file with the hydrogeological mixing proportions with the chemical composition of each of the component waters.

The *Equilibrium_Phases* option of the PhreeqC code is used to equilibrate each of the waters with some minerals. The selected minerals are present in the system and have fast kinetics for the simulated time intervals. The results obtained include the detailed chemical compositions of the groundwaters at each point and the amount of mass transfer for the equilibrated minerals.

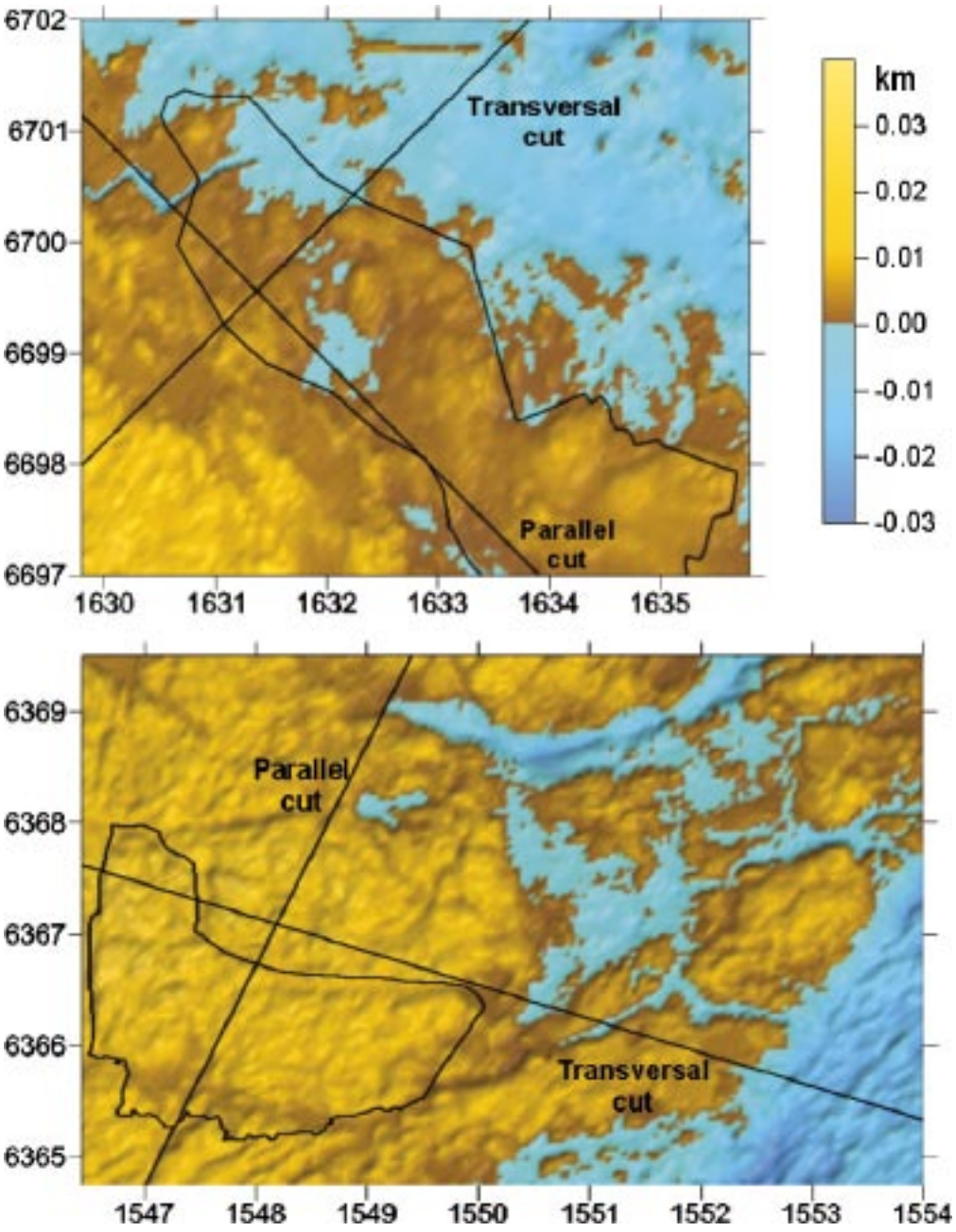

Figure 3-2. *Elevation maps for Forsmark (upper diagram) and Laxemar (lower diagram). Curves defining the repository candidate areas are indicated as well as lines defining the vertical cuts where geochemical simulations have been performed.*

This simulation methodology corresponds to the classical reaction-path calculations: mixing of waters constitute the irreversible process in the hydrochemical system evolution, while the equilibrium reactions represent reversible processes modifying its effects.

The large number of points (or waters) obtained in the hydrogeological spatial discretisation for which PhreeqC calculations had to be performed lead to the development of simple interface software in order to make the input and output of data automatically. All points in the grid of the hydrogeological model, with a spacing of either 100 or 50 m /Hartley et al. 2006a, 2006b/, were used in the calculations: no interpolation of data was performed within this work.

3.2.2 Key parameters for the geochemical calculations

In addition to the mixing proportions supplied by the hydrogeological models, the following parameters are fundamental for the geochemical evaluations:

- The thermodynamic database.
- The chemical compositions of the component waters of different origin (mixing components), as they condition the final composition of the mixed waters.
- The selected mineral equilibrium reactions.

Each of these is discussed in the following subsections.

Thermodynamic databases

The WATEQ4F.dat database, which is distributed with the PhreeqC code (version 2.12.5-669, released November 16, 2005 /Parkhurst and Appelo 1999/), has been used to carry out the mixing and reaction simulations.

Additions/modifications

A few modifications have been introduced that affect the solubility (equilibrium constants) of some important phases in the groundwater systems under study (see Appendix A). The affected phases are:

a) Iron(III) oxy-hydroxides and amorphous or crypto-crystalline iron mono-sulphides. Both groups of solids are involved in the redox processes that control the Eh of the groundwaters, and their solubility is highly dependent on the degree of crystallinity, specific surface area, and re-crystallization or ripening.

b) Aluminosilicate phases. They are present as rock forming minerals and as fracture filling minerals in most granitic systems. Due to extensive solid-solution between end-member phases, their thermodynamic properties are not well known.

Appendix A contains a detailed discussion of the main difficulties encountered when working with these type of phases, the range of solubility values found in the literature, and the values selected for the SR-Can modelling.

Overall redox equilibrium

Apart from these additions and corrections, the hypothesis of homogeneous equilibrium between all redox pairs in the groundwaters has been tested.

Among the variables required to define the geochemistry of groundwaters, the redox potential has been difficult to characterize and to model /Washington et al. 2004/. Often dis-equilibrium among the different redox pairs is found in natural waters /Lindberg and Runnells 1984, Stefánsson et al. 2005/ and therefore an overall Eh value for a groundwater is often impossible to assign /Thorstenson 1984, Nordstrom and Munoz 1985, Langmuir 1997/.

In speciation-solubility calculations with PhreeqC one option is to use an input redox potential to distribute the total concentration of all redox couples in solution /Parkhurst and Appelo 1999/. This type of calculation relies on the homogeneous redox equilibrium assumption which is very difficult to verify in natural waters. Alternatively, redox disequilibria is allowed in PhreeqC if the concentrations of each component for a redox pair is provided. In this case an Eh value may be calculated for each redox couple.

However, during the reaction-path calculations (e.g. chemical mixing or mixing and reaction calculations) all dissolved redox pairs are unavoidably equilibrated by PhreeqC defining a common redox potential (Eh). This procedure is common to almost all geochemical codes performing reaction-path and reactive transport simulations, see e.g. /Liu and Narasimhan 1989, Engesgaard and Kipp 1992, Freedman and Ibaraki 2003/.

The redox pairs involved in the SR-Can calculations are Fe, S and C. Some recent studies (e.g. /Washington et al. 2004/) indicate the occurrence of partial equilibrium or quasi-equilibrium among these redox pairs under the special conditions of depleted strong oxidants (e.g. O_2) and concentrations of redox species higher than 10^{-6}M. Therefore a homogeneous redox equilibrium approach with PhreeqC might be an acceptable approach to understanding the redox state of the groundwaters of Laxemar and Forsmark.

Other observations from the Fennoscandian sites indicate that there are also situations in which iron seems to be uncoupled with the rest of the redox pairs, that is, in redox dis-equilibrium (/Grenthe et al. 1992/ and Table 3-3, p. 292 in /SKB 2005a/). It would therefore be desirable to be able to simulate this redox dis-equilibrium in the SR-Can simulations.

It is furthermore well known that sulphate reduction and methanogenesis are microbially-mediated processes in low-temperature systems. Sulphate reduction requires either organic matter or other strong reductants such as H_2 or CH_4, and because energetically it is not very favourable, it normally does not take place if other electron acceptors are available, such as nitrate, Fe(III) or O_2. Methanogenesis may occur in very reducing environments in the presence of dissolved H_2. In the Forsmark and Laxemar sites this corresponds to large depths and highly saline waters and because the concentration of HCO_3^- decreases with depth, this process may be neglected in the SR-Can simulations.

Coupled and un-coupled databases

The only way to prevent equilibration between redox couples in PhreeqC is to define the individual redox states in each couple as separate "chemical elements", by modifying the thermodynamic database /Parkhurst and Appelo 1999/. In SR-Can a modified version of the thermodynamic database has been implemented in order to obtain redox disequilibrium between the HCO_3^-/CH_4, SO_4^{2-}/HS^- and $Fe(OH)_3/Fe^{2+}$ redox pairs. This modified database will be here named the "Un-coupled" database. The modification essentially avoids the redox pairs SO_4^{2-}/HS^- and HCO_3^-/CH_4 to participate in the homogeneous redox equilibrium during the chemical mixing and reaction simulations. This was achieved by removing the species CH_4 and, in the case of the sulphur redox species, the SOLUTION_MASTER_SPECIES (S(−2)) was removed and it was replaced by a new "chemical element" called "S_" with its corresponding species: $H_2S\_$, $HS\_^-$, $S\_^{2-}$, etc; and minerals: $FeS\__2$ (pyrite), CuS_ (covellite), etc.

In summary, the "un-coupled" database has allowed to obtain groundwater Eh values controlled by the iron system and the $Fe^{2+}/Fe(OH)_3$ redox pair. The resulting Eh values are similar to the ones measured in some of the Swedish groundwaters believed to be controlled by the electro-active $Fe^{2+}/Fe(OH)_3$ redox pair /Grenthe et al. 1992/. With the original "coupled" database the resulting Eh values correspond to homogeneous redox equilibrium, consistent with the agreement between Eh values for the $Fe(OH)_3/Fe^{2+}$, SO_4^{2-}/HS^- and HCO_3^-/CH_4 couples which has been observed in some groundwater samples at Laxemar and Forsmark /Gimeno et al. 2004, 2005/.

Therefore, the use of these two databases covers the measured and calculated Eh values in SKB's site characterisation studies and although some problems in the treatment and interpretation of redox potential still persist, this methodology can give a reasonable range of Eh values in the SR-Can simulations.

Component waters for the chemical mixing

All the geochemical calculations start with mixing proportions of the component waters instead of the chemical compositions, which therefore have to be calculated. The results will be strongly affected by the assumed original composition of the mixing components.

Table 3-1 shows the original compositions of the end-member waters that are being used in the M3 statistical analysis performed within SKB's site characterisation studies /SKB 2005a, 2006e/. Some of these waters are represented by real samples from natural systems and

Table 3-1. Compositions of end-member waters reported in /SKB 2005a, 2006e/. All concentrations in mg/L.

	Brine	Littorina	Glacial	Meteoric	Superficial granitic ground-water (Laxemar)	Superficial granitic ground-water (Forsmark)
pH	8.0†	7.6	5.8*		7.5	7.6
Eh (mV)	−300†					
Li	4.64	0.07			0.0	0.011
Na	8,500#	3,674	0.17	0.4	15.4	64.6
K	45.5	134	0.4	0.29	2.6	9.5
Ca	19,300	151	0.18	0.24	38.4	62.0
Mg	2.12	448	0.1	0.1	4.0	14.0
Sr	337	2.68			0.22	0.284
Fe	0.4‡	0.002			0.82	0.5
F	1.6‡	0.49			0.0	1.13
Cl	47,200	6,500	0.5	0.23	11.2	15.7
Br	323.6‡	22.2				
Alkalinity	14.1	93	0.12	12.2	137	310
SO_4^{2-}	906	890	0.5	1.4	7.5	18.6
Si	2.9	1.84	0.01*		6.06	9.78
Source:	KLX02 1,601–1,651 m depth, sampled 1993-Aug-03	p. 13 in /Pitkänen et al. 2004/	p. 32 in /Laaksoharju and Wallin 1997/	p. 32 in /Laaksoharju and Wallin 1997/	Selected in this work from sample: HBH05 16 m depth, see p. 356 in /SKB 2006e/.	Selected in this work from sample: HFM03 20 m depth

† From monitoring the 1,420–1,705 m depth section of this borehole.

The value in the Sicada data base is 8.2 g/L, which differs from the value used for the Brine end-member in SKB's geochemical analysis of site data, see e.g. p. 32 in /Laaksoharju and Wallin 1997/ and p. 348 in /SKB 2006e/. The reason for this discrepancy is being investigated.

‡ From a sampling 1994-Jan-17 at depth 1,392–1,670 m in the same borehole, having Cl = 45.5 g/L. Bromide contents re-scaled (from 312 g/L) to the higher salinity.

* pH and Si for Glacial mixing component from p. 13 in /Pitkänen et al. 2004/.

some others are estimated from diverse geological information. In both cases there are some fundamental parameters not known for some of these waters (pH, Eh, Al, Fe, or S^{2-}), and in order to have an estimation of them, a comprehensive evaluation of their chemical composition is presented below.

Brine

The chemical composition for the Brine[1] mixing component corresponds to the deepest and more saline water sampled in the Laxemar and Forsmark sites, which up to now is a sample from borehole KLX02 in Laxemar at 1,631–1,681 m depth with a salinity of 75 g/L TDS. The groundwaters sampled from the deepest part of this borehole are quite old (1.5 million years estimated from ^{36}Cl data /Louvat et al. 1997, 1999/) with a Ca-Na-Cl composition and with a significant deviation from the MWL (Meteoric Water Line in $\delta^{18}O$ vs δD plots) due to its long interaction time with the bedrock in a near-stagnant environment /Laaksoharju and Wallin 1997, Laaksoharju et al. 1999b/.

[1] Brine is normally defined as an aqueous solution having a salinity higher than that of sea water, i.e. > 35 g/L. However, in some contexts this term is reserved for waters with salinities above 100 g/L TDS, e.g. /Kharaka and Hanor 2005/.

In spite of the current controversy about the origin of the salinity in this kind of waters in crystalline rocks /Starinsky and Katz 2003, Gascoyne 2004, Casanova et al. 2005, Frape et al. 2005, Négrel and Casanova 2005, Smellie et al. 2006/, it seems reasonable, taking into account their high residence times, to assume that they are in equilibrium with the mineralogy of the bedrock /Gimeno et al. 2004/.

The groundwater sample used as the Brine mixing component in the Swedish site characterization programs lacks aluminium, Fe^{2+} and sulphide, as well as in situ determinations of pH and Eh. These data have been taken from a different sample from the same borehole KLX02 (1,420–1,705 m depth section) which turned out to be slightly less saline. The continuous logging of down-hole and surface instruments indicates pH = (8.0 ± 0.2). The Eh loggings show significant differences among the different electrodes (Pt, C and Au), at surface and at depth, but the stable and extended reading from the Pt electrode indicates a value of −300 mV.

An additional uncertainty related with the Brine mixing component is the apparent compositional variability found between sites. There are very few data of highly saline groundwaters in the Fennoscandian basement useful as a reference to evaluate the homogeneity of these waters. In SKB's site characterization programme, a common Brine end-member has been used for mixing proportion and mass balance calculations. However, up to now the more saline waters analysed in Forsmark show salinities clearly lower than in Laxemar (16 versus 47.2 g/L of chloride, respectively). This may be due to the more limited depth of the drilling campaigns in the Forsmark area, but in any case it introduces a reasonable doubt about the real composition of the saline waters in the Forsmark area and their similitude to those in Laxemar.

The main difference found from a comparison between the two sites occurs in the SO_4^{2-} contents /Gimeno et al. 2004, 2005/. Sulphate concentrations in the Laxemar area increases with chloride reaching a maximum (800–900 mg/L for chloride levels of 15,000 mg/L) when it attains equilibrium with gypsum. In Olkiluoto, the groundwaters with highest sulphate content have an intermediate salinity (5 to 6 g/L of Cl) and the sulphate concentrations decrease to very small values in the more saline groundwaters. This suggests a marine origin for the sulphate at the Olkiluoto site. In Forsmark the groundwater salinities are more limited than at Laxemar or Olkiluoto, but they appear to follow the same trend as in Olkiluoto. The origin of the difference in SO_4^{2-} concentrations between Laxemar and Forsmark still needs more detailed studies but it seems likely that it may be related to the presence or absence of gypsum as fracture fillings /Drake et al. 2006/.

Finally, all the brines and saline waters from the Finnish shield with TDS values higher than 20 g/L included in /Frape et al. 2005/ show SO_4^{2-} contents lower than 190 mg/L and most lower than 80 mg/L. This fact suggests that the Brine component defined from Laxemar samples (906 mg/L) may have an exceptionally large sulphate content.

In order to take this uncertainty into account a Brine mixing component with a very low sulphate content has been used as an alternative mixing component in the simulations for the Forsmark area.

Solid phases equilibrated with the brine component

Before the chemical mixing simulations, the Brine component was equilibrated with calcite, chalcedony, albite and K-feldspar at a fixed pH value of 8. The equilibrium assumption for these phases is reasonable as a result of the long residence time for this water and it has been confirmed with the saturation indices obtained for the real groundwaters from the two sites /Gimeno et al. 2004/.

The redox potential for these waters is assumed to be controlled by an iron mineral phase (haematite) with the equilibrium constant value proposed in /Grenthe et al. 1992/.

The final composition obtained for this mixing component is shown in Table 3-2.

Table 3-2. Calculated compositions of the mixing components after mineral equilibration. All concentrations in mol/L. For the calculations using the "un-coupled" database the only results given are those differing from the "coupled" database.

	Brine		Littorina		Glacial		Superficial GW Laxemar		Superficial GW Forsmark	
Temp.	15°C		15°C		15°C		15°C		15°C	
pH	8.00†		7.94		9.25		7.37		7.09	
Eh (mV)	−243	−359	−241	−378	−298	−251	−48	−46	+17	+19
Li	0.0007		1×10^{-5}						2×10^{-6}	
Na	0.380		0.162		7.4×10^{-6}		0.00067		0.0028	
K	0.0009		0.0035		1.0×10^{-5}		7×10^{-5}		0.00024	
Ca	0.494		0.0039		7.5×10^{-5}	7.6×10^{-5}	0.00090		0.0010	
Mg	9×10^{-5}		0.0187		4.1×10^{-6}		0.00016		0.00058	
Sr	0.004		3×10^{-5}				3×10^{-6}		3×10^{-6}	
Fe	7×10^{-8}	7×10^{-6}	9×10^{-6}		8.0×10^{-7}	1.3×10^{-7}	1.5×10^{-5}		1×10^{-5}	9×10^{-6}
Mn	3×10^{-6}		3×10^{-6}						3×10^{-6}	
Al	7×10^{-10}		1×10^{-7}		1.9×10^{-6}		3×10^{-8}		2×10^{-8}	
F	9×10^{-5}		3×10^{-5}						6×10^{-5}	
Cl	1.366		0.186		1.4×10^{-5}		0.00032		0.00044	
Br	0.0042		0.0003						0.0003	
C	3×10^{-5}		0.0016		8.9×10^{-5}		0.0023	0.0024	0.0048	
SO_4^{2-}	0.0097		0.0094		5.3×10^{-6}	5.2×10^{-6}	8×10^{-5}		0.00019	
HS^-	1×10^{-6}	1×10^{-7}	9×10^{-6}		1×10^{-11}	1×10^{-7}	3×10^{-29}	1×10^{-7}	3×10^{-35}	1×10^{-7}
Si	0.0013		0.0002		0.00025		0.0002		0.0002	
Database:	Coupled	Un-coupled	Coupled	Un-coupled	Coupled	Un-coupled	Coupled	Un-coupled	Coupled	Un-coupled
Minerals at equilibrium, saturation index imposed‡	Calcite, 0 Chalcedony, 0 Albite, 0 K-feldspar, 0 $Fe(OH)_3$(H_Gr), 0		Calcite, 0 Chalcedony, 0 Kaolinite, 0 FeS(ppt), 0		Calcite, −1. Chalcedony, 0 Kaolinite, 0 $Fe(OH)_3$(micr), 0		Calcite, −0.5 Chalcedony, 0 Kaolinite, 0 $Fe(OH)_3$(micr), 0		Calcite, −0.5 Chalcedony, 0 Kaolinite, 0 $Fe(OH)_3$(micr), 0	

† Fixed pH.

‡ The saturation index is defined as /Langmuir 1997, Appelo and Postma 2005/: log (IAP/K_{sp}) where IAP is the ionic activity product and K_{sp} the solubility product, which for calcite and chalcedony are those given in the original Wateq4F database provided with PhreeqC, while Appendix A contains a discussion and selection of the data for the iron(III) oxy-hydroxides, FeS(ppt) and the aluminosilicates.

Littorina

The chemical composition of seawater during the Littorina stage has been selected as one of the reference waters used in the hydrogeological and hydrogeochemical modelling of the Laxemar and Forsmark sites, as well as in other Fennoscandian sites with a similar palaeo-geographic evolution (for example Olkiluoto in Finland /Pitkänen et al. 1999, 2004/).

The Littorina stage in the postglacial evolution of the Baltic Sea commenced when the passage to the Atlantic Ocean opened through Öresund in the southern part of the Baltic Sea and sea water started to intrude at ≈ 6,500 BC. The salinity increased more or less continuously until ≈ 4,500–4,000 BC, reaching estimated maximum values twice as high as modern Baltic Sea and this maximum prevailed at least from 4,000 to 3,000 BC. This period was followed by a stage where substantial dilution took place. During the last 2,000 years the salinity has remained almost constant to the present Baltic Sea values.

Groundwaters with high proportions of Littorina Sea water are identifiable by their higher salinities and $\delta^{18}O$ values than the present Baltic Sea (as well as higher values for e.g. magnesium and sulphate).

The estimation of the original composition of the Littorina Sea is indirectly made from palaeontological studies (e.g. fossil assemblages), $\delta^{18}O$ measurements of molluscs and foraminifera, and ^{18}O analysis and trace-element content in sediments or minerals (see /Westman et al. 1999/ and references therein). With all these data an estimation of the salinity and the chloride concentration can be obtained. Then, from correlations between the different elements and chloride in sea waters, the rest of the chemical composition can also be estimated /Culkin and Cox 1966, Carman and Rahm 1997/.

The Littorina Sea composition used in this work is that used within the site characterisation studies /SKB 2005a, 2006e/, see Table 3-1. It is based in the maximum salinity estimation of 12‰ or 6,500 mg/L Cl^- /Kankainen 1986/, while the other main element concentrations were obtained by diluting the global mean ocean water /Pitkänen et al. 1999, 2004/.

However, the salinity was variable over the entire Littorina Sea period. Moreover, as it occurs in the present Baltic sea, salinity also varies vertically (depth) and laterally (geographical situation) e.g. /Sohlenius et al. 2001/, and palaeontological or palaeogeochemical studies reflect these variations with estimated maximum salinities between 8 and 24‰ for all the Baltic zone both for surface and deep sea waters (see Table 2-2 in /Westman et al. 1999/). The uncertainty related with the geographic variability can be minimised restricting the estimation to the areas of interest, that is, the island of Gotland and the Baltic Sea Proper. The maximum surface salinity during the Littorina Sea stage in these zones seems to has been between 10 and 13‰ (Cl = 5.5 to 7.2 g/L) as indicated by fossil assemblages; as well as from ^{18}O and trace-element content in sediments. The chloride concentration assigned to Littorina (6.5 g/L) can be representative of a mean value for the range of uncertainty (Cl = 5.5 to 7.2 g/L).

Similar results for the chloride contents during the maximum salinity of the Littorina stage have been found using different methodologies /Sjöberg et al. 1984, Laaksoharju and Wallin 1997, Pitkänen et al. 1999, 2004/.

In addition to the uncertainty in the Littorina Sea salinity, seawater intruding in the sub-surface may be modified by reactions in the sediments. The main processes are: sulphate reduction, carbonate precipitation and cation exchange. Because of these factors, it must be understood that the composition of the Littorina Sea component in chemical mixing calculations is quite uncertain.

Equilibrium calculations to obtain a Littorina Sea mixing component

In order to obtain important parameters such as pH, Eh, Fe, sulphide, etc, for Littorina Sea water intruding into the sub-surface, the initial seawater has been modified by imposing a few equilibrium processes. For example, it may be assumed that the original Littorina Sea water

was air-saturated, but this oxygen would quickly be consumed by microbial processes in marine sediments. Also carbonate precipitation would affect the original composition. Therefore, the Littorina Sea mixing component has been equilibrated with calcite, amorphous FeS, kaolinite and chalcedony.

Equilibrium with respect to FeS reflects the expected microbial sulphate reduction and the common presence of this sulphide phase in anoxic marine sediments. Equilibrium with chalcedony and kaolinite is an attempt to approximate the interaction with aluminosilicates in the sea sediments or in the first metres of the bedrock.

The final composition obtained for this mixing component is shown in Table 3-2.

Glacial

The Glacial component water represents the chemical composition of a meltwater from a previous glaciation (> 11,000 BC). The composition adopted in the site investigation programme (Table 3-1) corresponds to actual meltwaters from one of the largest glaciers in Europe, the Josterdalsbreen in Norway, situated on crystalline granitic bedrock /Laaksoharju and Wallin 1997/. This composition is similar to that estimated in /Pitkänen et al. 1999, 2004/ in a model study of the Olkiluoto site, Finland. Glacial meltwaters have a very low content of dissolved solids, even lower than present-day meteoric waters, and they represent the chemical composition of surface meltwaters prior to the infiltration in the basement, and therefore, prior to suffer water-rock interaction processes.

Groundwaters with a glacial component can be recognized by their relatively low salinity and their isotopically light signature (δD and $\delta^{18}O$). However, in the Forsmark and Laxemar areas the composition of these groundwaters has been drastically modified by mixing with waters of other origins. Therefore, there are no “undisturbed” or “pure” glacial meltwater remnants that could serve as a glacial mixing component.

The extent of water-rock interaction processes that can be reasonably expected as meltwaters infiltrate the ground may be inferred from the study of waters from zones with no mixing processes but with a clearly glacial or old meteoric origin. Despite the fact that many of the studied KBS-3 sites lack representative hydrochemical data (e.g. because of sampling problems leading to contamination from drilling water and/or other groundwater sources), some indications of ancient glacial melt water are apparent. For example, in Fjällveden according to /Wallin 1995, Tullborg 1997a/, groundwaters below 500 m depth may be residual meltwaters or any other meteoric water formed from a colder climate. A glacial origin is favoured in /Bath 2005/ where “apparent” ^{14}C ages around 12,000 to 14,000 years (i.e. late-glacial) are reported. At Gideå there may also be an indication of mixing between meteoric and post-glacial meltwaters /Wallin 1995/. Finally, groundwaters in Lansjärv also show the isotopically light signature ($\delta D = -109.3‰$ and $\delta^{18}O = -13.8‰$) typical of glacial or old meteoric waters from colder climates.

Compared with the original composition of glacial meltwaters, these waters show a slightly lower pH, although still alkaline (close or higher than 9) and higher TDS values as a consequence of water-rock interactions. The differences are of orders of magnitude, especially for chloride, sodium and alkalinity. However in absolute terms the final salt contents are still very low, even taking into account potential contamination. A further discussion is given in Appendix B. This means that, as expected, water-rock interaction modify the compositional characters in a quite limited scale. Similar conclusions have been obtained when analysing other old meteoric or glacial waters in crystalline basements /Degueldre 1994, Thury et al. 1994, Degueldre et al. 1996/.

Dissolved O_2 concentrations in glacial meltwaters could be high, about 1.4 mM or 45 mg/L. Reduced biological activity in the sub-glacial soil would not decrease this O_2-levels. It may therefore be envisaged that O_2-rich glacial meltwaters might penetrate the bedrock through conductive vertical fracture zones. Recent studies have indicated that O_2 may be strongly depleted in dissolved gases in basal ice (provided that contact with atmosphere does not occur) and much

lower O_2 concentration might be expected in meltwaters recharging the bedrock /Gascoyne 1999/. Moreover, no evidence has been found that oxidizing conditions have ever prevailed at depth neither in Sweden nor in Finland (see /Vieno and Nordman 1999, Puigdomenech et al. 2001b/ and references therein). This indicates that O_2 is depleted already in the near-surface zone. This important question from the standpoint of repository safety is further discussed in Section 4.2.4.

Equilibrium calculations for the Glacial mixing component

As for the Littorina case, some reactions have been considered to affect Glacial meltwaters intruding the bedrock in order to simulate water-rock interaction processes in the upper parts of the rock prior to mixing with other groundwater components.

In this case the calcite saturation index was fixed to −1.0 (originally glacial meltwaters are strongly under-saturated with respect to calcite). The redox potential for these waters has been assumed to be controlled by an iron mineral phase (microcrystalline $Fe(OH)_3$) common in environments that buffer the input of oxygenated waters. In addition, equilibrium with respect to chalcedony and kaolinite has been assumed.

The final results (Table 3-2) indicate an alkaline pH (≥ 9) common to other glacial groundwaters, see for example the Grimsel water in Table 2-1. As the buffer capacity of these waters is very low, very small changes in some of the components of the original meltwater can result in a drastic modification in the equilibrated final composition (e.g. alkalinity or Eh). In any case, these uncertainties do not affect the simulations involving the chemical mixing and reaction processes in SR-Can.

Superficial granitic groundwater of meteoric origin

This mixing component represents a typical shallow groundwater (less than 100 m depth) of recent meteoric origin and, therefore, it should reflect the chemical characteristics of meteoric waters after a short interaction with soils, overburden and granite. The selection of a representative composition for this dilute groundwater has been made from a large amount of available shallow groundwater samples from each of the Forsmark and Laxemar sites. Their tritium content and low chloride concentrations are representative of their recent meteoric origin and the absence of mixing processes with more saline waters.

All the groundwaters of this type sampled at the sites have low TDS. However their chemical composition can be very heterogeneous in detail. One representative superficial granitic groundwater has been selected for each site: for Forsmark a sample from borehole HFM03 at ≈ 20 m depth; and for Laxemar a sample from borehole HBH05 at ≈ 16 m depth. However due to the high variability observed in these systems, any of them could have been used for both sites.

As discussed in Appendix B, groundwaters of meteoric origin may be quite dilute, even at considerable depths. Because of the large relative impact of chemical mixing in the SR-Can simulations, a selection of proper compositions for superficial groundwaters is important, as it will have a large impact on the distribution of salinity with depth.

Solid phases equilibrated with superficial granitic groundwaters of meteoric origin

In this case, as the selected mixing component waters are real samples, the chemical compositions are well known but they do not have aluminium or measured Eh data. These values have been obtained by equilibrating the samples with kaolinite and micro-crystalline $Fe(OH)_3$. Moreover a calcite saturation index of −0.5 has also been imposed for these waters.

The final compositions for the superficial granitic groundwaters for Forsmark and Laxemar are shown in Table 3-2.

Mineral equilibrium reactions

The SR-Can simulations for the first temperate period after repository closure include both chemical mixing and equilibrium with some solid phases. A selection has been made of mineral reactions with rates fast enough for the time scale considered and involving mineral phases accessible to groundwaters in the system.

Calcite ($CaCO_3$) is ubiquitously present as fracture filling minerals, see Appendix C. It normally reacts rapidly with circulating groundwaters, which therefore are usually found to be saturated or close to saturation with this mineral. Chemical reactions involving calcite are important in regulating the acidity (pH) and alkalinity (HCO_3^-) of groundwaters. It may be shown that several of the calcite samples are hydrothermal, and therefore very old, while other samples have been precipitated from "cold" groundwaters, and could perhaps be younger than 2 million years, see the detailed discussion in Appendix C.

Silica (SiO_2) in the form of quartz is one of the components of the bedrock. Silica may adopt several crystalline forms, each with a different stability and solubility. Most groundwaters are found to be close to saturation with chalcedony, a silica polymorph.

Mineral equilibrium reactions affecting the redox state in groundwaters include two different mineral phases: *a*) crystalline $Fe(OH)_3$ (e.g. haematite) with the equilibrium constant deduced in /Grenthe et al. 1992/; and *b*) amorphous Fe(II) mono-sulphide (FeS(am)). These solids represent two different and alternative groundwater evolution scenarios: equilibrium with crystalline $Fe(OH)_3$ can represent a situation where the redox state is not affected by sulphate-reducing bacteria activity, while equilibrium with FeS(am) represents a situation with sulphate-reducing bacteria activity in the system (also identified at the sites). Apart from the redox effects of these reactions, they also affect the contents of iron and sulphide. Fe(III) oxy-hydroxides are quickly precipitated if the Fe(III)-concentration increases above its solubility limit at the prevailing pH. Also the precipitation of Fe(II)-sulphide is fast, and this sets constraints on the maximum levels of Fe(II) and sulphide.

3.2.3 Tests of alternative geochemical simulation strategies

Tests were initially made in order to check the influence of the following factors:

- Inclusion or exclusion of mineral reactions (calcite, chalcedony and $Fe(OH)_3$). These two alternatives are here denoted "only mixing" and "mixing + reaction", respectively.
- Suppression or inclusion of redox equilibrium for the SO_4^{2-}/HS^- and HCO_3^-/CH_4 redox couples, denoted as the "un-coupled" or "coupled" databases, respectively. Appropriate mixing components (Table 3-2) were used in the "mixing + reaction" simulations, see the figures in Section 3.3.
- Selection of a solid phase to control redox conditions (see Appendix A): either the Fe(III) oxy-hydroxide (Fe(OH)3(hematite_Grenthe)) or Fe(II) sulphide (FeS(ppt)).

Unless otherwise stated, the figures and tables in this chapter show results for "mixing + reaction" with the "coupled" database and the Fe(III) oxy-hydroxide as redox-conditioning solid. Alternative simulation strategies are discussed when appropriate.

In the light of the results obtained with these tests, some additional scoping calculations have been performed. Some of them considered the equilibrium with additional mineral phases (chlorite, illite, kaolinite and K-feldspar) and some other tested the influence of ionic exchange. The results of these tests, not presented in this report, showed that the inclusion of additional aluminosilicates, such as chlorite and illite had a negligible effect on the concentrations of Mg and K for Forsmark and Laxemar. The inclusion of ion-exchange processes, however, indicated that in some cases they could affect substantially the Ca, Mg and K concentrations. Not enough information is available on the ion-exchange capacity of the fracture surfaces of the sites, and this option was not further pursued, but it should be further investigated in future safety assessments.

In the specific case of Forsmark, some scoping calculations were performed using a different Brine groundwater with a very low sulphate content (10 mg/L), see Figure 3-1.

3.2.4 File nomenclature

Subsets with hydrogeological data

Because of the large number of points in the regional hydrogeological models, planar subsets of data were selected to aid the visualisation of results. The selected planes, one of which is obviously a horizontal cut at repository depth, are discussed in Section 3.2.1. These files were named by starting with "F_" or "L_" for the Forsmark or Laxemar simulations, followed by the year, e.g. 2020, and then:

- for all data at repository depth, added "_400" for Forsmark and "_500" for Laxemar,
- for all data at repository depth within the repository area, added "_400_ra" and "_500_ra" for Forsmark and Laxemar, respectively,
- for the vertical cut defined in Section 3.2.1 approximately perpendicular to the general coast direction: added "_T",
- for the vertical cut defined in Section 3.2.1 approximately parallel to the general coast direction: added "_II".

For example, the file "L_6000_500_ra.dat" contains all the hydrogeological results at 500 m depth within the repository area for the Laxemar model at year 6,000 AD, while the file "L_6000_500.dat" contains the data for the whole regional model at the same depth.

PhreeqC databases

The database distributed with PhreeqC version 2.12.5.669, released November 16, 2005, was modified as discussed in Section 3.2.2 and in Appendix A.

Two versions were prepared as discussed in Section 3.2.2: one which included overall redox equilibrium (the "coupled" database), and another that excluded sulphate and carbonate reduction (the "un-coupled" database). These files were named, respectively:

- wateq4f_SR-Can.dat
- wateq4f_SR-Can_no_S-redox.dat

PhreeqC input and output files

PhreeqC input files were automatically prepared by combining the subsets of hydrogeological data described above with the compositions of the mixing components listed in Table 3-2. The file names were composed by adding an appropriate text to the name of the corresponding hydrogeological file. The text is used to describe the simulation strategy outlined in Section 3.2.3:

- "_mixCoupled" for simulations including only mixing with the "coupled" database.
- "_mixUncoupled" for simulations including only mixing with the "un-coupled" database.
- "_FeOH3Coup" for "mixing + reaction" simulations including the redox-controlling mineral Fe(OH)3(hematite_Grenthe) and the "coupled" database.
- "_FeOH3Uncoupled" for "mixing + reaction" simulations including the redox-controlling mineral Fe(OH)3(hematite_Grenthe) and the "un-coupled" database.
- "_FeScoupled" for "mixing + reaction" simulations including the redox-controlling mineral FeS(ppt) and the "coupled" database.

For example, the file F_6000_T_FeOH3Coup.pqi contains the PhreeqC input file for a "mixing + reaction" simulation corresponding to the hydrogeological data for Forsmark at 6,000 AD using the redox-controlling mineral Fe(OH)3(hematite_Grenthe) and the "coupled" database. The label "_T_" in this file name indicates that the file contains only data corresponding to a vertical cut approximately perpendicular to the general coast line, as define in Section 3.2.1.

Extraction of results from PhreeqC output files

A simple software was used to extract data from the verbose output files from PhreeC into tables of data. The computer program scans the output file and writes a line for each mixture. Each line contains the X,Y,Z coordinates as well as desired information such as pH, total and free concentrations, saturation indices, etc.

The data files obtained in this way were named as the output files for PhreeqC, except that the extension was changed from the standard used by PhreeqC Interactive, "pqo", to "res" (for example: F_6000_T_FeOH3Coup.res). The data is separated by commas and column-wise, and therefore it can easily be read by spread sheet programs or graphical software.

3.3 Comparison of model results with present-day groundwaters

3.3.1 Introduction

In this section the outcome of coupling the hydrogeological results with geochemical mixing and mineral reaction modelling for 2,020 AD is compared with present-day groundwater characteristics such as redox potentials, pH, [Ca^{2+}], etc. In addition, some figures present a comparison between calculated reference water fractions provided by the hydrogeological modelling /Hartley et al. 2006ab/ with mixing proportions of end-member waters given in /SKB 2005a, 2006e/ calculated with the M3 code /Laaksoharju et al. 1999a, Gómez et al. 2006a/. The aim of these comparisons is to evaluate the effectiveness of the simulation strategy adopted and to explore the effects of alternative assumptions in the geochemical simulations.

For Forsmark, groundwater data collected before 27-May-2004 are included in the site description model (SDM) version 1.2 /SKB 2005a/, while the SDM version 2.1 includes the rest of samples analysed up to the 25-July-2005 "data freeze". The figures for Forsmark in this section include simulation points from two vertical sections (parallel and perpendicular to the general coast direction as described previously in Section 3.2) down to a depth of ~ 1.1 km.

For Laxemar, groundwater data collected before 22-November-2004 are included in the site description model (SDM) version 1.2 /SKB 2006e/, while the SDM version 2.1 includes the rest of samples analysed up to the 11-July-2005 "data freeze". The figures for Laxemar include simulation points from one vertical section (perpendicular to the general coast direction as described in Section 3.2 above) down to a depth of ~ 1.5 km.

3.3.2 Non-redox elements

As mentioned in Section 3.2.3, two geochemical simulation approaches were tested:

- Only chemical mixing and equilibrium reactions in the aqueous phase, excluding mineral precipitation-dissolution reactions. This alternative is designated as "only mixing" simulations.
- Inclusion of mineral-water reactions. This is the standard simulation procedure in this work, and it is named the "mixing+reaction" alternative when it is compared with the effect of suppressing mineral reactions, i.e. when results are compared with the "only mixing" alternative. Unless otherwise stated, the minerals included are: calcite, chalcedony and Fe(III) oxy-hydroxide (Fe(OH)3(hematite_Grenthe) as defined in Appendix A).

In most calculations the thermodynamic database used is the WATEQ4F.dat file supplied with the PhreeqC code with the few modifications described in Appendix A. In a few cases the "un-coupled" database (with suppressed redox equilibrium for the SO_4^{2-}/HS^- and HCO_3^-/CH_4 redox couples) has been used to test the effects on redox-sensitive elements. Unless otherwise stated all calculations are performed with the "coupled" database, where homogeneous redox equilibrium is allowed between all redox couples present in the groundwaters.

Present-day conditions at Forsmark

Plots of pH and of the concentrations of Na^+, K^+, Ca^{2+}, Mg^{2+}, SO_4^{2-}, and alkalinity (HCO_3^-) against [Cl^-] show overall good agreement between the calculated values and the groundwaters analysed in Forsmark (Figure 3-3 to Figure 3-6). However, the figures show that the modelling strategy gives a poor description of the most diluted samples, which correspond to the upper ~ 100 m of the rock volume. It may also be seen in the figures that the modelled results, which include the site in a large regional scale, show a larger range of concentrations than the groundwaters that have been sampled only in a few boreholes located within the repository candidate volume. A comparison of the "only mixing" and the "mixing+reaction" alternatives shows that the effect of including or excluding mineral equilibrium reactions (calcite, chalcedony, and either crystalline $Fe(OH)_3$ or amorphous FeS) is minimal, see Figure 3-6, indicating that mixing processes are quite important in regulating groundwater compositions for some of the main ions.

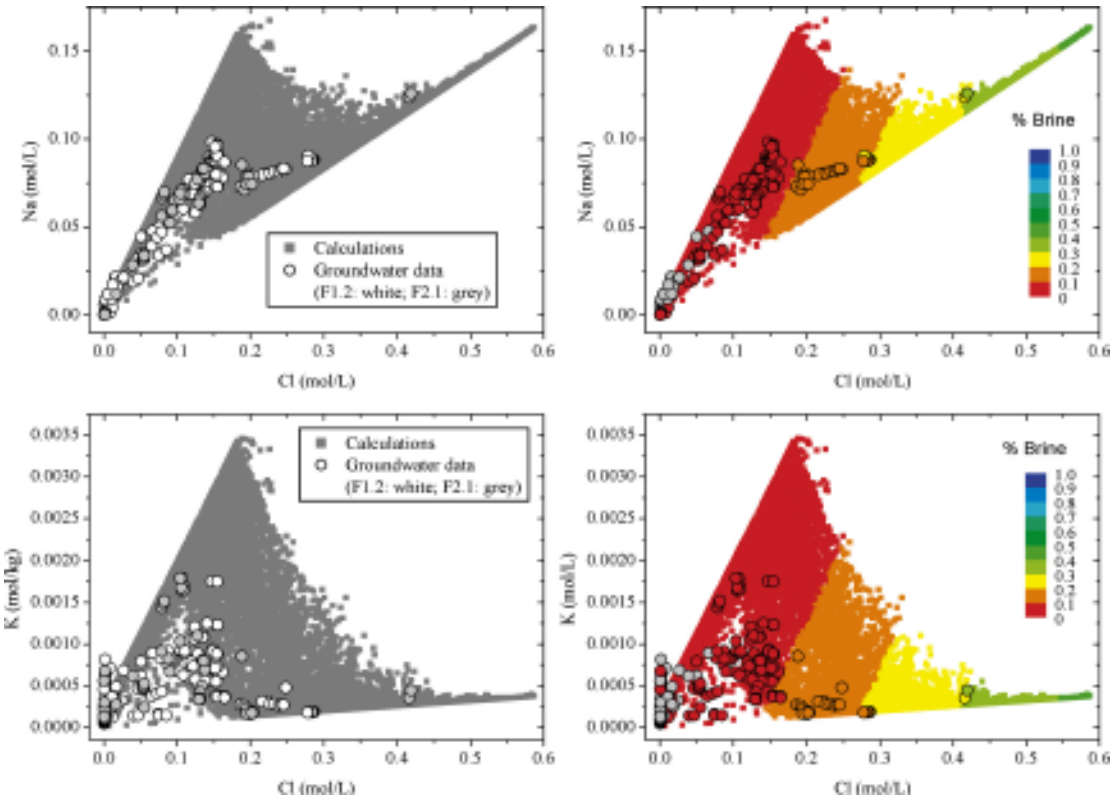

Figure 3-3. *Comparison between simulated and analysed Na and K in Forsmark groundwaters. The plots to the left show the groundwater samples from the 1.2 and 2.1 data freezes. The plots to the right show the calculated percentage of the "brine" component from the 2,020 AD hydrogeological model results /Hartley et al. 2006a/ compared with M3 results for sampled groundwaters (grey coloured samples have no calculated mixing proportions).*

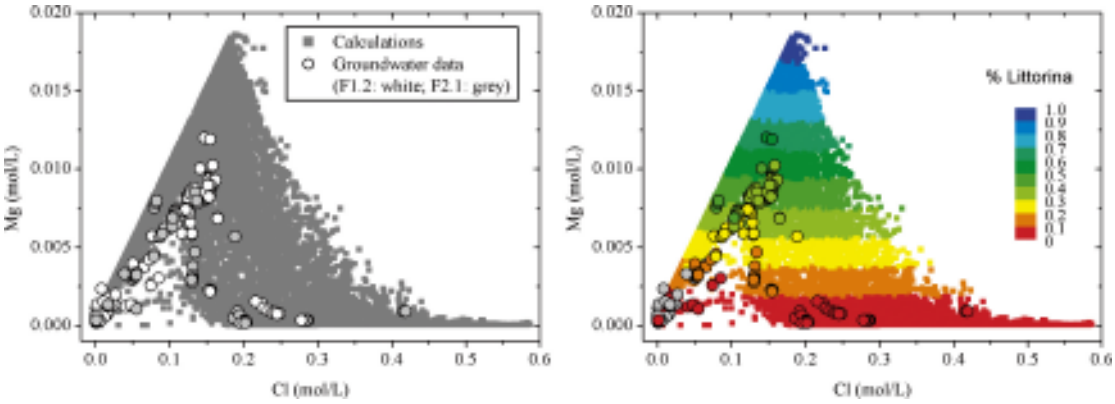

Figure 3-4. *Comparison between simulated and sampled Mg in Forsmark groundwaters. The plot to the left shows the groundwater samples from the 1.2 and 2.1 data freezes. The plots to the right show the calculated percentage of the "Littorina Sea" component from the 2,020 AD hydrogeological model results /Hartley et al. 2006a/ compared with M3 results for sampled groundwaters (grey coloured samples have no calculated mixing proportions).*

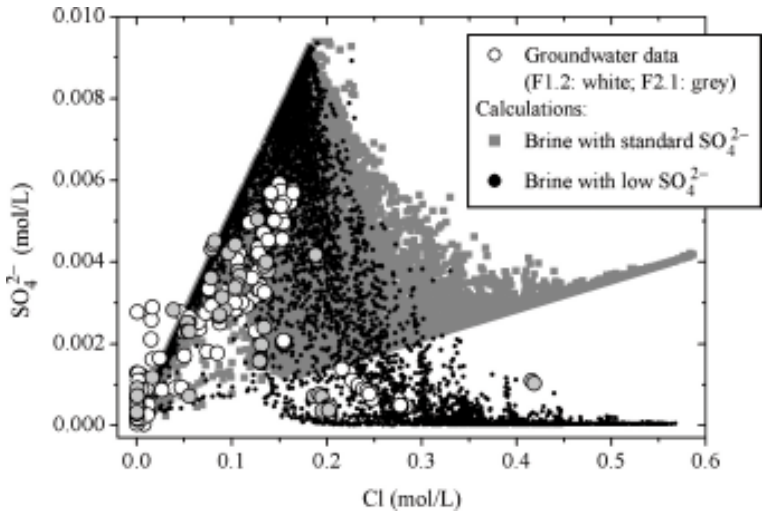

Figure 3-5. *Comparison between simulated and sampled sulphate in Forsmark groundwaters. The plot shows the groundwater samples from the 1.2 and 2.1 data freezes as well as the effect of using either the standard "brine" mixing component defined in Table 3-2 or the same "brine" component but setting* $[SO_4^{2-}] = 10^{-4}$ *M.*

The effect of a different sulphate composition for the Brine component may be seen in Figure 3-5. It is clear from the figure that the Brine component at Forsmark should have lower sulphate content than that at Laxemar. The simulations in this report have used a common Brine mixing component for both sites that is best suited for the Laxemar site, resulting in an over-prediction of the sulphate concentrations at Forsmark. It is to be expected that this question will be resolved in future site description models, and that for future safety assessments a better Brine mixing component will be available for the Forsmark site.

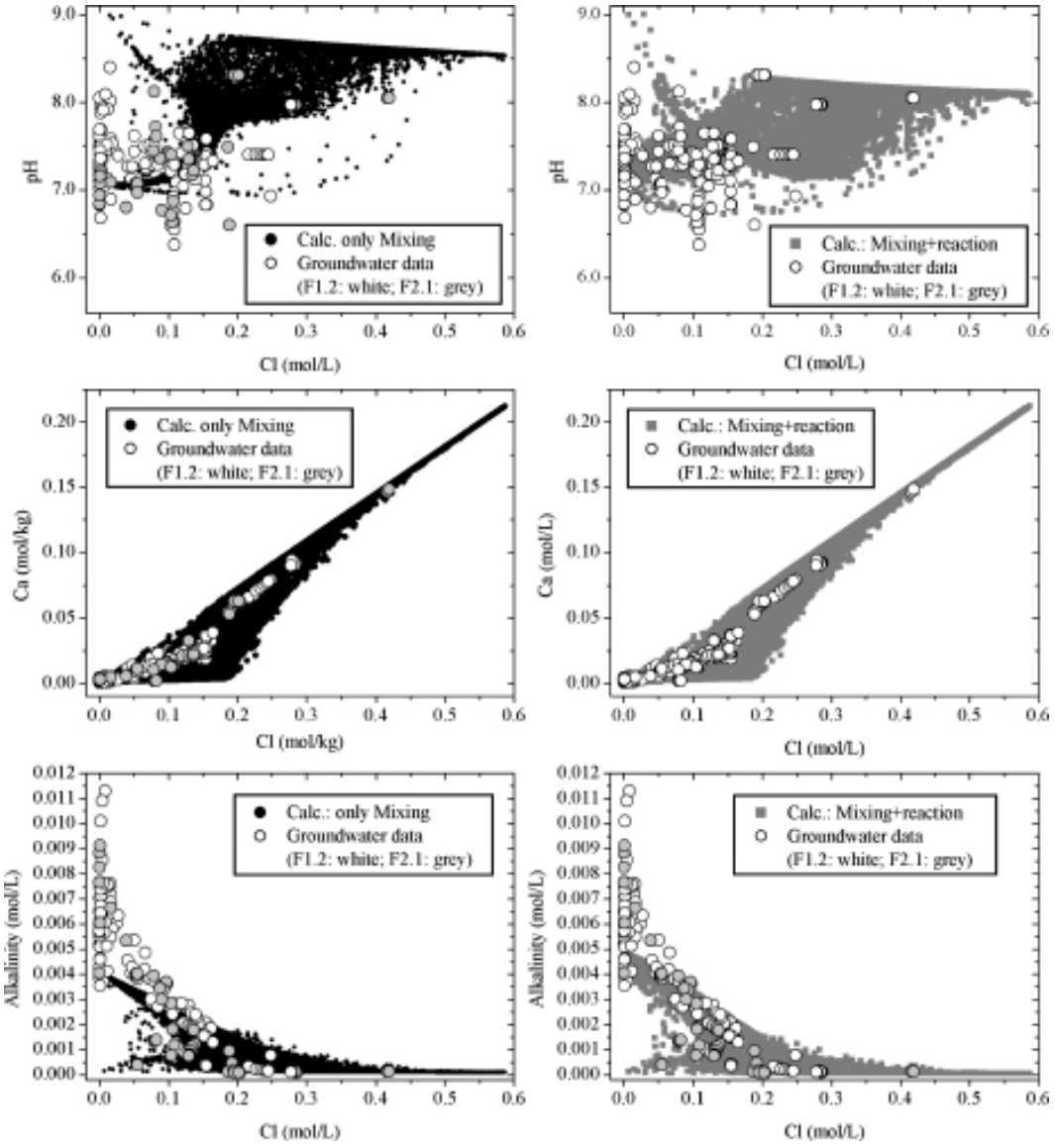

Figure 3-6. *Comparison between simulated and analysed pH, Ca and alkalinity in Forsmark groundwaters. The plots to the left show "mixing" simulations, i.e. where mineral reactions have been excluded. The plots to the right show simulations where both chemical mixing and mineral reactions have been included.*

Present-day conditions at Laxemar

As in the case of Forsmark above, plots of pH and of the concentrations of Na^+, K^+, Ca^{2+}, Mg^{2+}, SO_4^{2-}, and alkalinity (HCO_3^-) against [Cl^-] for Laxemar also show an overall good agreement between the calculated values and the groundwaters analysed in Laxemar, Äspö and Simpevarp, see Figure 3-7 to Figure 3-9, although the simulation results, that correspond to a regional model, show a larger range of concentrations than the sampled groundwaters.

Figure 3-9 also shows that the simulation strategy is not adequate to describe parameters such as pH or alkalinity for the most diluted waters, i.e. for samples close to the ground surface (less than ~ 100 m depth). This deficiency is also observed in the Forsmark simulations, see e.g. Figure 3-6.

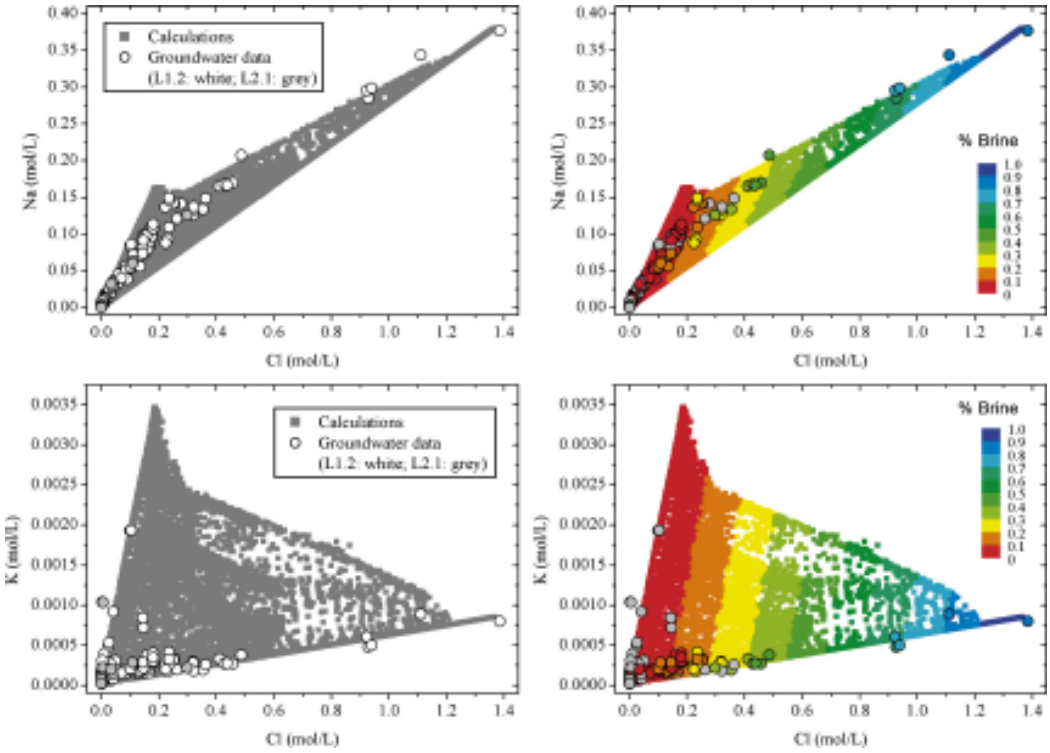

Figure 3-7. *Comparison between simulated and analysed Na and K in Laxemar groundwaters. The plots to the left show the groundwater samples from the 1.2 and 2.1 data freezes. The plots to the right show the calculated percentage of the "brine" component from the 2,020 AD hydrogeological model results /Hartley et al. 2006a/ compared with M3 results for sampled groundwaters (grey coloured samples have no calculated mixing proportions).*

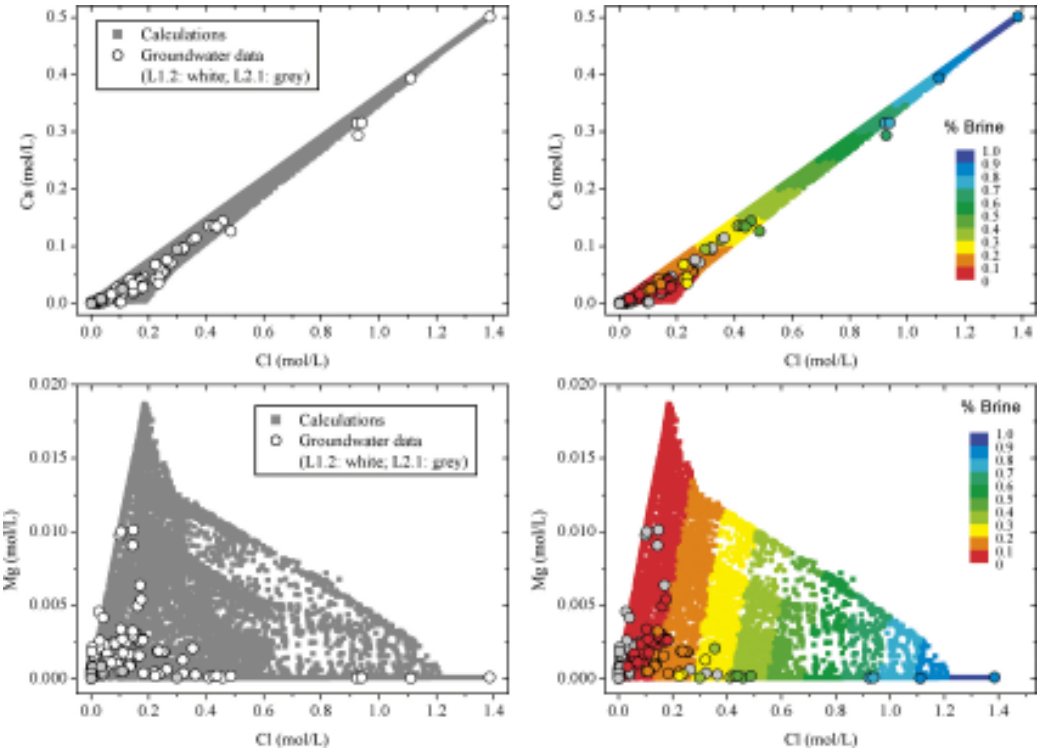

Figure 3-8. *Comparison between simulated and analysed Ca and Mg in Laxemar groundwaters. The plots to the left show the groundwater samples from the 1.2 and 2.1 data freezes. The plots to the right show the calculated percentage of the "brine" component from the 2,020 AD hydrogeological model results /Hartley et al. 2006a/ compared with M3 results for sampled groundwaters (grey coloured samples have no calculated mixing proportions).*

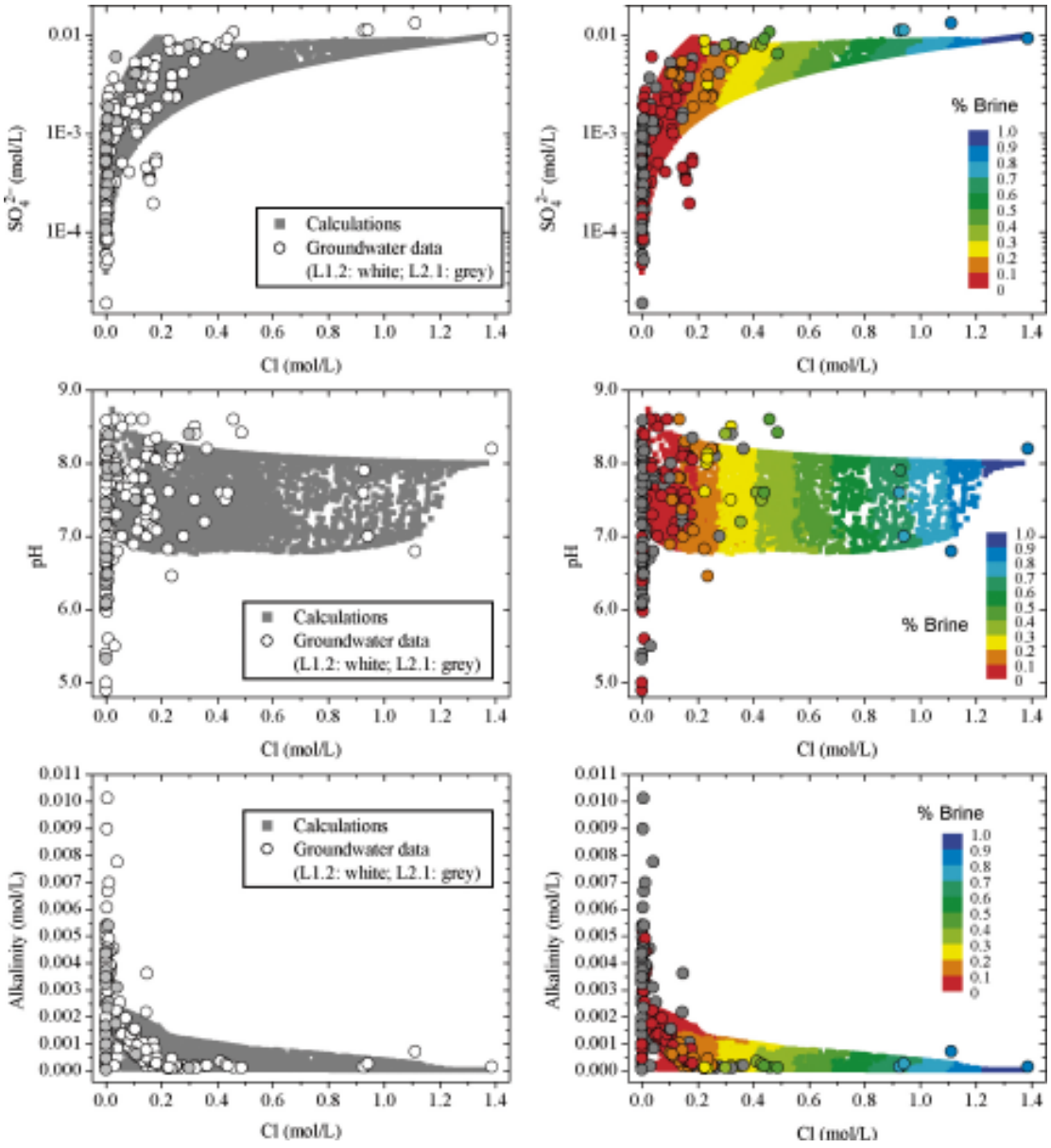

Figure 3-9. *Comparison between simulated and measured sulphate, pH and alkalynity in Laxemar groundwaters. The plots to the left show the groundwater samples from the 1.2 and 2.1 data freezes. The plots to the right show the calculated percentage of the "brine" component from the 2,020 AD hydrogeological model results /Hartley et al. 2006a/ compared with M3 results for sampled groundwaters (grey coloured samples have no calculated mixing proportions).*

3.3.3 Redox elements

Figure 3-10 shows the present-day redox potentials plotted against pH for both Laxemar and Forsmark compared with simulated values. The figure shows the dependence of redox potentials on two factors:

- The redox mineral phase at equilibrium. Two solid phases have been tested here: recently precipitated (amorphous) iron(II) sulphide FeS(ppt), and the iron(III) oxy-hydroxide proposed in /Grenthe et al. 1992/, referred in this document as $Fe(OH)_3$(hematite_Grenthe). The effect is not very pronounced in the SR-Can calculations at pH > 7, because under these conditions the values of Eh are regulated by the SO_4^{2-}/HS^- couple.

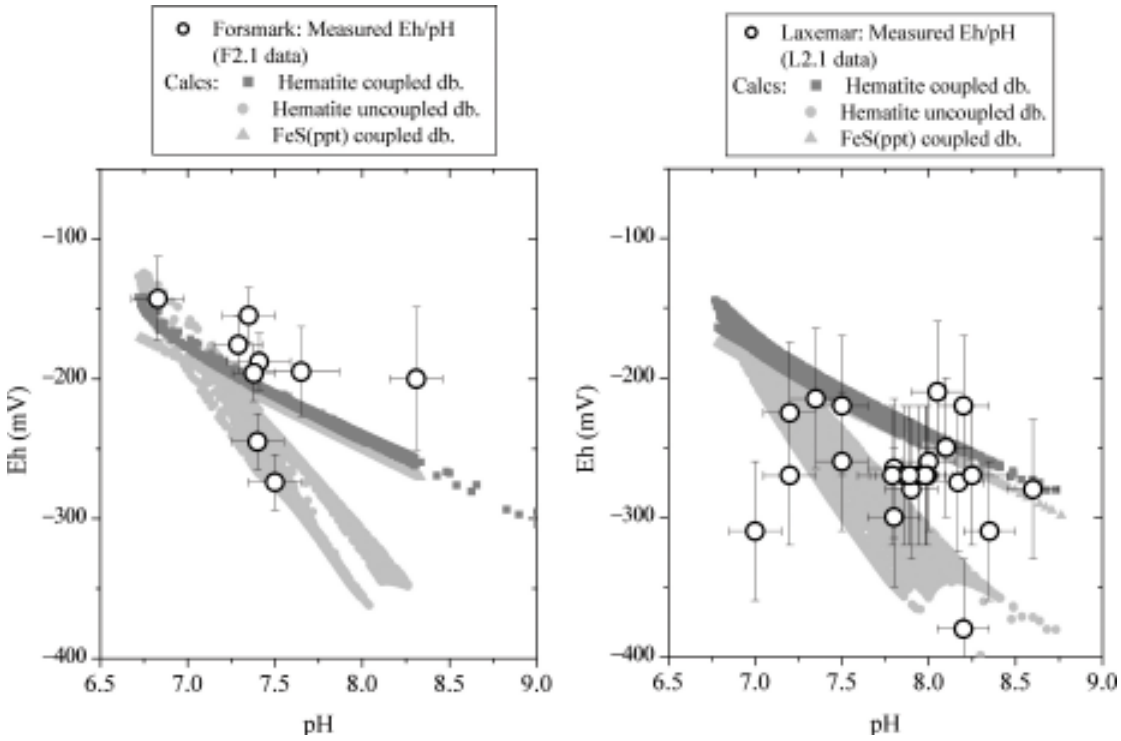

Figure 3-10. *Comparison between simulated and measured redox potentials in Forsmark and Laxemar groundwaters. The plots show the effects of different assumptions in the minerals assumed to be at equilibrium and of using different databases ("un-coupled" or "coupled" that exclude or include, respectively, redox equilibrium between SO_4^{2-} and HS^-).*

- If redox equilibrium between sulphate and sulphide is allowed or not (referred here as "coupled" or "un-coupled" database). Although oxidation of sulphide is a fast process, the reduction of sulphate to sulphide occurs only through the mediation of microbes, which require a reductant such as dissolved H_2, CH_4 or organic matter. It should be noted here that the mixing components used in the simulations (Table 3-2) are slightly different for the "coupled" and "un-coupled" databases.

A comparison between the calculated Eh values and measurements at Forsmark (left plot in Figure 3-10) indicate that overall there is a good agreement between the data obtained so far and the simulations. The limited pH-range of these groundwaters and the spread and the estimated uncertainty in the data (± 50 mV) do not allow to select a model that results in a better agreement with the measurements. For Laxemar (right plot in Figure 3-10) the Eh measurements are spread over a wider pH-range, and they also show a wider range of Eh-values. The Laxemar region is somewhat larger than that of Forsmark, and probably the depth distribution of redox processes is different for inland and coastal parts of the Laxemar site. Tentative mechanisms regulating the redox conditions at the sites are reported in /SKB 2005a, 2006e/ and improvements are expected for new versions of the site descriptive models as more data becomes available.

The plots of Eh against pH (Figure 3-10) indicate that overall the highest calculated values of Eh are obtained assuming equilibrium with either $Fe(OH)_3$(hematite_Grenthe) or FeS(ppt) and using the "coupled" database that includes redox equilibrium between sulphate and sulphide. Furthermore, when the redox potential is controlled by $Fe(OH)_3/Fe^{2+}$ couple, the calculated Eh values are lower, in particular at pH > 7.5, for the "un-coupled" database.

Because of higher Eh values are expected to be less favourable from the point of view of the performance of a radioactive waste repository, the calculations assuming equilibrium between groundwaters and $Fe(OH)_3$(Grenthe) and the "coupled" database are adopted as the reference method for the calculation of Eh potentials at the sites.

The results for other redox-sensitive groundwater components, total dissolved iron and sulphide, are illustrated in Figure 3-11. As in the case of the redox potential, the analysed groundwaters also show a large spread of Fe(II) and HS^- values. This large variation probably reflects the effects of several processes on components that have low concentrations: small changes have a large impact on the final concentration. Microbial processes in particular are expected to greatly influence the concentrations of iron(II) and sulphide.

The reference Eh calculation method (equilibrium with $Fe(OH)_3$(Grenthe)) gives quite low values of Fe(II), which is not supported by the present-day groundwater data, especially at the higher pH values, Figure 3-11. Nevertheless, the reference method selected is conservative in giving the highest Eh values and the lowest reducing capacity, i.e. lowest Fe(II) content.

It may be noted that the results assuming equilibrium with FeS(ppt) give in general higher $[HS]_{TOT}$ values than those analysed in the present-day groundwaters at the sites. Equilibrium with Fe(III) oxy-hydroxides results in a larger span of calculated concentrations for sulphide (Figure 3-11). Nevertheless, the assumption of equilibrium with FeS(ppt) gives results that agree better with the groundwater subset with the highest sulphide concentrations in Laxemar, in agreement with the observed activity of sulphate reducing bacteria (SRB) in some parts of

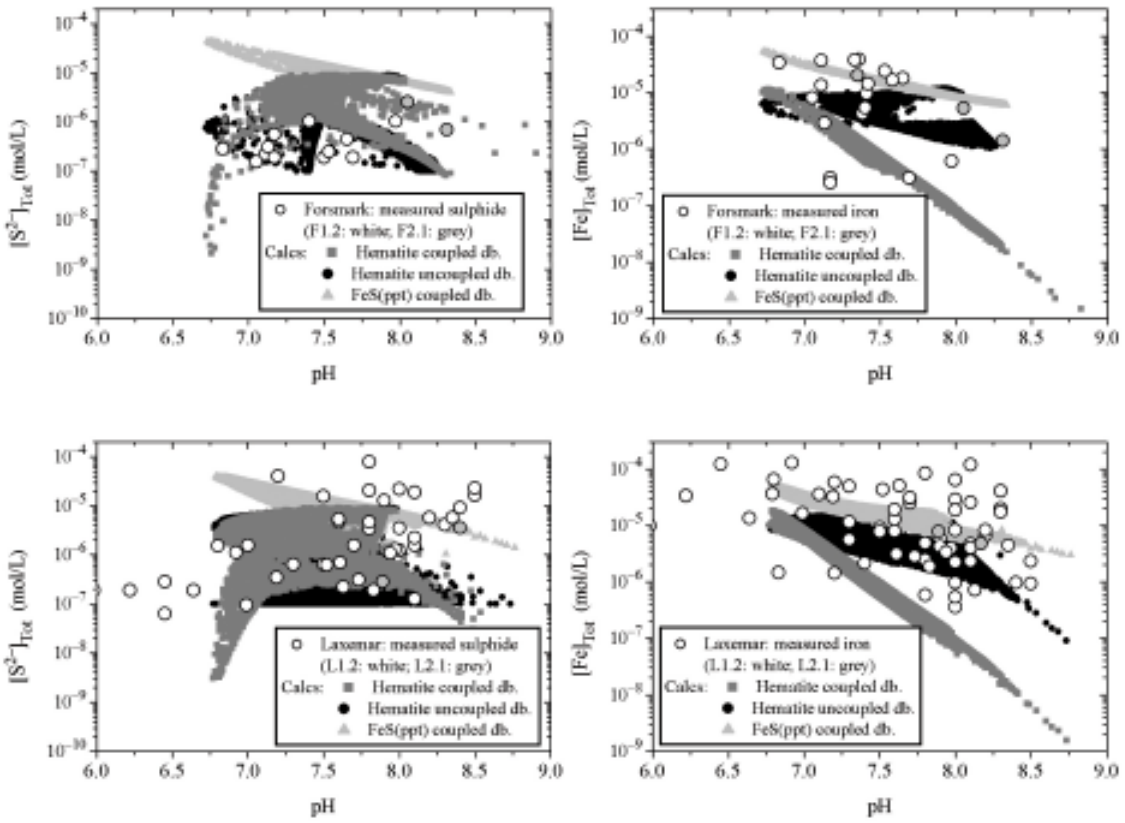

Figure 3-11. *Comparison between simulated and measured concentrations for sulphide (left) and iron (right) at Forsmark (upper plots) and Laxemar (lower plots). The plots show the effects of different assumptions in the minerals assumed to be at equilibrium and of using different databases ("un-coupled" or "coupled" that exclude or include, respectively, redox equilibrium between SO_4^{2-} and HS^-). The mixing components defined in Table 3-2 have been used.*

this site /SKB 2006e/. The SRB activity so far detected in Forsmark groundwaters is lower than in Laxemar /SKB 2005a/. It is not clear at present which factors control the intensity of SRB activity in these systems. Bacterial sulphide production would induce the precipitation of Fe(II) sulphide, which justifies including the assumption of equilibrium with FeS(ppt) among the redox models in SR-Can (see also the discussion below on sulphide in next section).

3.4 Simulation results for the entire temperate period

3.4.1 Introduction

One of the questions to be addressed for this period in SR-Can is whether the chemical environment will remain favourable after repository closure. The most important parameters are the redox properties and salinity. Other factors to consider are the effect of grouting and cement materials that could affect groundwater pH, as well as the groundwater content of K, HS^- and Fe(II), because these components might affect the chemical stability of the buffer and the canister.

3.4.2 Evolution of salinity

As mentioned previously in Section 2.3 the salinity distribution may initially be affected during repository operation by perturbations in the hydraulic conditions, although in the case of Forsmark this perturbation is negligible, and the data for Laxemar is too preliminary to allow definitive conclusions.

During the initial temperate period after repository closure, groundwaters will be affected by increasing amounts of waters of meteoric origin, see Figure 3-1. On a regional scale this corresponds to a gradual decrease of the groundwater salinity, especially in the upper part of the modelled rock volume, which is 2 km deep overall. The salinity distribution for this time period has been calculated using the ConnectFlow model /Hartley et al. 2006ab/. Figure 3-12 presents the calculated distribution of salinities at Forsmark and Laxemar at repository depths for three time steps. Towards the end of the modelled period over 70% of the groundwaters at the sites have less than 1 g/L of dissolved salts at repository depth, while a lesser proportions of the groundwaters had low salinities at the start of the simulation, that is, at repository closure.

In conclusion, the salinities during the first temperate period following repository closure will remain limited both at Forsmark and Laxemar, ensuring that the swelling properties of the buffer and backfill are not negatively affected.

3.4.3 Other natural groundwater components

The increasing proportions of groundwaters of meteoric origin will decrease the overall salt content of the groundwaters as discussed in the previous subsection. However, the effects on the individual chemical constituents will depend on their reactivity. The evolution of the different chemical properties of groundwaters has been estimated by coupling the results from the hydrological calculations with a mixing and chemical reaction model, as described above. The final objective has been to check if, during its evolution, the chemical environment around the repository fulfils at all times the safety function indicator criteria specified in Section 1.2. In this subsection, the results are discussed for divalent cations, potassium, sulphide and iron, as well as alkalinity and pH. The results for salinity are discussed in the previous subsection, whereas the results for redox conditions are presented below in the following subsection.

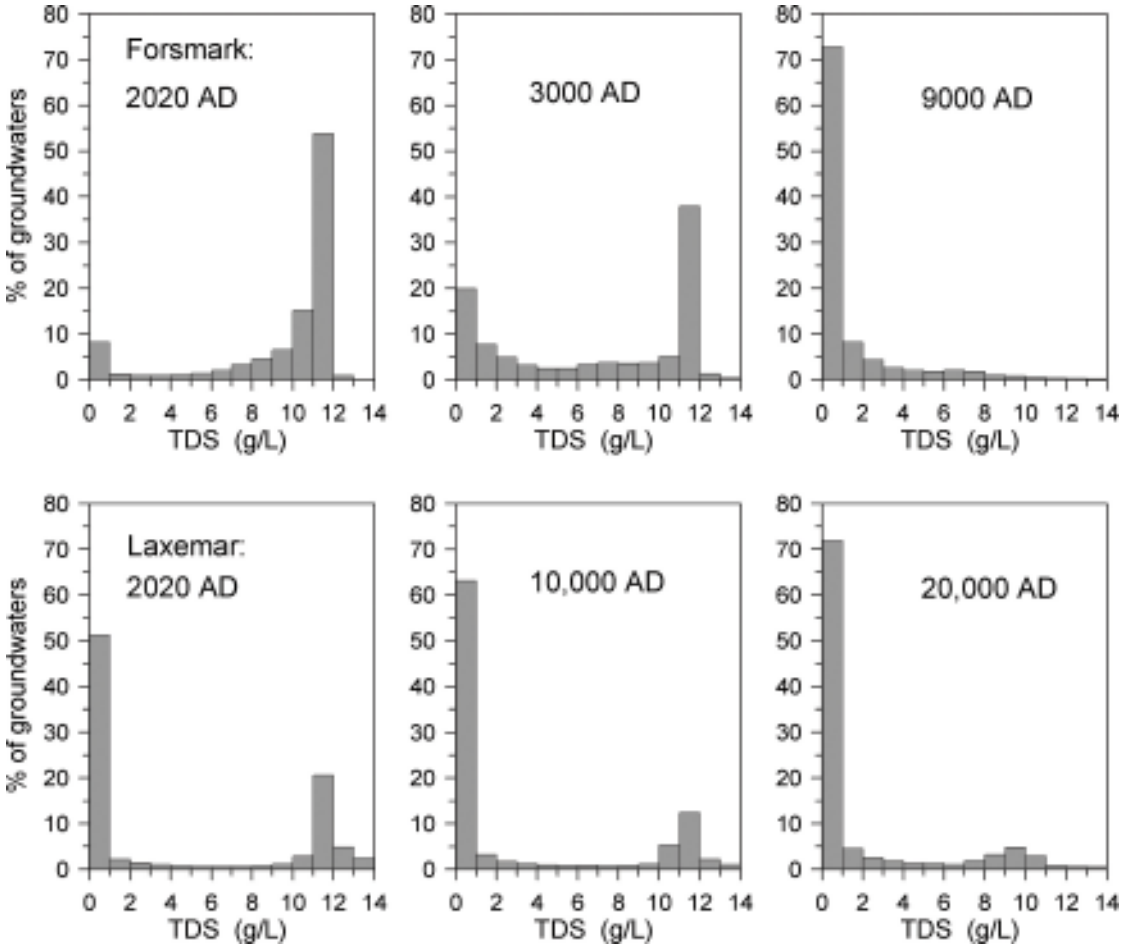

Figure 3-12. *Histograms showing the evolution of TDS (total dissolved solids) as a function of time. Upper diagram: evaluation for Forsmark at 400 m depth at times equal to (from left to right) 2,020 AD, 3,000 AD and 9,000 AD. Lower diagram: data for Laxemar at 500 m depth at times equal (from left to right) 2,020 AD, 10,000 AD and 20,000 AD. Diagrams calculated using the regional model results in /Hartley et al. 2006a, Hartley et al. 2006b/. The figure shows the effect at repository depth of the gradual inflow of rain water.*

Calcium

The concentration of divalent cations is important in that their presence decreases the stability of colloids (see the discussion on colloids later in this section). In groundwaters that are too dilute, colloids might enhance the transport of radionuclides. In addition, as the buffer swells into fractures, montmorillonite colloids may be transported away by dilute groundwaters. The criterion for the safety function indicator is $\sum [M^{2+}] \geq 0.001$ mol/L, as available experimental data suggests that montmorillonite colloids are not stable at concentrations above this limit.

Calcium participates in water-rock interactions (carbonates) and may be released from the weathering of feldspar. At Forsmark and Laxemar the deep saline groundwaters are quite rich in calcium, see Figure 3-13, and examination of the groundwaters at depths larger than ≈ 100 m shows that the calcium concentrations may be simulated by mixing of component waters and that the relative effects of chemical reactions are minor, Figure 3-6. The other major divalent cation is magnesium, which is normally regulated in granitic groundwaters by the precipitation and dissolution of chlorite, a mineral that may have a wide range of compositions. In general, magnesium concentrations in groundwaters are much lower than those of calcium, and because of the low solubility of chlorites and the uncertainty in the composition of this mineral, the modelling of Mg concentrations is much more uncertain than that of Ca. Magnesium ions, that have the same positive effect on safety as Ca ions are, therefore, pessimistically, disregarded in the SR-Can evaluation of the divalent cation component of groundwater composition.

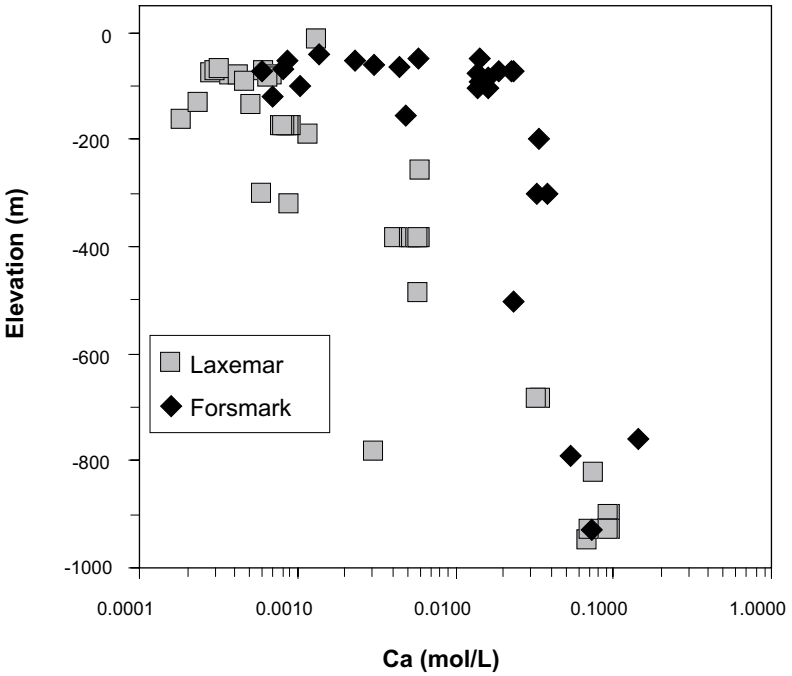

Figure 3-13. *Calcium concentrations in groundwaters sampled in Forsmark and Laxemar as a function of depth.*

The calcium concentrations observed at present at Forsmark increase rapidly with depth in the top ≈ 100 m of the bedrock, see Figure 3-13. For Laxemar, the increase of Ca with depth is gradual, and most of the samples at depths ≤ 200 m have Ca concentrations close to or below 0.001 mol/L. The selected meteoric water (superficial granitic groundwater) for Forsmark in the mixing and reaction calculations (Table 3-2) corresponds to groundwaters sampled at ~ 50 m depth, which have the composition expected for a rain water that has travelled a short distance in the fractures of the granite at the sites. In Figure 3-1 above, these superficial groundwaters correspond to the top few hundred metres in the south-west part of the modelled domain, and the hydrological calculations for 2,020 AD show that they are entirely "rain" water.

The results of coupling the hydrological model results with the mixing and reaction calculations, including equilibrium with calcite, are shown in Figure 3-14 and Figure 3-15, which illustrate the gradual dilution with time of the groundwaters due to the inflow of superficial waters of meteoric origin. Figure 3-16 shows the spreading of concentrations at repository depth, and Figure 3-17 shows a histogram of Ca concentrations for the two sites at the end of the simulations (9,000 and 20,000 AD for Forsmark and Laxemar, respectively), also at repository depth, when most of the groundwaters that were present at repository closure have been replaced by waters of meteoric origin. It should be noted that the Ca concentrations in groundwaters found at present in the upper 150 m vary approximately between 0.2 and 25 mM, according to the data shown in Figure 3-13. This spread of the data is not included in the meteoric component used in the mixing calculations, and, therefore, the variability shown in Figure 3-16 and Figure 3-17 is underestimated.

It may be concluded from these modelling results that for the whole temperate period following repository closure Ca concentrations at repository depth at Forsmark and Laxemar will decrease with time and they will reach values that, in general, will remain close to 0.001 mol/L, that is, near to the limit where montmorillonite colloids start to become unstable. It must be noted that two factors have not been considered here which will contribute to increase $[M^{2+}]$ in groundwaters of meteoric origin, namely, ion-exchange processes and magnesium ions.

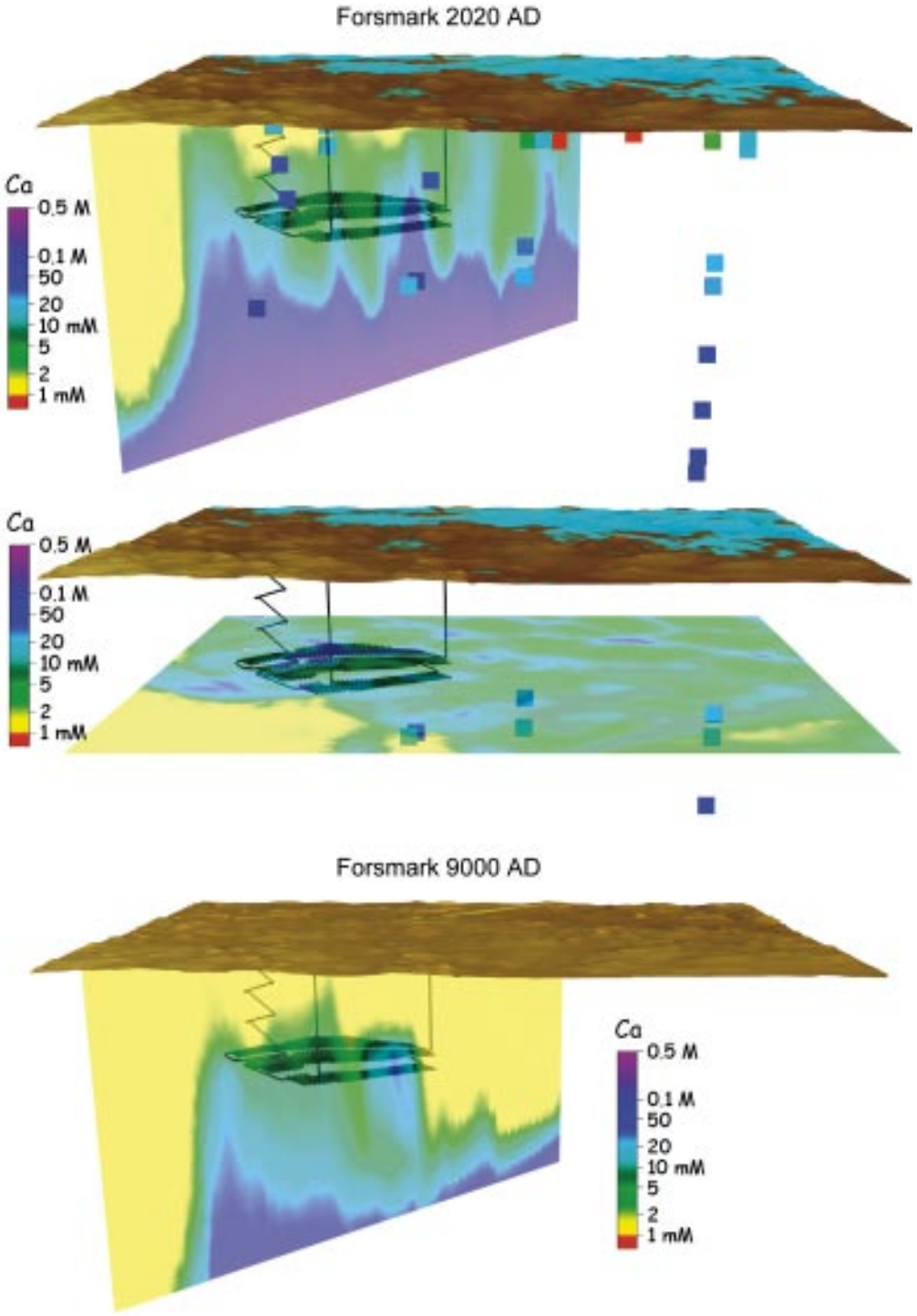

Figure 3-14. *Calculated Ca concentrations at the Forsmark site. Top: present-day groundwaters and a calculated vertical cut approximately perpendicular to general coast direction (upper picture) and horizontal cut at 400 m depth (lower picture). The top surface shows land and Baltic Sea areas. The repository layout is also shown. The vertical scale is exaggerated three times. Bottom: expected evolution of the groundwaters at the end of the temperate period, i.e. at year 9,000 AD. The coast has moved away from the site due to isostatic uplift and groundwaters become diluted due to the increased infiltration of meteoric waters.*

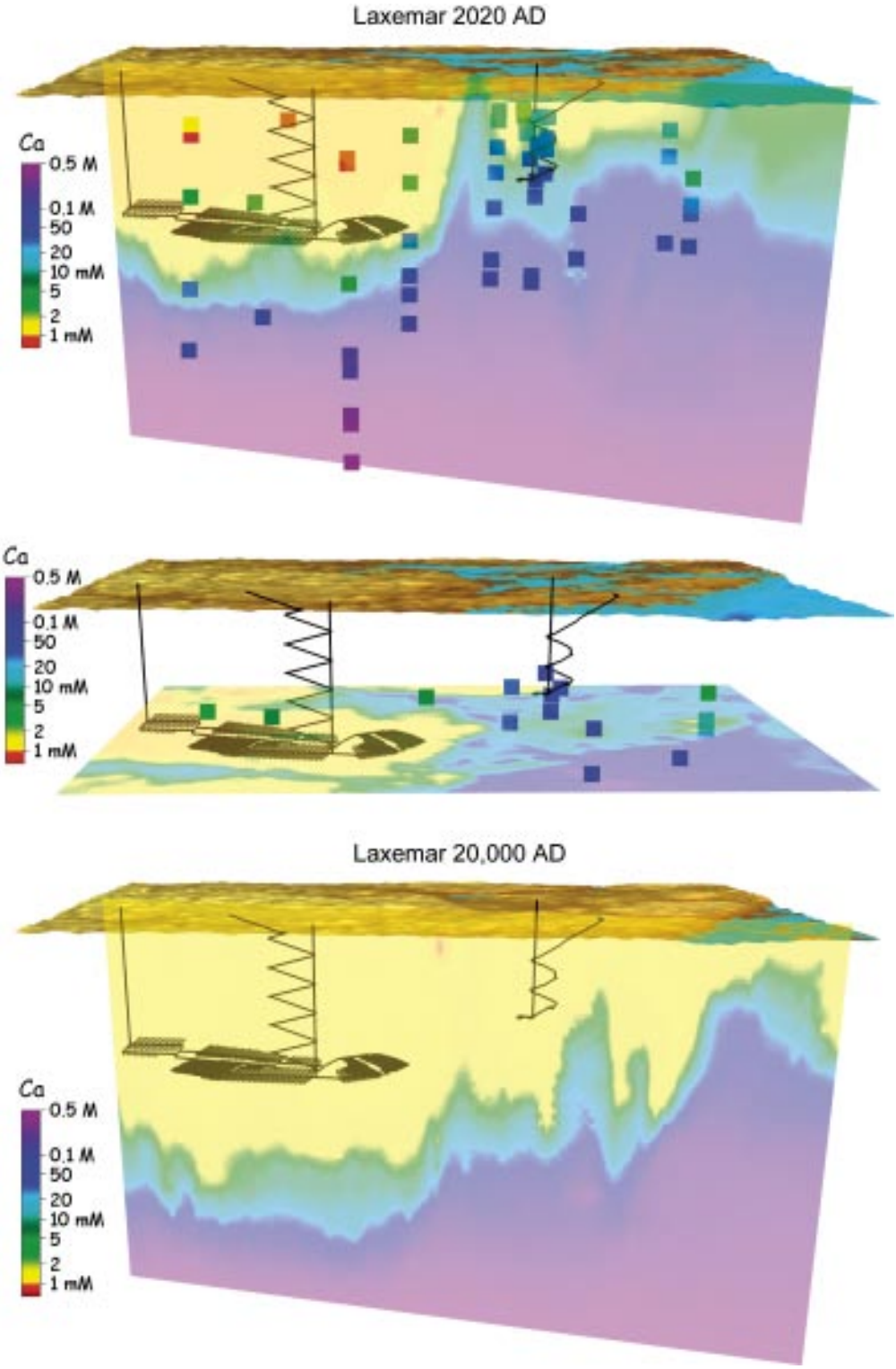

Figure 3-15. *Calculated Ca concentrations at the Laxemar site. Top: present-day groundwaters and a calculated vertical cut approximately perpendicular to general coast direction (upper picture) and horizontal cut at 500 m depth (lower picture). The top surface shows land and Baltic Sea areas. The repository layout and the Äspö Hard Rock Laboratory are also shown. The vertical scale is exaggerated three times. Bottom: expected evolution of the groundwaters at the end of the temperate period, i.e. at year 20,000 AD. The coast has moved away from the site due to isostatic uplift and groundwaters become diluted due to the increased infiltration of meteoric waters.*

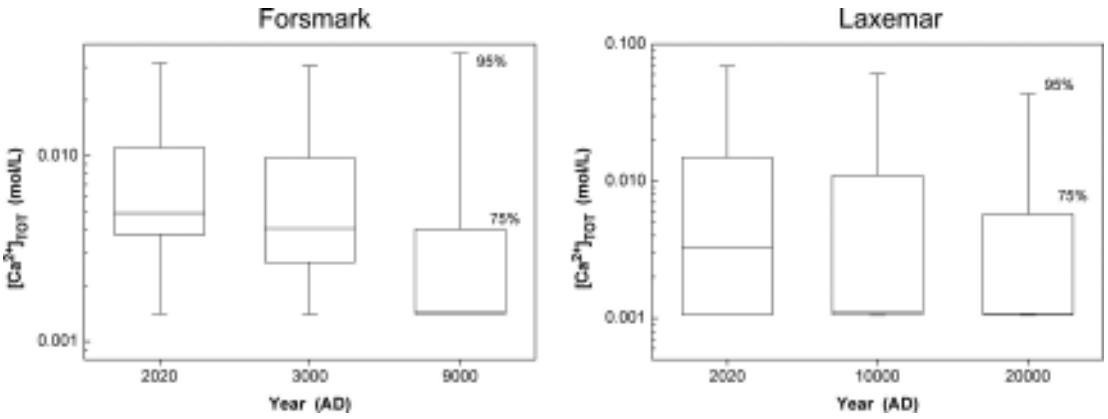

Figure 3-16. *Box-and-whisker plots showing the distribution of Ca concentrations at Forsmark and Laxemar at repository depth (400 and 500 m, respectively) as a function of time. The statistical measures are the median, the 25th and 75th percentile (box) and the 5th and 95th percentile ("whiskers").*

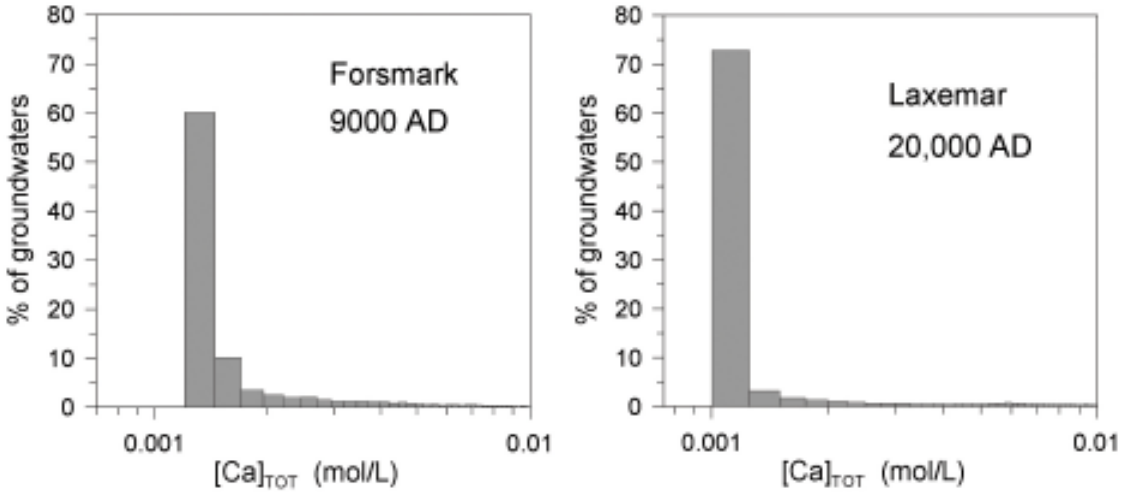

Figure 3-17. *Histogram showing the calculated distribution of Ca concentrations. Left: Forsmark at 400 m depth at 9,000 AD; right: Laxemar at 500 m depth at 20,000 AD.*

The sharp cut-off in Figure 3-17 is a consequence of excluding the uncertainty, shown in Figure 3-13, in the composition of meteoric water, and therefore it cannot be excluded that some of the groundwaters during the temperate period will have concentrations slightly lower than 0.001 mol/L and if so these waters would infringe the safety function indicator requiring $\sum [M^{2+}] \geq 0.001$ mol/L and they would increase the stability of bentonite colloids. It has not been possible to fully address this uncertainty within the SR-Can project. Uncertainty propagation analysis or a different process modelling strategy will be needed in future evaluations of groundwaters for performance assessments in Sweden.

A key point when assigning the composition of the superficial granitic groundwater of meteoric origin in the simulations is that these waters are slightly under-saturated with respect to calcite as indicated in Table 3-2. When these waters move further down into the rock domain the simulations presented here assume equilibrium with calcite, $CaCO_3$, and the Ca contents in the resulting groundwater increases slightly as compared with the initial meteoric mixing component. Calcite is a mineral often present in the fractures sampled in cored boreholes, Table 4-1, and it reacts relatively fast with groundwaters, which are therefore close to calcite saturation at depths below some tens of metres, as discussed in Appendix C. However, as shown below (Figure 3-21 and corresponding text) the total amounts of calcite dissolved are very small.

pH and bicarbonate

For pH and bicarbonate, the mixing and reaction calculations are dominated by the precipitation and dissolution of calcite. The results are summarised in Figure 3-18 and Figure 3-19. The models for both sites show that the pH values remain approximately in the range 7 to 8.7, and that bicarbonate values increase slightly with time, up to about 0.004 mol/L in Forsmark, see Figure 3-20. Although not shown in the figures, the calculated partial pressures of dissolved carbon dioxide increase with time, as it is assumed in the modelling that the infiltrating meteoric waters have a higher CO_2 content than the other waters in the system.

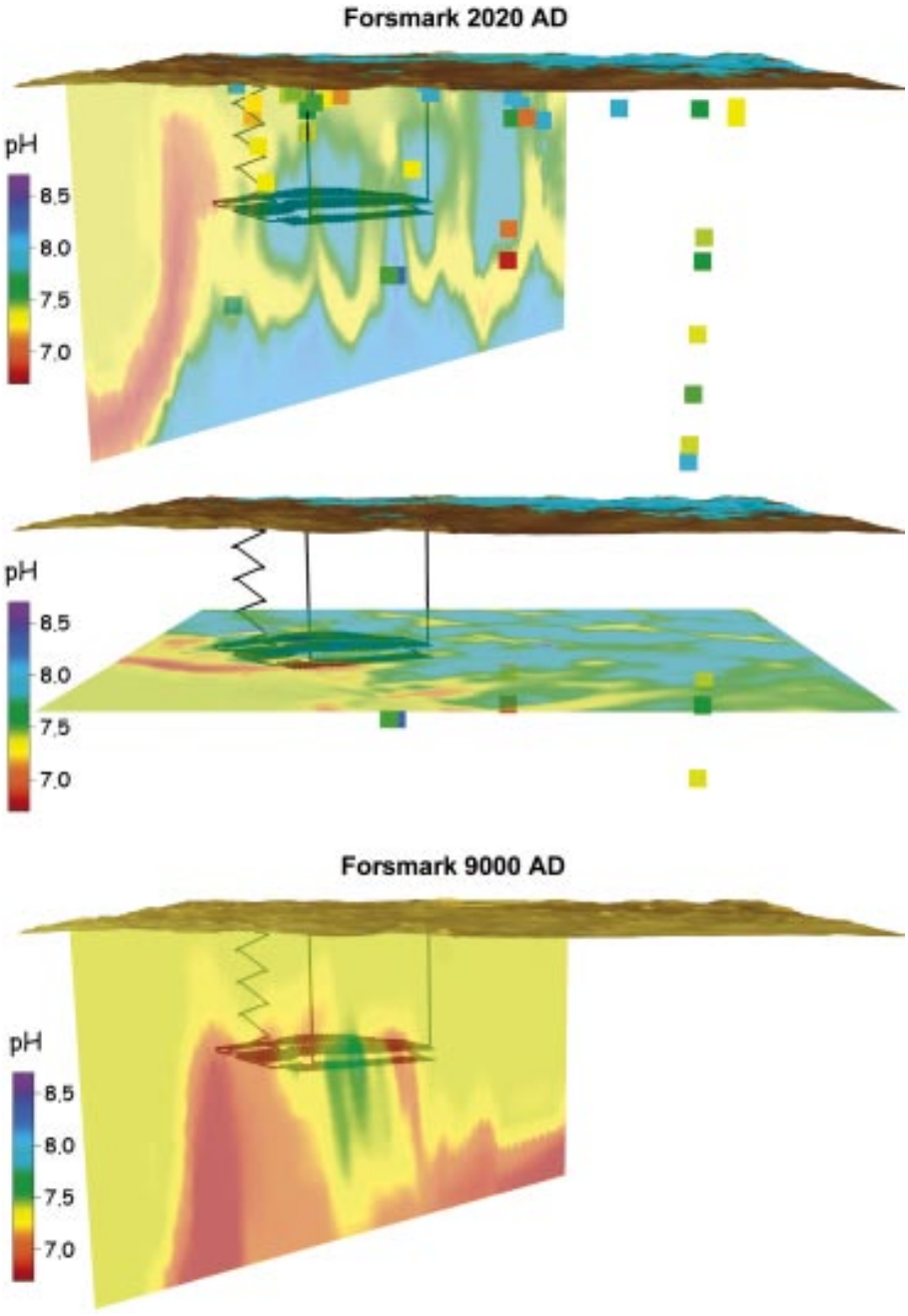

Figure 3-18. *Calculated pH values at the Forsmark site. Top: present-day groundwater pH values and a calculated vertical cut approximately perpendicular to general coast direction (upper picture) and a horizontal cut at 400 m depth (lower picture). The top surface shows land areas and the Baltic Sea. The repository layout is also shown. The vertical scale is exaggerated three times. Bottom: expected evolution of groundwater pH values at the end of the temperate period, i.e. at year 9,000 AD. The coast has moved away from the site due to isostatic uplift and overall groundwaters have higher pH values due to the increased infiltration of meteoric waters with pH ≈ 7.1.*

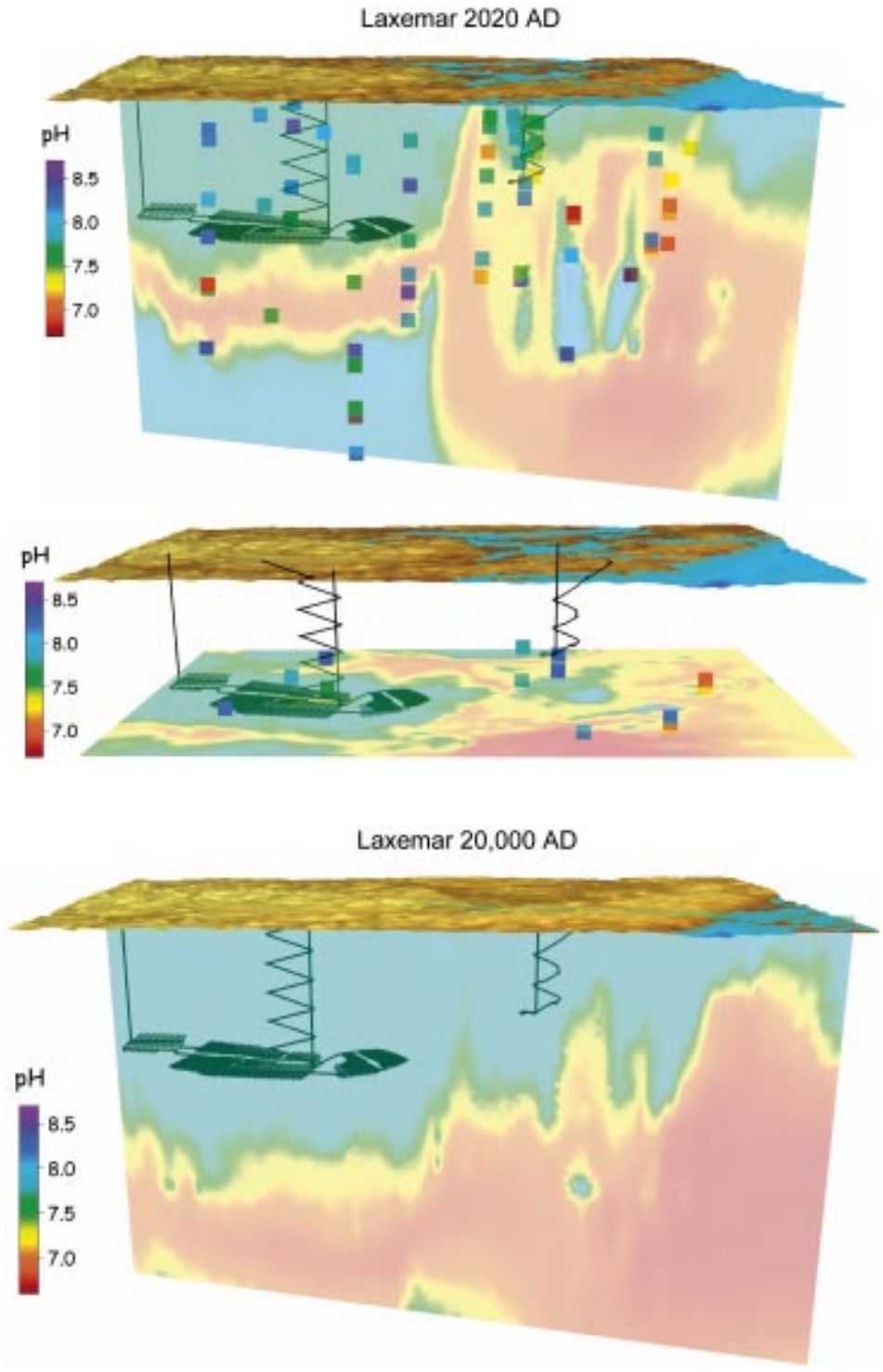

Figure 3-19. *Calculated pH values at the Laxemar site. Top: present-day groundwater pH values and a calculated vertical cut approximately perpendicular to general coast direction (upper picture) and a horizontal cut at 500 m depth (lower picture). The top surface shows land areas and the Baltic Sea. The repository layout and the Äspö Hard Rock Laboratory are also shown. The vertical scale is exaggerated three times. Bottom: expected evolution of groundwater pH values at the end of the temperate period, i.e. at year 20,000 AD. The coast has moved further away from the site due to isostatic uplift and the picture shows the influence of an increased infiltration of meteoric waters with pH ≈ 7.4.*

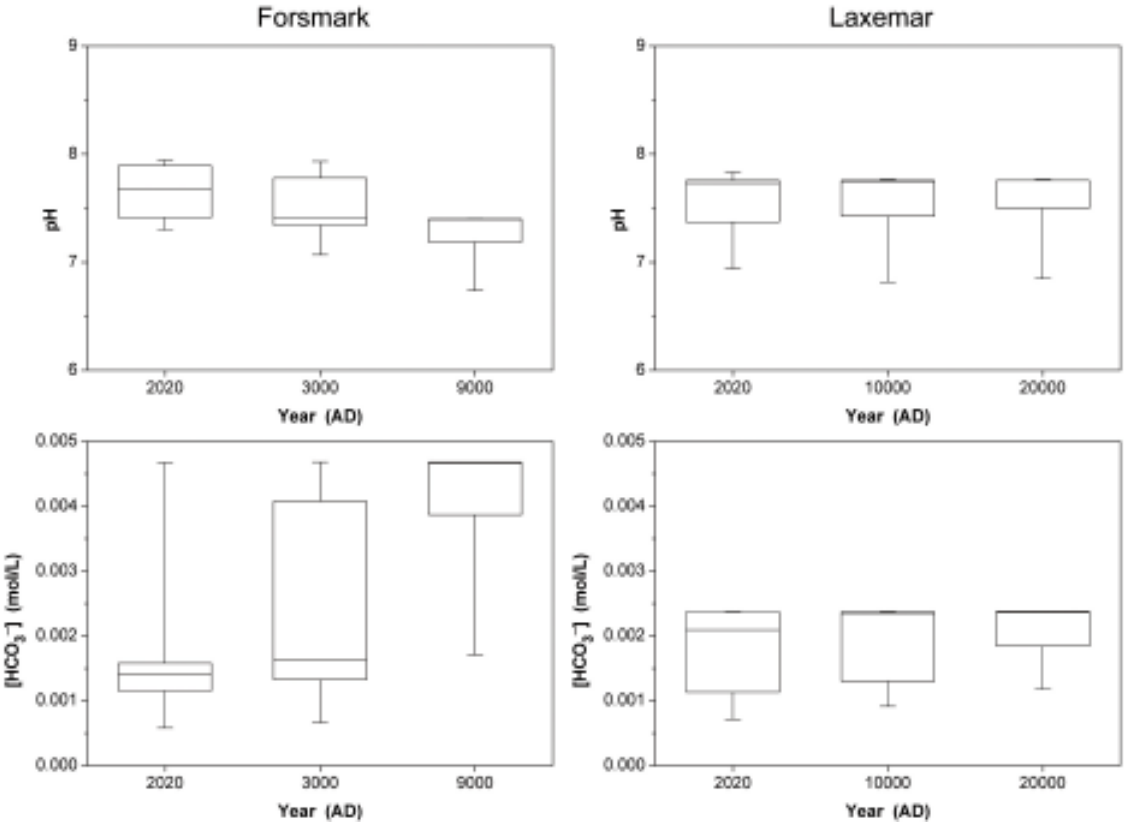

Figure 3-20. *Box-and-whisker plots showing the distribution of pH values (top) and of "free" bicarbonate concentrations (bottom) at Forsmark and Laxemar at repository depth as a function of time. The statistical measures are the median, the 25th and 75th percentile (box) and the 5th and 95th percentile ("whiskers").*

Figure 3-18 and Figure 3-19 show areas with lower pH values in the vertical cuts which move to greater depths with time. In the upper parts of the modelled domain meteoric waters infiltrate which are relatively acid (pH < 7.4) and have high bicarbonate and CO_2 content. These meteoric waters are slightly under-saturated with calcite and this mineral will therefore dissolve, as it is present in fracture infills (see Table 4-1 and Appendix C). Therefore pH is increased according to: $CaCO_3(cr) + H^+ \rightleftharpoons Ca^{2+} + HCO_3^-$. Deeper down, the waters have already reached equilibrium with calcite, but they are still somewhat rich in HCO_3^-, and calcite over-saturation occurs when they mix with deeper Ca^{2+}-rich waters. In this rock volume the pH is decreased according to: $Ca^{2+} + HCO_3^- \rightleftharpoons CaCO_3(cr) + H^+$. Groundwaters at larger depths have a higher pH ≈ 8 corresponding to that of the "brine" component in Table 3-2. The calculated amounts of dissolved and precipitated calcite for present-day conditions at Laxemar are shown in Figure 3-21. By comparing it with Figure 3-19 it may be seen that lower pH volumes coincide with those of calcite precipitation. The calculated amounts of calcite mass transfer are quite small, in absolute value less than 2×10^{-4} mol per litre of groundwater. Assuming an "ideal" fracture with an aperture of at most 1 mm and with 10% of the rock surface covered by calcite, this mass transfer corresponds to a change of less than 0.04 µm in the calcite thickness.

Because of the correlation between calculated redox potentials and pH, see Figure 3-10, the areas with lower pH, which are a consequence of calcite precipitation, correspond to areas with *higher* calculated Eh. This is further illustrated in the figures of Section 3.4.4.

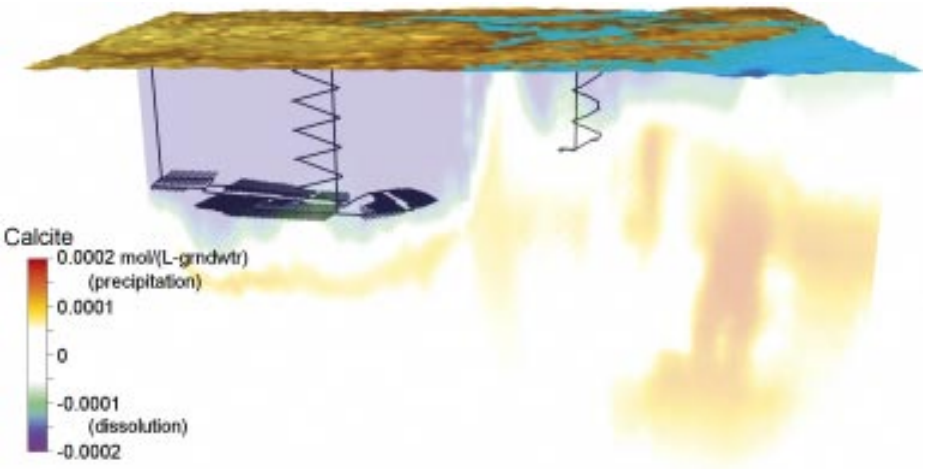

Figure 3-21. *Calculated mass transfer for calcite ($CaCO_3$) at the Laxemar site for present-day conditions shown for a vertical cut approximately perpendicular to general coast direction. The top surface shows land areas and the Baltic Sea. The repository layout and the Äspö Hard Rock Laboratory are also shown. The vertical scale is exaggerated three times. The model indicates dissolution of calcite in rock volumes with groundwater predominantly of meteoric origin, and precipitation of calcite in volumes where bicarbonate-rich groundwaters mix with Ca-rich deep groundwaters.*

Potassium, sulphide and iron

Potassium concentrations are generally low in the groundwaters sampled at both sites, as observed also in other Fennoscandian sites in granitic rocks, see for example Table 2-1. Solubility control by sericite has been proposed as a mechanism controlling the maximum concentrations of potassium /Nordstrom et al. 1989/, but ion-exchange processes can not be ruled out. Even if the exact mechanism is not known all available groundwater data indicate that the increased infiltration of waters of meteoric origin will not increase the potassium concentrations found at present. The reaction modelling performed within SR-Can is not well suited to constrain potassium concentrations because, as mentioned, there is not enough information available on the possible reactions that could control this element. The mixing calculations give maximum values of $[K^+]$ below 0.004 mol/L at any time for both Laxemar and Forsmark, that is, the potassium concentration of the Littorina Sea mixing component.

Sulphide concentrations have not been extensively modelled in the site characterisation models, mainly because the data are scarce: sulphide concentrations are usually below the detection limit. Under oxidizing conditions, for example in superficial waters, sulphide is quickly oxidized to sulphate. Under reducing conditions, dissolved Fe(II) is normally present and the maximum sulphide concentrations are regulated by the precipitation of Fe(II) sulphide according to:

$$HS^- + Fe^{2+} \rightleftharpoons FeS(s) + H^+$$

with $\log_{10}K = \log_{10}\left([H^+] \left([Fe^{2+}] [HS^-] \right) \right) \approx 3$; see the discussion in Appendix A.
At pH = 7 to 8 this expression gives: $\log_{10}([Fe^{2+}][HS^-]) \approx -10$ to -11. In most groundwaters $\log_{10}[Fe^{2+}] \geq -6$ (see Table 2-1) which sets the maximum $\log_{10}[HS^-]$ in the range -4 to -5.

This is confirmed by the data from groundwater analyses from the sites, see Figure 3-22. The maximum value for Forsmark is $\log_{10}[HS^-] = -5.1$ (0.26 mg/L) from KFM07A at 780 metres depth. For Laxemar the highest value is $\log_{10}[HS^-] = -4.1$ (2.5 mg/L) in an older sample from KLX01 at 670 metres depth. These are, however, exceptions and, for many of the groundwaters, sulphide is below the reporting limit of the analytical methods (9×10^{-7} M or 0.03 mg/L).

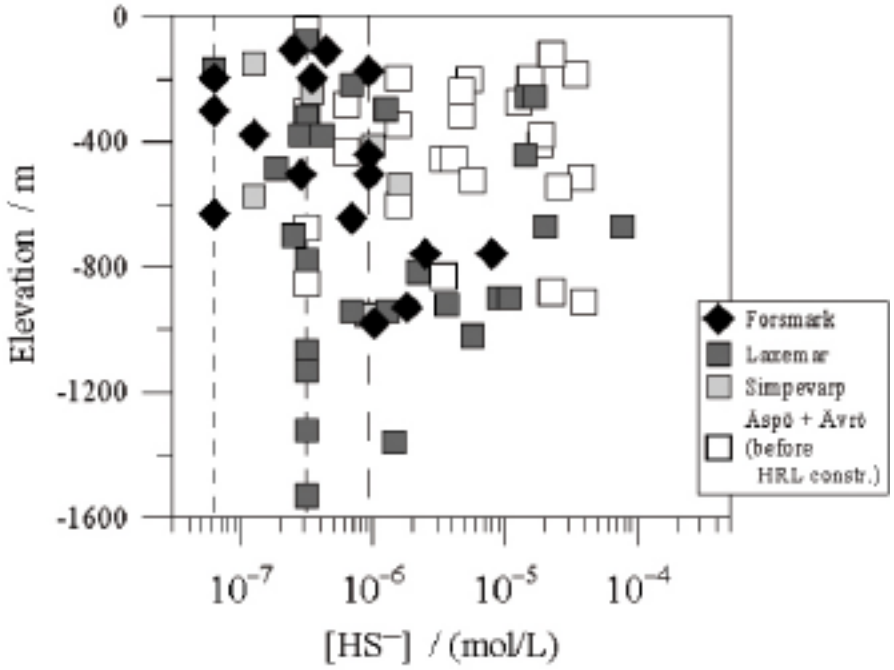

Figure 3-22. *Sulphide concentrations in contemporary groundwaters of the Forsmark and Simpevarp areas. Only one value has been selected for any given depth section of each borehole for cases where several analyses have been performed, and all data selected as reliable by the site description modelling are included. The dashed lines correspond to 0.03, 0.01 and 0.002 mg/L, representing the reporting limit, and two detection limits for the analytical methods used when obtaining the data. Values plotted at such a limit indicate that sulphide concentrations were analysed and found to be below the limit.*

The results of mixing the marine component with the other waters are shown in Figure 3-23. A slight decrease in sulphide values as meteoric waters become increasingly dominant with time is shown in Figure 3-24. A process not taken into account in the modelled sulphide concentrations is the possible dissolution of pyrite during the increased infiltration of meteoric waters with time.

The concentrations of methane and hydrogen are also of importance as nutrient sources for microbially mediated sulphate reduction to sulphide:

$SO_4^{2-} + CH_4 \rightarrow HS^- + HCO_3^- + H_2O$

$SO_4^{2-} + 4H_2 + H^+ \rightarrow HS^- + 4H_2O$

In Figure 3-25 it is seen that the maximum possible contribution to sulphate reduction from H_2 is modest. If all hydrogen was quantitatively used by microbes in sulphate reduction, at most the sulphide concentration would increase by $10^{-5.6}$ M. The figure also shows that methane concentrations are as a rule below 10^{-5} M. From this, from the data in Figure 3-22, and from the results of the hydrogeological and geochemical modelling described above, it may be concluded that sulphide concentrations, including the potential contribution from methane, averaged over the temperate period will be at the levels found at present at the sites or lower, that is, $\leq 10^{-5}$ M for any deposition hole. This is regarded as a cautious assumption: for any given deposition hole oscillations in sulphide levels will take place, but the time-averaged concentrations are expected to be $\leq 10^{-5}$ M.

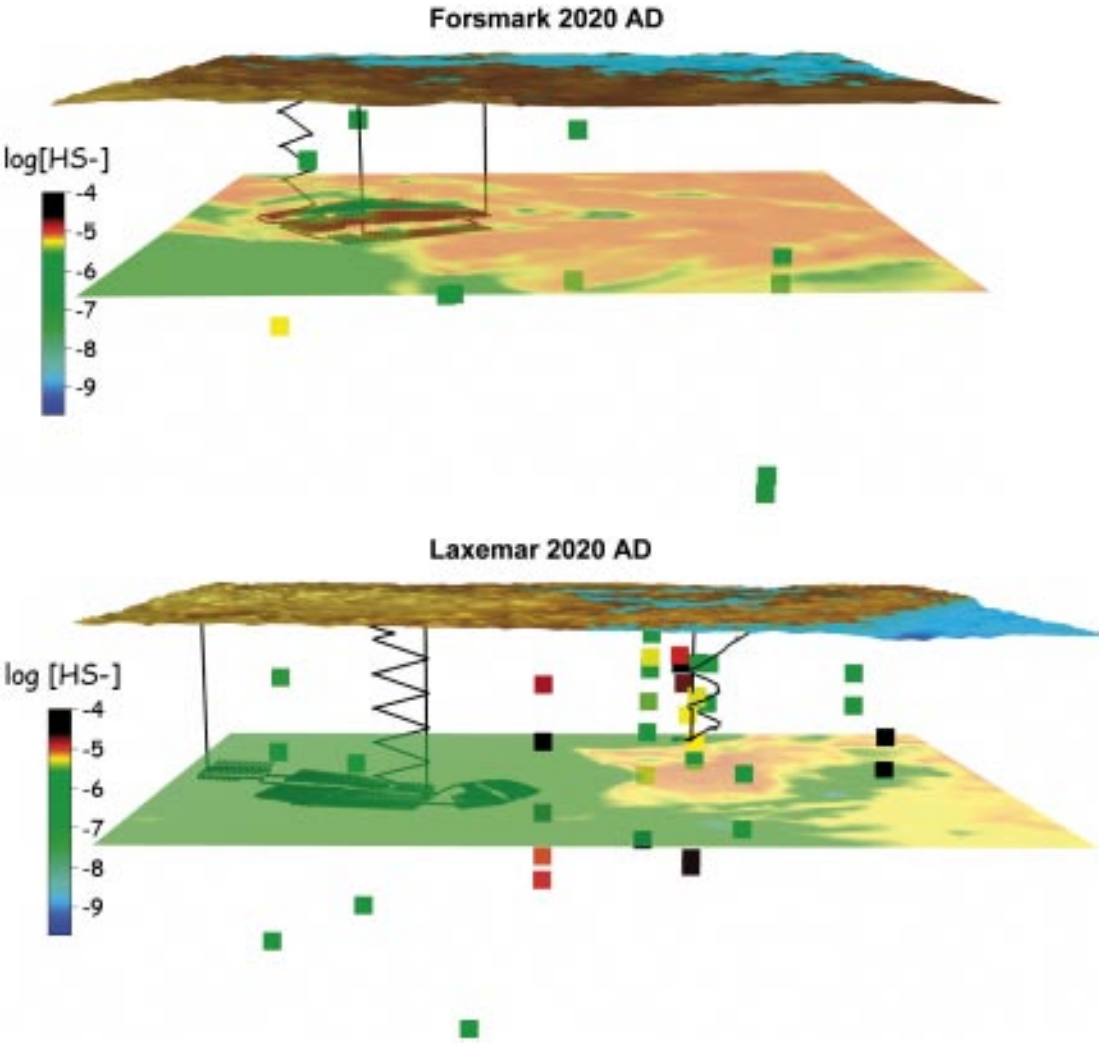

Figure 3-23. *Calculated present-day sulphide concentrations at the Forsmark and Laxemar sites. Groundwater data and calculated horizontal cuts at repository depth. The top surfaces shows land and Baltic Sea areas. The repository layouts are shown, and for Laxemar also the Äspö Hard Rock Laboratory. The vertical scale is exaggerated three times. The figure shows higher calculated sulphide concentrations in areas under the Baltic Sea.*

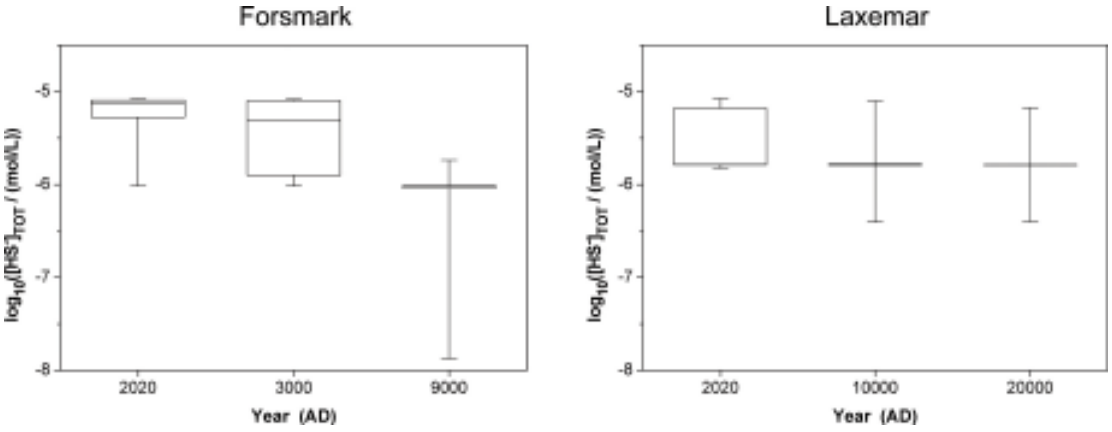

Figure 3-24. *Box-and-whisker plots showing the distribution of sulphide concentrations in Forsmark and Laxemar at repository depth as a function of time. The statistical measures are the median, the 25th and 75th percentile (box) and the 5th and 95th percentile ("whiskers").*

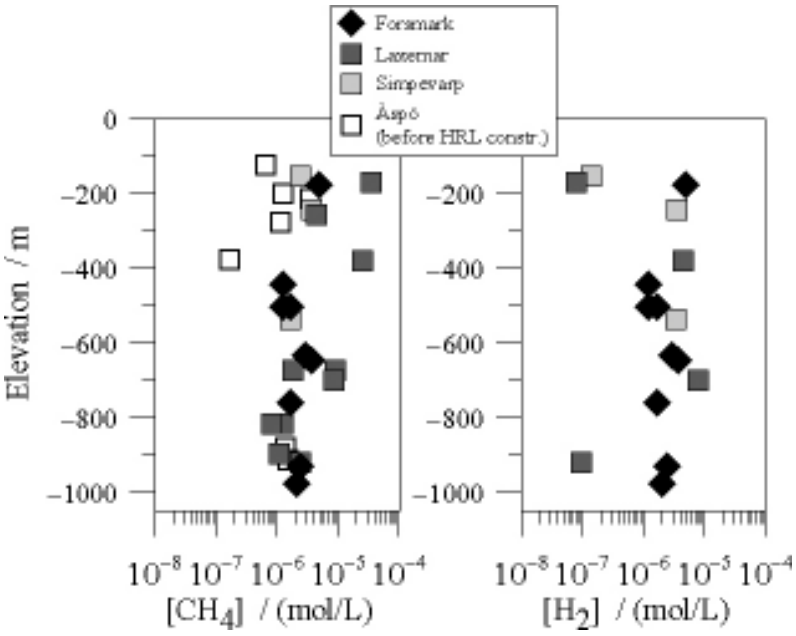

Figure 3-25. *Methane and hydrogen concentrations in contemporary groundwaters at the Forsmark and Simpevarp areas.*

The concentration of Fe(II) is regulated by a complicated set of reactions including the slow dissolution of Fe(II)-silicates, such as chlorite and biotite, the precipitation of Fe(II) sulphides and redox reactions. The concentrations of Fe(III) are in general negligible in granitic groundwaters, as the oxy-hydroxides of Fe(III) are quite insoluble and they precipitate quickly. For the reaction modelling in SR-Can, it has been assumed that Fe(III) oxy-hydroxide is at equilibrium, and this assumption has some effect both on redox potentials, discussed below, and on total iron concentrations. Figure 3-26 shows the Fe concentrations of groundwaters at repository level. The concentration levels are regulated by the interplay between groundwater flow (mixing of component waters) and the redox equilibrium between Fe(II) and Fe(III) oxy-hydroxide, which is also controlled by pH.

In conclusion, during the initial temperate domain following repository closure at the two sites evaluated, the potassium concentrations are expected to remain ≤ 0.004 mol/L, sulphide concentrations are expected to be ≤ 10^{-5} mol/L for any deposition position averaged over the temperate period and iron concentrations are expected to gradually increase up to 10^{-5} mol/L.

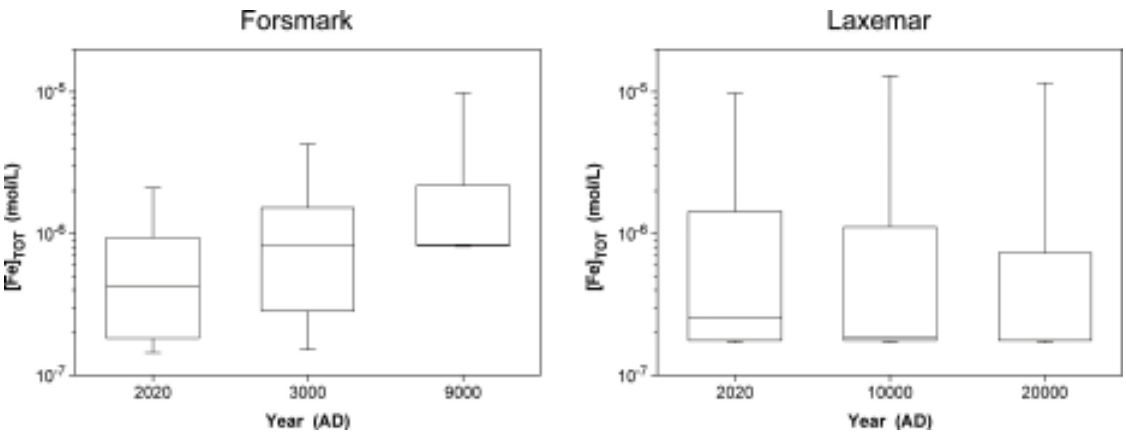

Figure 3-26. *Box-and-whisker plots showing the distribution of iron concentrations in Forsmark and Laxemar at repository depth as a function of time. The statistical measures are the median, the 25th and 75th percentile (box) and the 5th and 95th percentile ("whiskers").*

Chloride and sulphate

Although chloride and sulphate are not listed among the safety function indicator criteria of Section 1.2, chloride is used when selecting radionuclide transport properties (sorption coefficients) and sulphate is important when determining the solubility limits for radium. Both Cl^- and SO_4^{2-} behave almost conservatively, i.e. they rarely participate in chemical reactions, and they have been modelled by mixing calculations in SR-Can. Figure 3-27 shows that the groundwater concentrations of chloride and sulphate at repository level tend to decrease with time as waters of meteoric origin become increasingly dominant.

Colloids

Colloids are partly stabilised by neutralising electric repulsions between charges in their surfaces. Some of these charges arise from the dissociation of acid-base groups, and are, therefore, pH dependent. The presence of ions in the water counteracts these charge effects, and, therefore, most colloids quickly sediment in waters containing more than either 1 mM of Ca^{2+} or 100 mM Na^+. The results from the modelling calculations show that colloids will not be especially stable during the temperate period, because the pH values, salinities and calcium concentrations will be high enough to destabilise them. The conclusion is that colloid concentrations are expected to remain at the levels that have been measured during the site investigations, i.e. less than 100 mg/L /SKB 2005a, 2006e/.

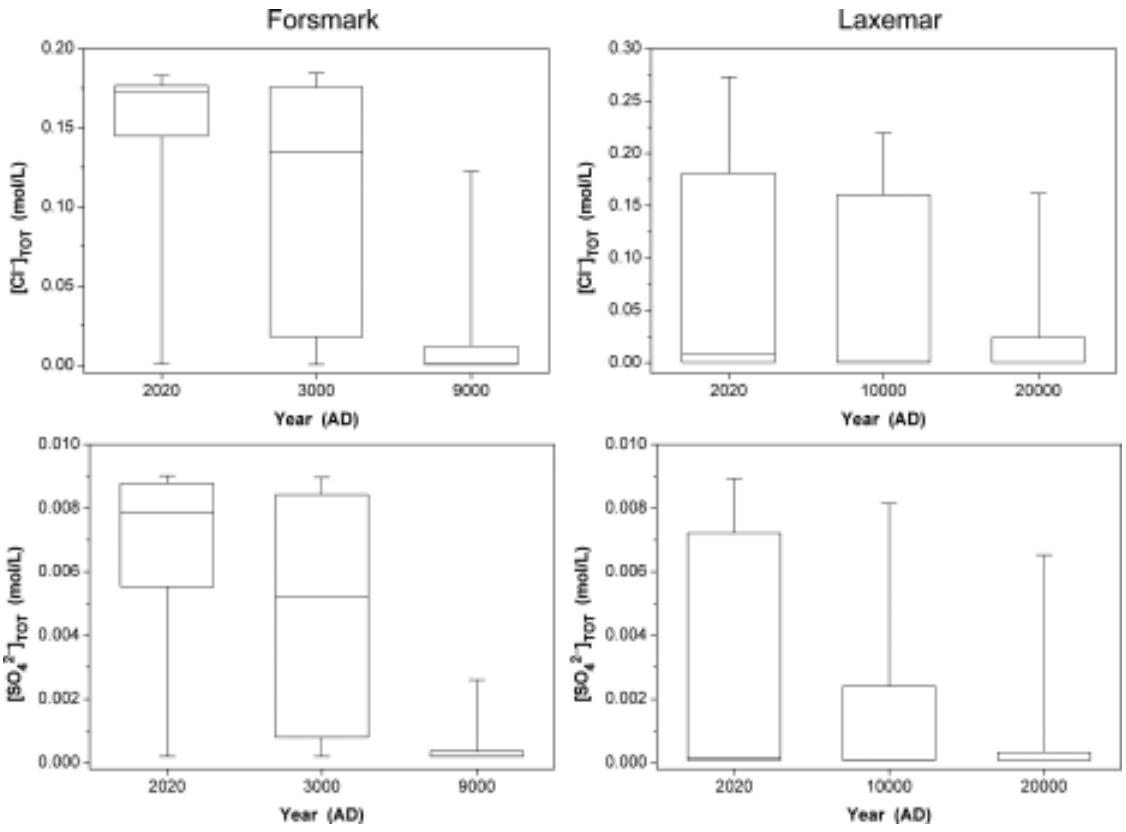

Figure 3-27. *Box-and-whisker plots showing the distribution of chloride concentrations (top) and of sulphate concentrations (bottom) at Forsmark and Laxemar at repository depth as a function of time. The statistical measures are the median, the 25th and 75th percentile (box) and the 5th and 95th percentile ("whiskers").*

3.4.4 Evolution of redox conditions

Evidence from the Äspö laboratory and other Swedish sites, shows that anoxic conditions prevail in the host rock even at a short distance from tunnel walls or from the ground surface. Air will be entrapped in the buffer and backfill, but anoxic conditions are expected to be established soon after the tunnels become re-saturated /Grandia et al. 2006/. Even if the buffer or backfill do not become fully saturated during this period, oxygen consumption processes will take place in the partially saturated materials, as shown from the data obtained at the Febex and Prototype experiments /Jockwer and Wieczorek 2003, Pedersen et al. 2004/.

The hydrological modelling of the sites /Hartley et al. 2006ab/ shows that the proportion of waters of meteoric origin at repository depth will increase with time, see Figure 3-1. This evolution is not expected to change the reducing characteristics of the groundwater, as infiltrating meteoric waters become depleted of oxygen by microbial processes in the soil layers of the site, if there are any, or after some tens of metres along fractures in the bedrock, as shown by the data collected within the Rex experiment /Puigdomenech et al. 2001a/ and from waters sampled at 40 to 70 m depth during the "Redox Zone" experiment at Äspö /Banwart 1999, Banwart et al. 1999/.

The SR-Can calculations include equilibrium with an Fe(III) oxy-hydroxide /Grenthe et al. 1992/. If reduction of sulphate is not allowed, the reaction controlling the redox properties of the groundwater is:

$$Fe(OH)_3(s) + 3\ H^+ + e^- \rightleftharpoons Fe^{2+} + 3\ H_2O$$

and the resulting redox potential is strongly correlated to pH, which is also reflected in the results of the simulations, see Figure 3-10. If the reduction of sulphate to sulphide is allowed, the following reaction takes place:

$$SO_4^{2-} + 9\ H^+ + 8e^- \rightleftharpoons HS^- + 4\ H_2O$$

and in this case the dependency between Eh and pH shows a less pronounced slope (Figure 3-10).

Figure 3-28 and Figure 3-29 present the Eh values calculated from the chemical mixing and mineral reaction modelling in SR-Can. Figure 3-30 shows that redox potentials increase slightly with time at Forsmark but remain well below −100 mV at the end of the simulation period, while for Laxemar the variation of Eh with time at repository depths is small. The figures show zones with Eh values which are higher than those of the surrounding rock volumes. The figures also show that the calculated values for the redox potential at the end of the temperate period are higher at depth (1 km for Forsmark and 1.5 km for Laxemar) than in the upper parts of the rock domain. This remarkable effect is due to the correlation between calculated Eh and pH values indicated in Figure 3-10. As indicated above when discussing simulated pH-values, see Figure 3-18, Figure 3-19 and Figure 3-21, calcite precipitation results in zones with lower pH, and they correspond to areas with *higher* calculated Eh. When meteoric groundwaters move further down in the rock, the zone where calcite precipitation takes place also moves down, with corresponding lower pH and higher Eh values.

It may be concluded from these results that the anoxic groundwater conditions now prevailing at repository depth will continue for the whole temperate period following the closure of the repository, in spite of the increasing proportion of meteoric waters with time.

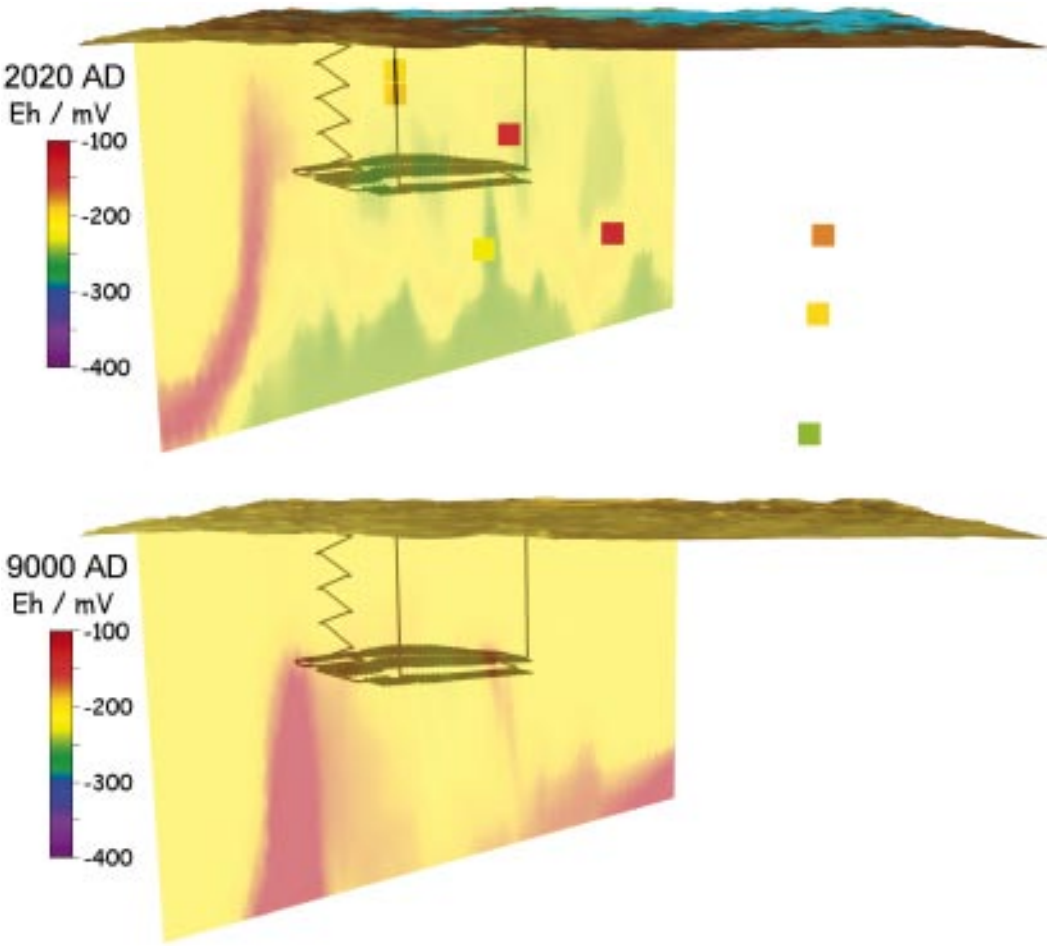

Figure 3-28. *Calculated Eh values at the Forsmark site. Upper picture: present-day groundwater Eh values and a calculated vertical cut approximately perpendicular to general coast direction. The top surface shows land areas and the Baltic Sea. The repository layout is also shown. The vertical scale is exaggerated three times. Lower picture: expected evolution of groundwater Eh values at the end of the temperate period, i.e. at year 9,000 AD. The coast has moved away from the site due to isostatic uplift.*

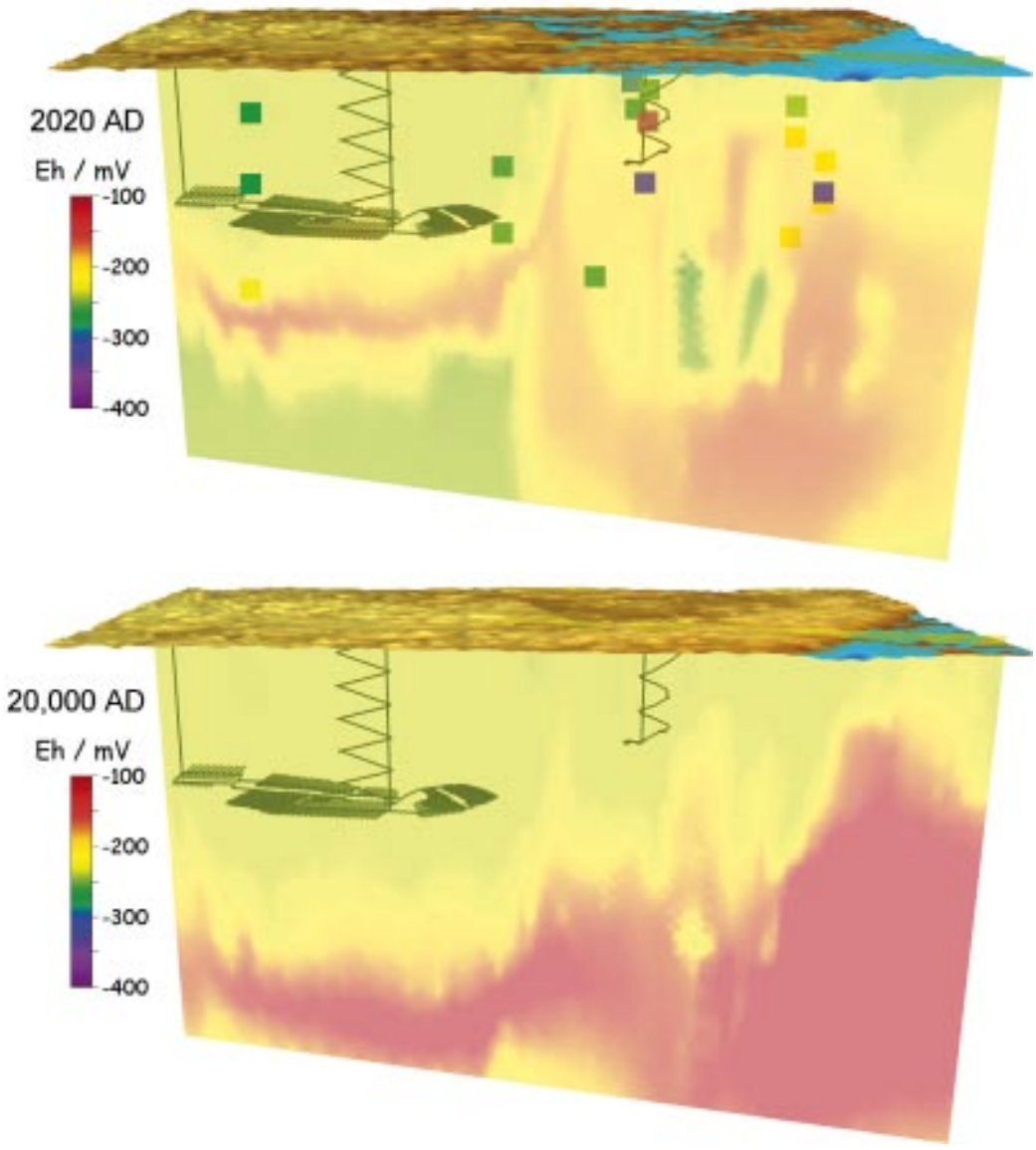

Figure 3-29. *Calculated Eh values at the Laxemar site. Upper picture: present-day groundwater Eh values and a calculated vertical cut approximately perpendicular to general coast direction. The top surface shows land areas and the Baltic Sea. The repository layout is also shown. The vertical scale is exaggerated three times. Lower picture: expected evolution of groundwater Eh values at the end of the temperate period, i.e. at year 20,000 AD. The coast has moved away from the site due to isostatic uplift.*

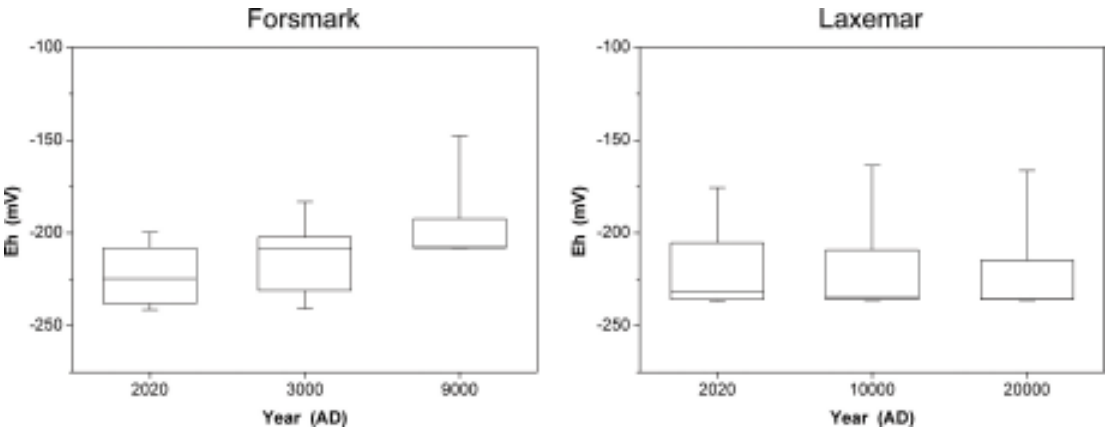

Figure 3-30. *Box-and-whisker plots showing the distribution of Eh values (redox potential) at Forsmark and Laxemar at repository depth as a function of time. The statistical measures are the median, the 25th and 75th percentile (box) and the 5th and 95th percentile ("whiskers").*

3.5 Compositions of groundwaters within the repository volume during the temperate period

The compositions of groundwaters within the repository candidate volumes are outlined in Table 3-3 and Table 3-4 for Forsmark and Laxemar, respectively.

These tables include a typical groundwater composition as well as statistics for each groundwater parameter (pH, Eh, and chemical elements). Data for 2,020 AD, 3,000 AD and 9,000 AD are provided for Forsmark, and data for 2,020 AD, 10,000 AD and 20,000 AD are provided for Laxemar.

Disagreements in the ranges for groundwater data given in Table 3-3 and Table 3-4 with those indicated in the box-and-whisker plots in Sections 3.4.3 and 3.4.4 are due to two factors: a) the tables summarise the data within the candidate areas at repository depth, instead of the whole regional model perimeter considered in the figures in Section 3.4; and b) the ranges in the tables correspond to the 1% and 99% percentiles while the box-and-whisker figures reflect the 5% and 95% percentiles.

3.6 Uncertainties

The model implemented in this work, which includes chemical mixing and equilibrium reactions with a few minerals, is not well suited to describe the acquisition of solutes by water-rock interactions in parts of the rock domain dominated by infiltrating meteoric waters. Therefore, the model results should not be expected to be relevant for the upper ~ 100 m at the sites. An attempt to improve the model has been to use superficial groundwaters as the mixing component, instead of "rain", see Section 3.2.2 and Figure 3-2. Because meteoric waters become increasingly dominant at repository depths during the temperate period, and because calcium is an important parameter for the stability of the bentonite buffer, improved modelling strategies should be evaluated in the future.

The Laxemar site descriptive model 1.2 is not sufficiently representative of the potential repository volume to allow definite conclusions to be drawn regarding groundwater compositions at the repository. In particular, the hydraulic interpretation of the site is based on data obtained outside the candidate volume and this affects directly the evaluation of groundwater geochemistry. It is to be therefore expected that future evaluations of the compositions of groundwaters within the repository volume may be substantially different than those presented in Section 3.5.

Table 3-3. Calculated chemical compositions of Forsmark groundwaters at 400 m within the repository area. All concentrations and ionic strength in mol/L. The concentration ranges correspond to the 0.1% and 99.9% percentiles.

	2,020 AD Example of result	Median	Range		3,000 AD Example of result	Median	Range		9,000 AD Example of result	Median	Range	
pH	7.67	7.67	7.15	– 8.67	7.34	7.40	6.89	– 8.59	7.34	7.37	6.75	– 8.31
Eh (mV)	–224	–224	–189	– –278	–204	–208	–170	– –278	–202	–205	–148	– –263
TDS (g/L)	9.90	9.88	0.63	– 12.5	3.19	3.08	0.51	– 13.3	0.82	0.71	0.51	– 9.95
Ionic Strength	0.192	0.193	0.004	– 0.240	0.061	0.062	0.008	– 0.259	0.015	0.013	0.008	– 0.194
Alkalinity	0.0013	0.0016	0.0001	– 0.0048	0.0038	0.0034	0.0001	– 0.0048	0.0046	0.0045	0.0003	– 0.0047
$[HCO_3^-]_{free}$	0.0011	0.00044	0.0001	– 0.0047	0.0036	0.0032	0.0001	– 0.0047	0.0044	0.0044	0.0003	– 0.0047
$[SO_4^{2-}]_{TOT}$	0.0071	0.0070	0.0002	– 0.0094	0.0022	0.0015	0.0002	– 0.0094	0.0004	0.0002	0.0002	– 0.0072
$[Cl]_{TOT}$	0.154	0.154	0.0027	– 0.194	0.044	0.044	0.0004	– 0.208	0.0057	0.0044	0.0003	– 0.154
$[Ca]_{TOT}$	0.0083	0.0065	0.0014	– 0.047	0.0033	0.0046	0.0014	– 0.046	0.0019	0.0022	0.0014	– 0.039
$[Mg]_{TOT}$	0.014	0.014	1×10^{-5}	– 0.019	0.004	0.003	0.001	– 0.018	0.0009	0.0006	0.0005	– 0.014
$[Na]_{TOT}$	0.125	0.123	0.004	– 0.163	0.038	0.029	0.0028	– 0.165	0.006	0.004	0.003	– 0.124
$[K]_{TOT}$	0.0026	0.0026	3×10^{-5}	– 0.0035	0.0009	0.0006	9×10^{-5}	– 0.0034	0.0003	0.0003	0.0002	– 0.0027
$[Fe]_{TOT}$	4×10^{-7}	4×10^{-7}	2×10^{-9}	– 4×10^{-6}	1×10^{-6}	9×10^{-7}	4×10^{-9}	– 9×10^{-6}	1×10^{-6}	1×10^{-6}	1×10^{-8}	– 1×10^{-5}
$[HS^-]_{TOT}$	7×10^{-6}	7×10^{-6}	1×10^{-10}	– 9×10^{-6}	3×10^{-6}	2×10^{-6}	1×10^{-7}	– 9×10^{-6}	1×10^{-6}	1×10^{-6}	1×10^{-8}	– 7×10^{-6}
$[Si]_{TOT}$	0.0002	0.0002	0.0002	– 0.0002	0.0002	0.0002	0.0002	– 0.0002	0.0002	0.0002	0.0002	– 0.0002

Table 3-4. Calculated chemical compositions of Laxemar groundwaters at 500 m within the repository area. All concentrations and ionic strength in mol/L. The concentration ranges correspond to the 0.1% and 99.9% percentiles.

	2,020 AD Example of result	Median	Range		10,000 AD Example of result	Median	Range		20,000 AD Example of result	Median	Range	
pH	7.76	7.76	7.01	– 7.97	7.76	7.76	7.05	– 7.78	7.76	7.76	7.03	– 7.76
Eh (mV)	−236	−236	−181	– −246	−236	−236	−185	– −236	−236	−236	−184	– −236
TDS (g/L)	0.26	0.26	0.25	– 5.0	0.25	0.26	0.25	– 2.57	0.25	0.26	0.25	– 2.54
Ionic Strength	0.004	0.004	0.004	– 0.111	0.004	0.004	0.004	– 0.059	0.004	0.004	0.004	– 0.058
Alkalinity	0.0024	0.0024	0.0010	– 0.0024	0.0024	0.0024	0.0017	– 0.0024	0.0024	0.0024	0.0018	– 0.0024
$[HCO_3^-]_{free}$	0.0024	0.0024	0.0009	– 0.0024	0.0024	0.0024	0.0016	– 0.0024	0.0024	0.0024	0.0016	– 0.0024
$[SO_4^{2-}]_{TOT}$	8×10^{-5}	8×10^{-5}	8×10^{-5}	– 0.0022	8×10^{-5}	8×10^{-5}	8×10^{-5}	– 0.0004	8×10^{-5}	8×10^{-5}	8×10^{-5}	– 0.0004
$[Cl]_{TOT}$	0.00036	0.00033	0.00031	– 0.082	0.00031	0.00032	0.00031	– 0.041	0.00031	0.00032	0.00031	– 0.041
$[Ca]_{TOT}$	0.0011	0.0011	0.0010	– 0.024	0.0011	0.0011	0.0011	– 0.015	0.0011	0.0011	0.0011	– 0.015
$[Mg]_{TOT}$	0.0002	0.0002	0.0002	– 0.004	0.0002	0.0002	0.0002	– 0.0004	0.0002	0.0002	0.0002	– 0.0002
$[Na]_{TOT}$	0.0007	0.0007	0.0007	– 0.043	0.0007	0.0007	0.0007	– 0.013	0.0007	0.0007	0.0007	– 0.012
$[K]_{TOT}$	7×10^{-5}	7×10^{-5}	7×10^{-5}	– 0.0007	7×10^{-5}	7×10^{-5}	7×10^{-5}	– 0.0001	7×10^{-5}	7×10^{-5}	7×10^{-5}	– 0.0001
$[Fe]_{TOT}$	2×10^{-7}	2×10^{-7}	6×10^{-8}	– 6×10^{-6}	2×10^{-7}	2×10^{-7}	2×10^{-7}	– 5×10^{-6}	2×10^{-7}	2×10^{-7}	2×10^{-7}	– 5×10^{-6}
$[HS^-]_{TOT}$	2×10^{-6}	2×10^{-6}	9×10^{-7}	– 3×10^{-6}	2×10^{-6}	2×10^{-6}	1×10^{-6}	– 2×10^{-6}	2×10^{-6}	2×10^{-6}	1×10^{-6}	– 2×10^{-6}
$[Si]_{TOT}$	0.0002	0.0002	0.0002	– 0.0002	0.0002	0.0002	0.0002	– 0.0002	0.0002	0.0002	0.0002	– 0.0002

3.7 Conclusions for the temperate period

The analysis of the evolution of the geochemical conditions at the Forsmark and Laxemar sites results in the following conclusions:

- Reducing conditions are expected to be re-established shortly after closure. This conclusion is based on several observations in similar systems and supported by the understanding of the underlying phenomena. Also, infiltrating meteoric water will be depleted of oxygen in the relatively thin soil layer of the site, or in the first few metres along fractures in the bedrock by microbial processes.
- At repository depth, the maximum salinity is expected during operation and immediately after closure, 12 g/L (corresponding to 0.2 M Cl^-) at Forsmark and lower at Laxemar. The salt content is expected to decrease during the first temperate period due to the progressive inflow of waters of meteoric origin.
- Concentration of divalent cations: during the first 1,000 years calcium concentrations are expected to be around 50 mM at repository depth. A decrease will take place with time due to the progressive inflow of waters of meteoric origin.
- Concentrations of other natural groundwater components: for potassium the expected average concentration is no larger than 4 mM, and for iron $\approx 10^{-5}$ M, whereas for sulphide the concentrations are expected to be $\leq 10^{-5}$ M for any deposition position averaged over the temperate period.
- The results of the geochemical analyses indicate that groundwater pH at the Forsmark site will be around 7 to 8. Similarly, the results for Laxemar indicate pH values between 6.5 and 8.5. Regarding effects of shotcrete and grout on groundwater composition, it is concluded that a plume of pH around 9 may develop in grouted fractures intersected by deposition tunnels and to a minor extent also in the backfill material. This plume may persist for up to one hundred thousand years. This could affect the retention properties of the transport pathways for radionuclides.

4 Evolution for the remaining part of the reference glacial cycle

For the remaining of the reference glacial cycle the hydrodynamic modelling is non-site specific, and the focus in SR-Can has been to estimate the reactions between fracture filling minerals and intruding glacial melt waters.

The successions of temperate, permafrost and glacial climate domains will affect the flow and composition of the groundwaters around the repository. The evolution between climate domains will be gradual, without a clear boundary between them. For example, during a temperate domain, temperatures may slowly decrease such that permafrost regions slowly develop within parts of the repository region. In SR-Can the evaluation of geochemical effects is restricted to using separate specifications for the different climatic domains. It is expected that different groundwater compositions will prevail around the repository as a result of the different types of climate domains and their corresponding hydraulic conditions. This section discusses the groundwater chemistry for periods in which the repository is below permafrost or an ice sheet, whereas the conditions expected under a temperate domain are discussed in Chapter 3.

For permafrost and glacial conditions, the following issues are treated:

- Evolution of salinity.
- Evolution of redox conditions.
- Evolution of concentrations of other relevant natural groundwater components.
- Effects of grouting, shotcreting and concrete on pH.

4.1 Permafrost conditions

4.1.1 Salinity

In the reference evolution of the repository, it is estimated that at Forsmark the ground will be frozen to a depth of 50 m or more for around 30 percent of the time in the glacial cycle of the reference evolution, see /SKB 2006b/. According to this scenario, the permafrost will not occur over a continuous period of time, but rather thawing will occur between more or less short periods of permafrost. Some of these permafrost periods will furthermore coincide with the time when the site is covered by an ice sheet, “basal frozen” conditions in Figure 1-1 and Figure 1-2.

Salt rejection

When water freezes slowly, most of the solutes present in the water will not be incorporated in the crystal lattice of the ice. During this process, salts that have been present in the surface waters and groundwaters will tend to accumulate at the propagating freeze-out front. This front is, however, not necessarily sharp, because e.g. freezing will take place over a range of temperatures, depending on the salinity and on the ratio between “free” and tightly adsorbed water molecules. The freezing process can give rise to an accumulation of saline water at the depth to which the perennially frozen front has reached. The saline waters formed in this manner within fractures and fracture zones will sink due to density gradients.

Generic calculations have been performed /Vidstrand et al. 2006/ to evaluate the fate of saline groundwaters produced during the freezing process. The concentration of the out-frozen salt has been estimated in these generic calculations assuming that before the onset of the permafrost the

salinity[2] distribution is linear from zero at the surface to 1.5% at 300 m depth. It was assumed that at the start of the simulations the frozen front had instantaneously reached 300 m depth and that the groundwater in a 10 m thick layer under the frozen rock had a salinity of ≈ 22%, that approximately represents the sum of all the salt available within the overlying 300 metres (this corresponds to a groundwater with ≈ 4.2 M Cl^-). This highly saline 10 m thick layer is located at the beginning of the simulation on top of groundwaters having a salinity increasing from ≈ 1.5% at the bottom of the permafrost to 10% at 2,000 m depth, which is also set as the bottom of the model. The DarcyTools model was used on the Laxemar-Simpevarp site using the boundary conditions and site properties from the site description model SDM v.1.1. The larger scale deformation zones in the model have an average transmissivity of 1.2×10^{-5} m^2/s. Further details are given in the original report /Vidstrand et al. 2006/. The model calculations show that saline waters generated in the deformation zones will move to deeper regions due to gravitational effects in periods shorter than 300 years. In these highly conductive parts, the salinity peak at repository depth may be for a few years as high as 9% (corresponding to a groundwater with ≈ 1.6 M of Cl^-). However, in less conductive portions of the rock, outside fracture zones, saline waters are practically immobile on the time scale of the simulations (300 years). The calculations are so far quite generic, and several factors remain to be investigated, such as the effect of regional flow fields and the effect of taliks on the hydrological conditions at repository depth. Furthermore, the onset of the permafrost has been considered in the modelling to be instantaneous, releasing highly saline groundwater immediately under the frozen rock.

As mentioned above, the concentration of the out-frozen salt has been estimated in these generic calculations assuming that before the onset of the permafrost the salinity distribution is linear from zero at the surface to 1.5% at 300 m depth. From the results in Section 3.4.2 this appears to be an overestimation, as the groundwaters at the sites will become gradually more diluted before the start of the permafrost. Therefore, a more realistic estimate of the concentration of the salt out-frozen from the top 300 m and distributed into a 10 m thick layer would be ≈ 2% (≈ 0.34 M Cl^-) instead of 22%. Another factor that would decrease the concentration of the out-frozen salt is the fact that the downward movement of the saline waters within fracture zones appears to be faster or at least to have a velocity similar to the advance of permafrost. Moreover it can not be excluded that pockets of un-frozen saline waters could become confined in the permafrost volume within the less permeable bedrock, depending on the geometry and thermal- and hydraulic properties of the fracture system. This would also reduce the amount of salt rejected to the bottom of the frozen rock.

Upconing of saline waters under permafrost conditions

The possibility of upconing of deep saline groundwater to repository depths during permafrost conditions was addressed in /King-Clayton et al. 1997/. This may possibly occur in the vicinity of permanent discharge features such as some taliks. Such discharge features mainly occur along more extensive conductive deformation zones, which are avoided in the repository design. However, it cannot be ruled out that saline waters may be transported through minor features to the repository area if the process occurs for long periods of time. This process is nevertheless not deemed to be a matter of concern, but may require some further assessment to be conclusively ruled out.

[2] The hydrological calculations in this section and in Section 4.2.2 make use of the groundwater salinity (weight%) as a function of space and time to evaluate density-driven groundwater flow. These salinity values may be converted into TDS (total dissolved solids): TDS (g/L) = $\rho\, S/100$; where S is the salinity in weight%; and ρ is the density (kg/m^3) of the groundwater. The density may be estimated according to /Svensson 1999/: $\rho = \rho_o(1+\alpha S)$; where ρ_o is the density of pure water, assumed to be 1,000 kg/m^3, and α a constant (= 0.00741). Values of individual groundwater components, such as chloride, calcium and sodium, may be estimated from the correlations shown in the figures of Section 2.2.1.

Permafrost decay

When the permafrost melts and decays there will be a release of dilute water from the upper part of the highly permeable network of fracture zones and perhaps also from confined individual fracture zones at depth, since these will have undergone salt-exclusion. At this stage the low permeable matrix which has preserved (or accumulated) its salinity, especially at greater depths, will probably be more saline than the surrounding groundwaters. The resulting chemical gradient will then cause a gradual transfer of salinity to the more permeable rock mass. In all probability this will be a slow process and dilution by mixing will occur also within the more permeable rock mass. The more dilute waters will tend to stay on the top layers of the rock mass due to their lower density.

4.1.2 Permafrost: Redox conditions

Geochemical processes are strongly influenced by the location of the upper boundary of the permafrost. For example, a widespread degradation of illite and the weathering of iron-containing minerals (e.g. chlorite) with further iron migration within the shallow active layer and its precipitation at the cryogenic barrier (e.g. as lepidocrocite) has been reported in /Alekseev et al. 2003/. Therefore, with respect to the overburden soils and shallow bedrock levels, all indications are that prior to, during and following permafrost decay, shallow groundwaters will be reducing due to a combination of microbial and geochemical reactions and processes.

The perennial freezing of rock volumes will effectively shut down the hydraulic circulation in the bedrock, at least locally. In this way, microbial populations could be isolated from the surface and also methane gas could be trapped as clathrates. Microbes present in the upper bedrock will survive in the permafrost and will become active during the subsequent melting. No changes in redox conditions are, therefore, to be expected unless the nutrient sources become exhausted. However, if clathrate formation has occurred, the dissociation of these compounds to release methane during permafrost decay would add to the nutrient sources for microbial populations in the bedrock, see for example the discussion in the /SKB 2006d/. In conclusion, it is not expected that redox conditions will change at repository depth during the formation or decay of permafrost, remaining reducing.

4.1.3 Permafrost: Other relevant natural groundwater components

There is very little information concerning the chemical conditions in groundwaters under permafrost. This is due to practical difficulties when drilling and sampling at ambient temperatures where freezing of drilling fluids and groundwater samples occurs.

Chemical components not participating extensively in chemical reactions, for example chloride, sodium, calcium and sulphate are expected to follow the patterns mentioned in the previous subsection describing the evolution of salinity during periods of permafrost.

Other components, being controlled by chemical reactions, are expected to be almost unaffected by the permafrost. The study at the Lupin Mine in N. Canada /Ruskeeniemi et al. 2004/ may be used to illustrate this: the pH values for sampled groundwaters vary between 6 and 9 and bicarbonate concentrations are found to be below 5×10^{-3} mol/L. For potassium, the concentrations are higher than for the groundwaters sampled at Forsmark or Laxemar: sub-permafrost groundwaters at Lupin have $< 2.6\times10^{-3}$ mol/L. For iron, most of the groundwaters sampled at Lupin had $< 54\times10^{-6}$ mol/L. Thus, the concentrations and pH values found are not far from those for groundwaters sampled elsewhere, for example at Forsmark, see Table 2-1.

The intensity of the production of sulphide due to microbially mediated SO_4^{2-} reduction will probably decrease due to the lower temperatures. As a consequence of the freeze-out of salts, sulphate concentrations might increase as compared with those at the end of a preceding temperate period, when groundwaters of meteoric origin predominate. Reducing agents are required for any sulphate reduction to take place, and under permafrost conditions the inflow of organic matter from the surface will become negligible. However, SO_4^{2-} reduction could be

sustained by the gaseous groundwater components methane and hydrogen, as already mentioned in Section 3.4.3. If microbial sulphide production occurs during this period, it will be limited mainly by the availability of CH_4 but also of SO_4^{2-} and. The amounts of methane and hydrogen will be controlled by their production and flow from the deeper parts of the bedrock, by the impervious frozen layers at the top of the site, and by their incorporation in the ice as clathrates. There is not enough data at present to quantify these processes, but there are no indications that either CH_4 or H_2 should increase in concentration during this period, and there is no evidence to support increased sulphide production at permafrost sites.

It is concluded that under permafrost conditions at the sites, following a relatively long period when diluted groundwaters of meteoric origin predominate, the production and concentrations of sulphide and methane will not be larger than those found at present, i.e. after a recent period of intrusion of marine sulphate-rich waters. Based on the arguments presented in Section 3.4.3 and present-day data (Figure 3-22 and Figure 3-25) it is to be expected that the sum of CH_4 and HS^- concentrations during permafrost periods will be at the levels found at present at the sites or lower, that is, on the average $\leq 10^{-5}$ M.

For major groundwater components, such as Cl, Na, Ca and sulphate the conclusion is that they will follow the trends of salinity discussed above. Other components, such as bicarbonate, potassium, iron, etc., as well as pH, that are controlled by fast chemical reactions are expected to remain mostly unaffected by permafrost.

4.1.4 Permafrost: Discussion and conclusions

Although groundwaters will become progressively diluted during the temperate period following the closure of the repository, permafrost can move salts to repository depth from the upper parts of the site. All arguments indicate that groundwaters below permafrost will not become more diluted than under temperate conditions. Rather, salt may move downwards within conductive fracture zones. Thus the concentrations of divalent cations (Ca^{2+}, Mg^{2+}, etc) are expected to increase during permafrost periods and they will satisfy the criteria concerning the safety function indicator: $\sum[M^{2+}] > 1\times10^{-3}$ mol/L (Section 1.2). However, the concentration of salts at repository level due to out-freezing will not become as high as to hamper the swelling of he buffer and the backfill, among other reasons because of the downward gravity-driven flow of saline waters. This situation will not be changed during permafrost decay as a transition to a temperate period occurs.

It should be noted that to date there is no supporting hydrochemical or mineralogical evidence indicating the occurrence of permafrost conditions having occurred in the Fenniscandian Shield. Any accumulation of increased salinity, for example, has long since been flushed out of the system, and any expected mineral phases (e.g. mirabilite, $Na_2SO_4\times10H_2O$) disappear rapidly with the onset of permafrost decay.

4.2 Glacial conditions

4.2.1 Introduction

For the glacial cycle of the reference scenario (about 120,000 years) the Forsmark site is covered by inland ice during a few periods with a total duration of about 30 thousand years, while for Laxemar the total duration is shorter /SKB 2006b/, see Figure 1-1 and Figure 1-2.

Groundwater flow in the glacial domain has been estimated using a generic model representing a large area (400×22 km) including the Laxemar site /Jaquet and Siegel 2006/. The model is equivalent to that used for the temperate period and summarised in Section 3.1.3, but the properties from an earlier site description for the Simpevarp subarea were used instead. The results of that model include evaluations of the salinity distribution beneath an ice sheet. Two extreme situations are discussed below: when the repository is entirely covered by a warm-based ice sheet, and when the ice sheet is advancing.

4.2.2 Glaciation: Evolution of salinity

Advancing warm-based ice sheet

Model results reported in /Jaquet and Siegel 2006/ illustrating the upconing of deep saline waters under an advancing warm-based ice-sheet are presented in Figure 4-1, which shows that salinities up to 5% (≈ 52 g/L TDS) may be reached locally at repository depth. In this model the ice sheet is advancing on a site that originally has groundwaters with salinities around 1–2% at repository depth. Because the advancement of the ice sheet is a relatively fast process and the retreat even more so, the high salinity conditions are predicted to last only a few centuries at most.

In conclusion: upconing is not expected to affect the swelling capacity of the backfill, according to the criterion indicated in Section 1.2.

The repository area covered by a stationary warm-based ice sheet

According to the results of the hydrogeological model, dilute waters are expected under a warm-based ice sheet at repository depth; see Figure 4-2 which shows that most of the waters have a calculated salinity ≤ 0.1 g/L. The composition of these waters is expected to be similar to those sampled at the Grimsel tunnel where cold meteoric waters are transported along fractures in granitic rocks. Figure 4-2 also shows that the salinity is not homogeneously distributed, and that waters having salinities between 0.1 and 10 g/L ([Cl^-] 0.0017 to 0.17 M) are not uncommon, although less frequent.

Therefore, it may not be excluded that when an ice sheet covers the repository area, dilute melt waters would occur at repository depth, violating the criterion for the safety function indicator which requires ∑[M^{2+}] to be larger than 1 mM (Section 1.2).

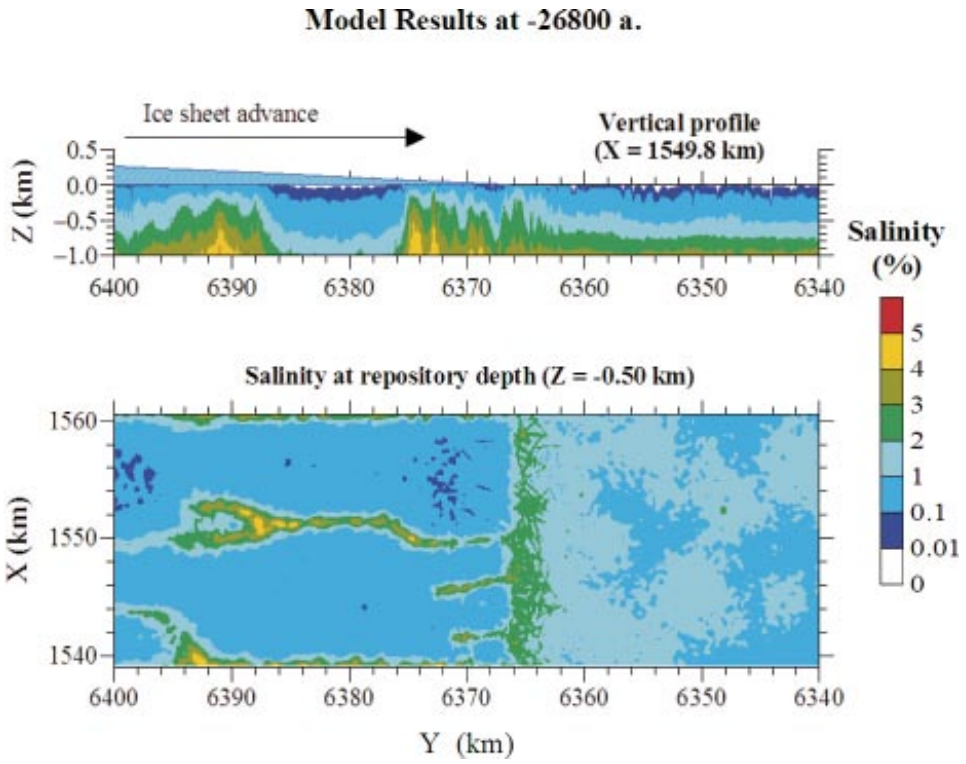

Figure 4-1. *Contour plots showing the salinities for a site affected by an advancing ice sheet calculated using the model described in /Jaquet and Siegel 2006/. The plots are focused on the Oskarshamn area: the upper diagram shows a north-south depth profile centred at the site (vertically exaggerated), and the lower diagram a slice at 500 m depth. The data indicate that groundwaters at repository depth can reach salinities up to 5% (≈ 52 g/L) due to the upconing of deep saline waters. However, most of the waters at repository depth a few kilometres under the ice margin have salinities between 0.1 and 1%.*

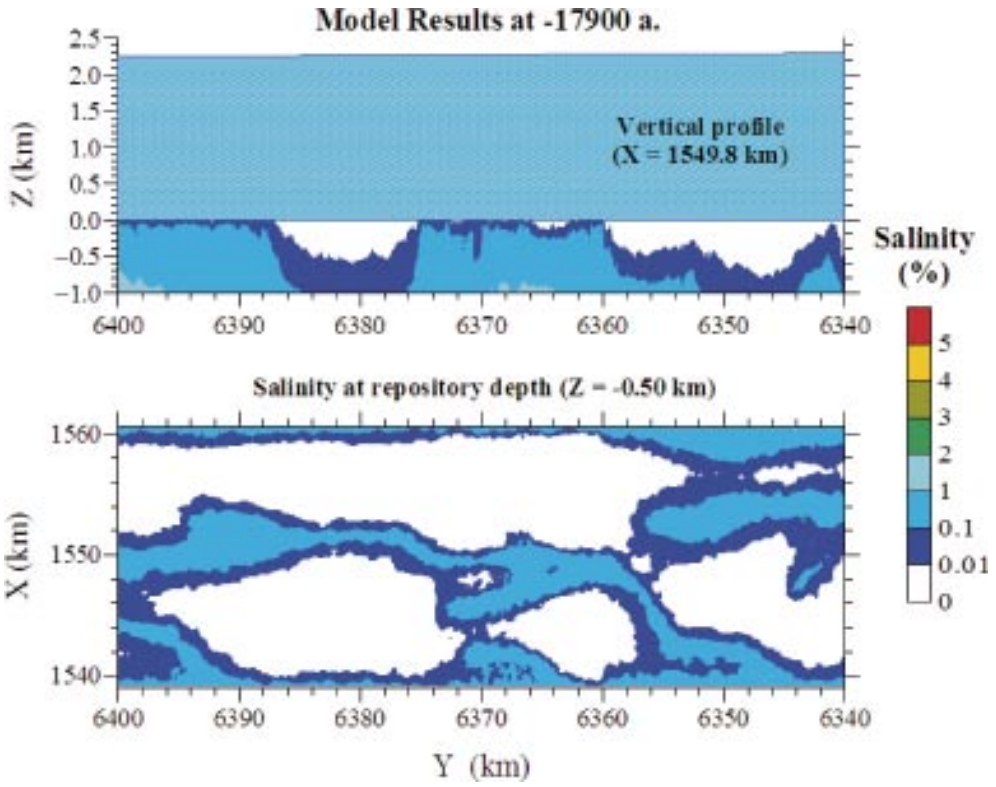

Figure 4-2. *Contour plots showing the salinities for a site under a warm-based ice sheet calculated using the model described in /Jaquet and Siegel 2006/. The plots are focused on the Oskarshamn area: the upper diagram shows a north-south depth profile centred at the site (vertically exaggerated), and the lower diagram shows a slice at 500 m depth. The data indicate that at repository depth most of the waters have salinities below 0.01% (≈ 0.1 g/L) although some waters have salinities as high as 1% (≈ 10 g/L TDS).*

Retreating warm-based ice sheet

The modelling study reported in /Jaquet and Siegel 2006/ shows that the hydrological results for a retreating ice sheet are similar to that of an advancing ice sheet, but the calculated salinities, shown in Figure 4-3, are quite different as much of the rock surface is devoid of overburden material and the underlying rock volume has already been extensively washed out by glacial melt waters. Figure 4-3 shows that the groundwater salinities are in this case essentially equivalent to those illustrated in Figure 4-2 for a stationary ice sheet, except for a slight upconing effect at the ice margin. According to these model results upconing is not expected to increase the groundwater salinities to such high levels that they would affect the swelling capacity of the backfill during the ice sheet retreat. It may be instead expected that when a warm-based ice sheet retreats dilute melt waters would occur at repository depth, violating the criterion for the safety function indicator which requires $\sum[M^{2+}]$ to be larger than 1 mM (Section 1.2).

Immediately after retreat of an ice sheet

As described in /SKB 2006b/, immediately after the retreat of an ice sheet, isostatic depression will maintain the ground surface at the repository site below the Baltic Sea surface level for a period of time. In the reference scenario of SR-Can, which is a repetition of the latest glacial cycle, the Weichselian, the Forsmark and Laxemar sites are expected to be below melt water lakes, and sea or brackish waters during a period of time between a few thousand years up to perhaps ten thousand years. Modelling of the Forsmark site since the retreat of the last ice sheet to the present-day situation shows a relatively fast turnover of groundwaters, where glacial melt is replaced by a succession of waters penetrating from the surface: the Yoldia sea, the glacial lake, the Littorina sea gradually evolving into the present day Baltic sea, and finally modern

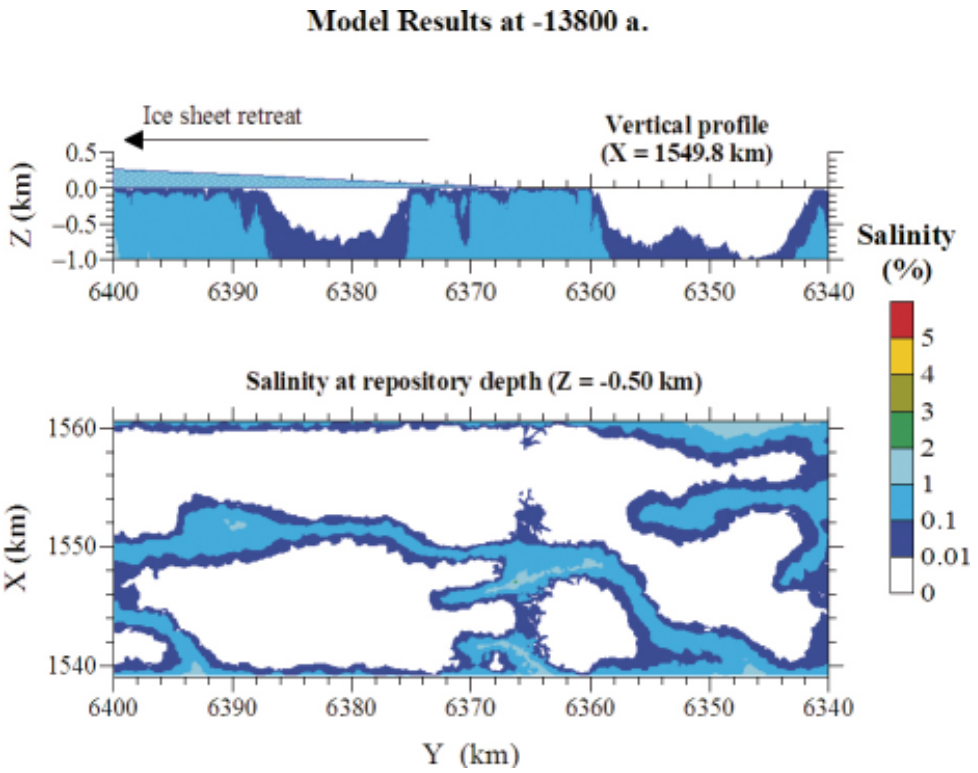

Figure 4-3. *Contour plots showing the salinities for a site under a retreating warm-based ice sheet calculated using the model described in /Jaquet and Siegel 2006/. The plots are focused on the Oskarshamn area: the upper diagram shows a north-south depth profile centred at the site (vertically exaggerated), and the lower diagram shows a slice at 500 m depth. The data indicate that at repository depth most of the waters have salinities below 0.01% (≈ 0.1 g/L) although some waters have salinities as high as 1% (≈ 10 g/L TDS). A slight upconing effect may be seen in the lower graph as a band of increased salinities at the ice margin.*

meteoric waters /SKB 2005a, 2006e/. The infiltration for relatively short periods of time of waters of marine origin will increase the salinity of groundwaters at repository depth that, as described above, had been diluted under a warm-based ice-sheet. It is, therefore, expected that during this period the concentration of divalent cations around the repository will increase as well to > 0.001 mol/L, corresponding to compliance with the safety function indicator, see Section 1.2. As the salinities are not expected to increase above those of sea water, the swelling capacity of the backfill will not be affected.

4.2.3 Glaciation: Other natural groundwater components

There is no experimental information concerning the chemical conditions in groundwaters under ice sheets. Whereas the expected salinities have been explored in the previous subsection with the help of a hydrological model, chemical reasoning must be used to estimate the consequences that a glaciation can have on specific aspects of groundwater chemistry.

As in the case of the temperate domain (Chapter 3) and the permafrost case discussed above in this section, chemical components not participating extensively in chemical reactions, such as Cl, Na, sulphate, and perhaps to some extent Ca, will follow the salinity patterns under the ice sheet described above.

Figure 4-2 above shows that most of the waters under a warm-based ice sheet have low contents of salts, ≤ 0.1 g/L, due to the continuous influx of glacial melt waters. The composition of glacier melt waters has been reviewed in /Brown 2002/. Although as expected some of these waters are extremely dilute (≈ 1 mg/L), there are several meltwaters that have gained solutes

from mineral weathering reactions, reaching salinities up to 0.2 g/L. Other examples of dilute granitic waters are those sampled in Gideå (0.33 g/L) and Grimsel (0.08 g/L), see also Appendix B. Although dilute, these waters are close to saturation with calcite. The relatively high pH values, ≈ 9, originate from the weathering of bedrock minerals.

For upconing groundwaters that may have salinities up to ≈ 50 g/L, see Figure 4-1, mixing calculations between a deep brine and glacial meltwater and simultaneous equilibration with calcite shows that such a groundwater would have the following composition (concentrations in mol/L): Ca 0.33; Na 0.25; K 5×10^{-4}; Fe(II) 5×10^{-6}; Cl 0.9; total carbonate 2×10^{-4}; sulphate 0.0064; and pH = 7.3, Eh ≈ −200 mV.

As in the case of permafrost, the intensity of microbially mediated SO_4^{2-} reduction to produce sulphide will probably decrease under an ice sheet due to the lower temperatures. Compared with a preceding permafrost period, sulphate concentrations might increase during the short periods of upconing waters and they will decrease substantially during the longer periods of intrusion of glacial melt waters. Therefore, SO_4^{2-} reduction may only occur during periods of upconing. In any case, reducing agents are required for any sulphate reduction to take place, and under glacial conditions the inflow of organic matter from the surface will become negligible. Sulphate reduction could still be sustained by the gaseous groundwater components methane and hydrogen, as discussed in Section 3.4.3. If microbial sulphide production occurs during upconing periods, it will be limited by the availability of both SO_4^{2-} and mainly CH_4. The amounts of methane will be controlled by its production and flow from the deeper parts of the bedrock. The production of CH_4 at depth is believed to be an abiotic hydrothermal process /Apps and van de Kamp 1993/. There is not enough data at present to quantify this process, but there are no indications that methane should increase in concentration during such periods, and there is no evidence to support increased sulphide production under glaciers.

It is concluded that for glacial conditions at the sites the production and concentrations of sulphide will not be larger than those found at present, i.e. after a recent period of intrusion of marine sulphate-rich waters. Based on the arguments presented in Section 3.4.3 and present-day data (Figure 3-22 and Figure 3-25), it is expected that the sum of methane and sulphide concentrations during glacial periods will not be larger than the values found at present at the sites, that is, on the average $\leq 10^{-5}$ M.

It may, finally, be concluded that major groundwater components, such as Cl, Na, sulphate, and perhaps Ca, will follow the trends of salinity discussed in subsection above. Other components, such as bicarbonate, potassium, iron, sulphide and pH that are controlled by relatively fast chemical reactions will be less affected by the glacial conditions, and their maximum concentrations will be governed by reactions with minerals. Nevertheless, as mentioned above all the evidence points towards dilute waters with relatively high pH. Therefore the criteria concerning the safety function indicators in Section 1.2 will be fulfilled in that pH will remain < 11 and the concentrations of K, HS^- and Fe will remain limited.

Colloids: As indicated previously, salinity levels are expected in general to decrease during glacial periods. Colloids are known to be strongly destabilised at high ionic strengths, and at high concentrations of divalent cations (Ca^{2+}) in particular. Therefore, during periods of glaciation, with predominantly dilute groundwaters, it cannot be excluded that colloids may perhaps be generated and transported by groundwater easily. However, a high potential stability of colloids does not necessarily implicate a high colloid concentration. It has, for example, been shown that the granitic groundwaters at Grimsel, which are quite dilute and where colloids, if formed, are quite stable, have low concentrations of colloids (≤ 0.1 mg/L). The reason for this is not clear: there might be some unknown mechanism that removes colloids at that site, or perhaps there is no significant generation of colloids at Grimsel. The conclusion is, therefore, that there is a potential for higher colloid concentrations in groundwaters during a glacial period, especially during the advance and retreat of an ice sheet when groundwater velocities are highest. An upper limit would be the highest measured colloid concentrations in groundwaters at repository depths, ≈ 1 mg/L.

4.2.4 Glaciation: Redox conditions

Background

As already mentioned in Section 4.2.1, hydrological models indicate that the advance of an ice sheet induces large changes in the groundwater conditions as compared with those prevailing today at the sites, e.g. /Svensson 1999, Boulton et al. 2001, Jaquet and Siegel 2006/. Short periods of upconing of deep reducing groundwaters, illustrated in Figure 4-1, will be followed by longer periods where glacial melt waters, more or less slowly, intrude into the rock. After some time the situation may look as in Figure 4-2, i.e. with groundwaters that originate almost entirely from ice melt water in large volumes of rock. Arguments have been put forward that if glacial melt waters were rich in dissolved atmospheric gases such as O_2, then reducing conditions might no longer prevail at repository depth, infringing one of the safety function indicator criterion given in Section 1.2, see e.g. /Puigdomenech et al. 2001b/.

Oxygen consuming microbial activity under glacial conditions is probably very limited and any estimates of such oxygen consumption are very uncertain. It may be envisaged that methane and hydrogen dissolved in deep groundwaters can be used by microbes to consume oxygen infiltrating from the ground surface. Preliminary modelling shows however this is of minor importance, as the infiltrating O_2-rich glacial melt waters push away the CH_4-containing groundwaters and mix only to a very limited extent with them. Taking these arguments into account, only inorganic reactions are taken into account in SR-Can as processes limiting the O_2 inflow with glacial melt waters.

Hydrogeological characteristics

The hydrogeological modelling of a moving glacier in SR-Can has been introduced above in Section 4.2.2. The study reported in /Jaquet and Siegel 2006/ indicates that, when the ice front is on top of the repository area, an increased downwards hydraulic flow occurs. The period for this enhanced groundwater flow has been estimated in SR-Can as follows /SKB 2006g/: Assuming that the repository area is 1 km long in the direction of the ice movement, and taking into account the time for each passage of the ice sheet, the total accumulated time for the steep first 1,000 m of the ice front covering a site is calculated to 40 years for a typical glacial period (here denoted **Case A**) or to 1,300 years in an extreme case in which the ice front comes to a temporary halt with the frontal-near part above the repository (here denoted **Case B**).

The ice profile becomes progressively steeper closer to the margin. An average surface slope of 20.7 degrees (0.35 m/m) is obtained for the first 1,000 m of the ice thickness profile /SKB 2006b/. In the Oskarshamn area, the regional gradient is approximately 0.2% /Follin and Svensson 2003/. The gradient imposed by the glacier is assumed to be 32% (0.35×0.9). Thus, the gradient during the glacial advance is 160 times larger than the gradient imposed by the regional topography, and for both Case A and B the Darcy velocity and the head gradient could increase by a factor of 160.

Oxygen content of meltwaters

Glacier ice may contain large amounts of air that has been incorporated during the formation of the ice /Martinerie et al. 1992, Ahonen and Vieno 1994/. Thus, glacier meltwater may initially contain dissolved carbon dioxide and oxygen at above the concentrations expected for aerated waters. The O_2 concentration for pure water in equilibrium with air is temperature dependent, ≈ 15 mg/L at 0°C. For glacial melt waters, based on theoretical constraints, the maximum O_2 concentration has been estimated to be 45 mg/L /Ahonen and Vieno 1994/, as observed in some samples of glacier ice thawed under laboratory conditions. However, it has been noted that much lower values are normally measured in sampled glacial melt waters in the field, in the range 0–5 mg/L /Gascoyne 1999, Puigdomenech et al. 2000/. Degassing prior to sampling can not be excluded, and degassing of melt waters prior to infiltration underground can not be accounted for in SR-Can. However, the analysed O_2 levels in meltwaters are often below

those corresponding to waters in equilibrium with air, and therefore, degassing can not be the only reason for the observed low O_2 concentrations. A process that could result is a complete disappearance of dissolved O_2 is reactions with minerals at the interface between the ice and the rock. Physical abrasion of the rock surface results in a continuous exposure of Fe(II) minerals, including some pyrite. Although melt waters are diluted, their sulphate content is believed to originate from pyrite oxidation /Brown 2002, Cooper et al. 2002/:

$$4\ FeS_2 + 14\ H_2O + 15\ O_2 \rightarrow 16\ H^+ + 8\ SO_4^{2-} + 4\ Fe(OH)_3$$

Sulphate concentrations of 0.1 mM (equivalent to the reduction of 6 mg of O_2/L) are not unusual in glacier meltwaters, and concentrations up to 1.1 mM have been reported /Brown 2002/. In addition, microbial activity under or within the ice sheet can not be excluded /Brown et al. 1994, Sharp et al. 1999, Tung et al. 2005/.

Fracture properties

Reducing capacity

Molecular oxygen is a quite reactive compound that spontaneously and easily reacts with a large number of materials. In such reactions oxygen accepts electrons from compounds that readily donate them. Electron donors are also called reductants, while electron acceptors, such as O_2, are called oxidants. In a redox reaction the oxidant is reduced, while the reductant is oxidized.

Dissolved hydrogen, methane and organic compounds are electron donors (reductants) normally present in groundwaters. These compounds however do no react readily with dissolved O_2, although microbes may use these electron donors and oxygen as electron acceptor to gain energy. In Forsmark and Oskarshamn, H_2 concentrations in groundwaters are $(0.1 \text{ to } 10)\times10^{-6}$ mol×L^{-1}, while for CH_4 there is a somewhat larger variation: $(0.1 \text{ to } 50)\times10^{-6}$ mol×L^{-1}, see Figure 3-25. Given the stoichiometry of the reactions with oxygen:

$$H_2 + ½\ O_2 \rightarrow H_2O$$

$$CH_4 + 4\ O_2 \rightarrow H_2CO_3 + H_2O$$

even if a complete mixing of infiltrating waters rich in O_2 would take place with groundwaters containing H_2 and CH_4, the amounts of these reductants are too small to significantly reduce the concentration of oxygen, unless it may be demonstrated that there is a large source and possibility for flow of methane or hydrogen to renew their concentrations.

Other prominent reductants in granitic groundwaters that react easily with oxygen are iron(II) and sulphide. Although other electron donors, such as manganese(II) are normally present, they will be neglected here. Typical Fe(II) concentrations for groundwaters in granitic rocks in Scandinavia are above 10^{-6} mol×L^{-1} (> 0.06 mg×L^{-1}). Sulphide concentrations are limited by the precipitation of iron(II) sulphide. Usually the sulphide concentrations are below 10^{-5} mol×L^{-1} (≤ 0.3 mg×L^{-1}), but often below the detection limit of the analytical methods (≤ 0.03 mg×L^{-1}). The reactions with oxygen:

$$Fe^{2+} + ¼\ O_2 + 2.5\ H_2O \rightarrow Fe(OH)_3(s) + 2H^+$$

$$HS^- + 2O_2 + OH^- \rightarrow SO_4^{2-} + H_2O$$

indicate that the capacity of groundwater to limit the inflow of oxygen in infiltrating waters is negligible. There are however sources of Fe(II) and sulphide that may renew these reductants when they become depleted in groundwater, namely the Fe(II)-containing aluminosilicates and the pyrite present in the granitic rock and in the minerals fillings and fracture coatings. This reducing capacity may be obtained by analysing their Fe(II) content. The available data are summarised in Table 4-1. From the low connected porosity of the rock matrix it may be argued that only a fraction of the reducing capacity is in contact with the rock pore water. Nevertheless, the reducing capacity of the rock matrix is quite high. Assuming 1% by weight of Fe(II) in the rock, a porosity of 0.3% results in a reducing capacity of 160 mol Fe(II) per litre of pore water.

Table 4-1. Redox characteristics and main fracture filling mineralogy for the Forsmark and Laxemar sites. Summary of data from /Drake et al. 2006/.

	Forsmark	Laxemar
Rock	85% granite to granodiorite 5 (± 4)% biotite ≈ 1.3% Fe(II)[†] Connected porosity: (0.1–0.6)%	80% Ävrö granite 10 (± 8)% biotite ≈ 1.7% Fe(II)[‡] Connected porosity: (0.1–0.6)%
Open fractures	– no fillings in 11% – chlorite: ≈ 1.5 (min.0.015) kg/m^2 (≈ 175 (min.1.7) g Fe(II)/m^2)[*] in 71% – pyrite < 50 g/m^2 in 9% – clays in 16% – calcite ≈ 680 (min.2.7) g/m^2 in 50%	– no fillings in 3% – chlorite: ≈ 0.75 (min.0.015) kg/m^2 (≈ 116 (min.2.3) g Fe(II)/m^2)[#] in 74% – pyrite < 5 g/m^2 in 18% – clays in 38% – calcite ≈ 410 (min.2.7) g/m^2 in 71%
Crushed zones[a]	– no fillings in 7% – chlorite in 23% – pyrite in 1% – clays in 27% – calcite in 23% – in fillings containing chlorite: 2 to 9% (of the bulk weight) is Fe(II) (5 to 18% Fe_2O_3 of which 70% is Fe(II))	– no fillings in 0.5% – chlorite in 90% – pyrite in 11% – clays in 59% – calcite in 84% – in fillings containing chlorite: 0.8 to 6% (of the bulk weight) is Fe(II) (2 to 15% Fe_2O_3; 60% Fe(II))

[†] From Fe analyses given as Fe_2O_3 content and comparison with $Fe(II)/Fe_{Tot}$ ratio data from Äspö.

[‡] From Fe analyses given as Fe_2O_3 content and measured $Fe(II)/Fe_{Tot}$ ratios.

[*] Assuming an Fe(II) content, given as FeO, of 15%.

[#] Assuming an Fe(II) content, given as FeO, of 20%.

[a] "Crushed zones" here refers to the boremap core logging classification corresponding to more than 20 fractures/metre. Deformation zones usually coincide with sections mapped as crushed zones.

Even if only 0.1% of this reducing capacity is available for reaction, it remains very high. The capacity of granitic rocks to react with oxygen has been confirmed experimentally /Torstenfelt et al. 1983, Pirhonen and Pitkänen 1991, Grenthe et al. 1992/. Fracture minerals and bentonite clay have also been shown to be able to deplete O_2 /Lazo et al. 2003, Rivas Perez et al. 2005/.

Groundwater flow path and transport times

The infiltration of glacial meltwaters will take place preferentially along deformation zones. The repository layout in SR-Can has been based on a respected distance of 100 m /SKB 2006g/, which requires that no deposition holes will be located within a band 100 to 200 m from a major deformation zone. The calculated fraction of canisters being intersected by so called discriminating fractures, those with radius larger than 75 m, is about 1.5 percent using estimated parameter values from the geological DFN model of rock domain RFM029 in Forsmark /SKB 2006g/. Therefore, the fastest way for glacial meltwaters to reach a deposition hole, is to travel first through some hundreds of metres in a deformation zone and then through at least 100 m in single fractures.

For temperate conditions the advective transport times between canister positions and the ground surface are modelled in /Hartley et al. 2006ab/. The models produce a wide distribution of advective transport times, reflecting the spreading in the fracture properties used, but the shorter times are calculated to be of the order of one year for the worst placed canister positions. It may not be ruled out that such short advective transport times are model artefacts. Under a glaciation period the groundwater head gradient and the groundwater velocities may on the average increase by a factor of 160, as described above. If applied linearly to all transport pathways, this would lead to shortest advective transport times of about 3 days and flow rates that seem unrealistic. In the following, it will be assumed that the *shortest realistic advective travel times are about a few years*, even for the Cases A and B defined above for the passage of the glacier margin above the repository.

The shortest advective transport paths start at deposition holes intersected by single fractures with radii of 75 m or more which in turn intersect a large deformation zone. The advective travel time, which is constrained to about one year, may be evaluated from the groundwater travel path, which should be perhaps 400 m in the deformation zone and 100 m in the fracture, and the groundwater velocity, $v = T \times i/\delta$ (where T is the fracture transmissivity, v is the groundwater velocity, i the hydraulic head gradient and δ the fracture aperture).

As it will be shown below, for very transmissive deformation zones matrix diffusion becomes negligible, and because the interaction between groundwater and fracture minerals is controlled by the rate of dissolution of these minerals, the water residence time, i.e. its velocity, is an important parameter.

Values of T may be measured experimentally, while the ratio i/δ needs to be estimated. The single fracture intersecting both the deposition hole and the deformation zone would have a transmissivity probably not larger than $T \approx 10^{-7}$ m^2/s, while the deformation zone might have transmissivities of at most $\approx 10^{-4}$ m^2/s. With these maximum transmissivities and with the constraint that the advective travel times should be as short as a few years, it follows that i/δ must be > 20 m^{-1} for the fracture and > 0.2 m^{-1} for the deformation zone. Down-hole imaging of boreholes shows that single fractures have apertures below 1 mm while channel apertures within deformation zones may be a few millimetres, see e.g. /Drake et al. 2006/. Thus a plausible combination of parameters that yield advective travel times of a few years, is a hydraulic head gradient of 0.01 (units-less), combined with a single fracture aperture of about 0.5 mm, while for the deformation zone the total aperture for the groundwater channels would be ≈ 5 cm.

A deformation zone may extend several km and have a thickness between one or a few metres up to perhaps 60 metres. The entire deformation zone is usually rich in smaller fractures and it has a higher porosity than "intact" rock. The highly transmissive fractures are, however, usually few. The mineral fillings in these fractures consist of coatings on the rock walls but also on fragments and grains of altered wall rock, chlorite and clay minerals.

A single fracture may be characterised by a void/channel, where water circulates. Fracture filling minerals are normally found as coatings (typically chlorite and calcite) on the rock walls but may also include more loose and porous materials. All situations in between these two extremes may be expected. The consumption of O_2 by reaction with dissolved Fe(II) may take place inside the "fracture", that is, between the two rock walls, and in the rock matrix when O_2 is driven into it by diffusion, originating from the large concentration gradient between the fracture groundwater and the rock porewater.

Consumption of oxygen in single fractures: matrix diffusion

Reactions in the rock matrix alone are able to reduce infiltrating O_2 in a single fracture. A model describing this has been presented in /Neretnieks 1986, Sidborn and Neretnieks 2006/. The model includes flow in the fracture, diffusion in the rock matrix, the dissolution of Fe(II) minerals in the rock matrix, and the reduction of O_2 by iron(II) in the pore water according to the following reactions:

$$KMg_{2.5}Fe_{0.5}AlSi_3O_{10}(OH)_2 + 3.5H_2O \rightarrow K^+ + 2.5\ Mg^{2+} + \tfrac{1}{2}\ Fe^{2+} + \tfrac{1}{2}\ Al_2Si_2O_5(OH)_4 + 2SiO_2 + 7OH^-$$

$$Fe^{2+} + \tfrac{1}{4}\ O_2 + 2.5H_2O \rightarrow Fe(OH)_3 + 2H^+ \qquad (5.1)$$

It may be shown that in most cases the rate of mineral dissolution is fast as compared with the diffusion process /Sidborn and Neretnieks 2006/. Microbial O_2 consumption with pyrite within the fracture has been shown to be important during initial stages /Sidborn and Neretnieks 2003, 2004/ but for longer periods of time the uptake of O_2 is controlled by matrix diffusion. According to the model, which includes fracture flow and matrix diffusion and it assumes that the dissolution of matrix Fe(II) minerals is relatively fast, the maximum penetration of dissolved O_2 at a given time t along a flowing fracture is given by:

$$x_{O_2=0} = \frac{Q_{flow}}{W}\sqrt{2\frac{c_{O_2}^{x=0}}{D_e\, f\, c_{Fe}}t} \qquad (5.2)$$

where D_e is the effective diffusivity of O_2 in the rock matrix (as a first approximation may be taken to be $D_e = 5\times10^{-14}$ m²/s); W is the width of the fracture; Q_{flow} the flow rate; f is a stoichiometric coefficient (in this case ¼, see reaction (5.1)), $c_{O_2}^{x=0}$ is the concentration of oxygen at the fracture inlet, which may be assumed to be at most 2.5×10^{-4} mol/L (8 mg/L) for water that has already been through a deformation zone and c_{Fe} is the concentration of Fe(II) in the rock matrix available for reaction (for 1% Fe(II) in the rock, as suggested by the data in Table 4-1, $c_{Fe} = 480$ mol Fe(II)/m³).

The relative effects of advection and matrix diffusion are included in the quotient $W/Q_{flow} = (v\times b)^{-1} = (T\times i)^{-1}$ (where v is the groundwater velocity; b half the fracture aperture; T the transmissivity; and i the head gradient). For the "worst case" fracture path mentioned above, with a transmissivity of $T \approx 10^{-7}$ m²/s, and using a head gradient around 0.01, the calculated maximum penetration along the fracture is 10 m for **Case A** (40 years of passage of the glacier front above the repository) and 60 m for **Case B** (for a total of 1,300 years). According to the criteria described in /Sidborn and Neretnieks 2006/ assuming that the rate of mineral dissolution is fast as compared with the diffusion process is not correct for a time period of 40 years (Case A), and longer penetration depths should be expected in that case.

Although some parameters are somewhat uncertain, e.g. W/Q_{flow}, D_e and $c_{O_2}^{x=0}$, it is clear from the calculation example given above that matrix diffusion has a large potential to retard the advance of O_2 in single fractures.

Another extreme case would be that of a single fracture reaching repository depth. In a most pessimistic choice of parameters the groundwater velocity would be $v = T\times i/\delta = 10^{-5}$ m/s to give a water advection time of 1.6 years to travel 500 m; giving a penetration depth for O_2 of 580 m for the most pessimistic **Case B** (a total of 1,300 years). If the concentration of dissolved oxygen in the meltwaters at the base of the ice sheet is increased, then the penetration depth increases as indicated by Equation (5.2). For the extreme case of $c_{O_2}^{x=0} = 45$ mg/L it would require more than 150 years with maintained high values of W/Q_{flow} for oxygen to reach repository depth, which is considered unlikely.

The processes described above and an equivalent model were confirmed experimentally when the "redox fronts" at the Osamu Utsumi mine were studied. Redox fronts in bedrock are created, for example, when: 1) recharging oxidizing groundwater is increasingly reduced at depth by the buffering capacity (i.e. available Fe(II)) of the host bedrock (as in the case of glacial melt waters), and 2) discharging reducing groundwaters are oxidized when approaching the shallow bedrock/overburden surface. In both cases a redox boundary is formed between two rock/groundwater systems with different oxidation environments. The precise localisation of these redox fronts is best exemplified in sedimentary rocks, in particular sandstones and claystones which often show clear colour differences. In crystalline rock environments, however, there is little optical evidence of redox fronts and detailed mineralogy, geochemistry and isotope studies are necessary to determine the transition from oxidizing to reducing. Consequently, sampling becomes problematical since initially there is no clear indication of where the redox front is actually positioned.

The most detailed investigations of redox front phenomena were undertaken in the Osamu Utsumi uranium mine, Poços de Caldas, Brazil /Chapman et al. 1992/. At this site sub-tropical conditions have led to the low temperature development of deep recharge weathering profiles and the formation of supergene uranium remobilisation deposits (as pitchblende) at and adjacent to the migrating redox front systems (Figure 4-4). Weathering has resulted in further argillisation of the rocks, together with small-scale remobilisation of REEs and other trace elements in association with the redox fronts.

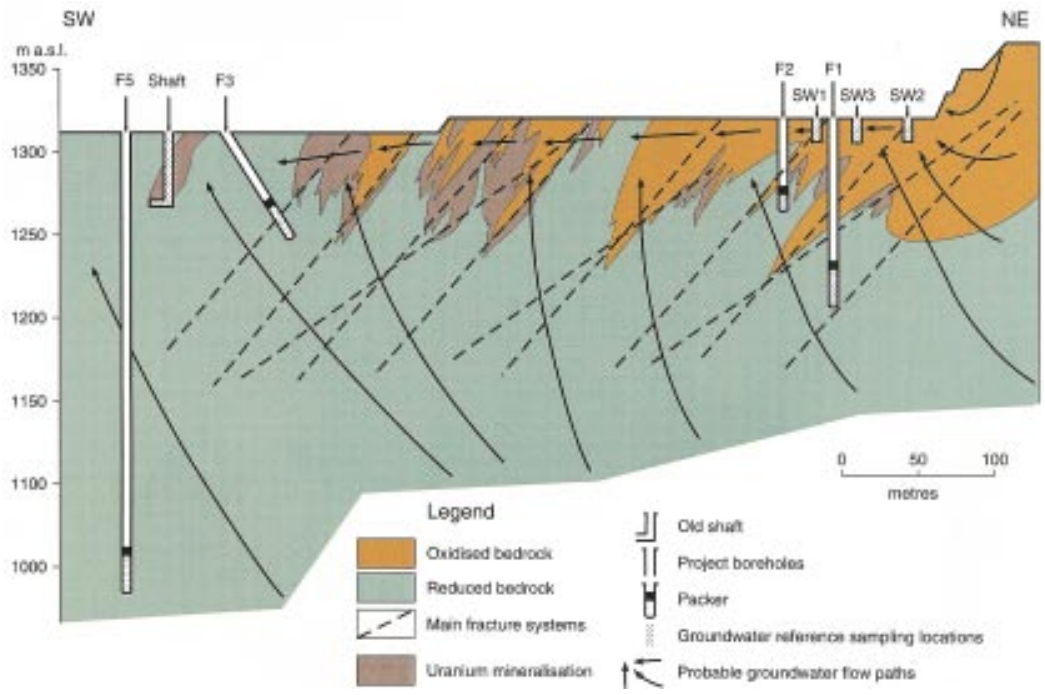

Figure 4-4. *Cross-section of the Osamu Utsumi uranium mine showing the location of the boreholes, the redox fronts, the major areas of reduced/oxidized bedrock, and probable flow directions of the modern groundwaters*

In general, the groundwaters at the Usamu Utsumi mine are of unusual dilute composition and indicate intensive weathering from actively circulating fresh groundwaters in contact with the highly leached potassic-rich rock mass /Nordstrom et al. 1992/. As a result, the waters are essentially of K-Fe-SO_4 character. Oxidation of pyrite (dispersed throughout the reduced bedrock) due to the mixing of reducing discharge waters and near-surface oxidizing waters within the upper 50 m of the mine bedrock, has produced acid mine water at and near the surface. At greater depths the groundwaters are more reducing in character and some redox trends are indicated. Tritium and stable isotopic data support this groundwater flow model.

The recharge permeation by advective flow of these recharging dilute groundwaters is strongly controlled by the fracture networks shown Figure 4-4. The phonolites and related volcanic rocks of the mine tend to be evenly fractured with relatively high hydraulic conductivities (10^{-5} to 10^{-7} $m \times s^{-1}$). Where major fracture zones are present, the oxidation fronts have penetrated significantly further into the rock than in the more uniformly fractured regions (left in Figure 4-5). The nature and extent of the redox fronts at the mine are clearly distinguished by sharp colour contrasts between reduced (blue-grey) and oxidized (brownish-red) phonolite bedrock (Figure 4-5). The oxidized colour is the result of alteration of disseminated pyrite to iron oxy-hydroxides.

The rate of front movement was addressed geochemically and geormorphologically. Uranium-series disequilibrium analyses revealed that over a period of at least 10^6 years advective flow has occurred along the fractures and parallel to the redox front. Diffusive transport of dissolved species occurred perpendicular to the fractures /MacKenzie et al. 1992/. Based on estimated geomorphological erosion rates of the Poços de Caldas plateau, assuming that the downward migration of redox fronts was dependent on the rate of erosion, the average rate of redox front movement was calculated to be around 12 m per million years over the last 10 million years /Holmes et al. 1992/.

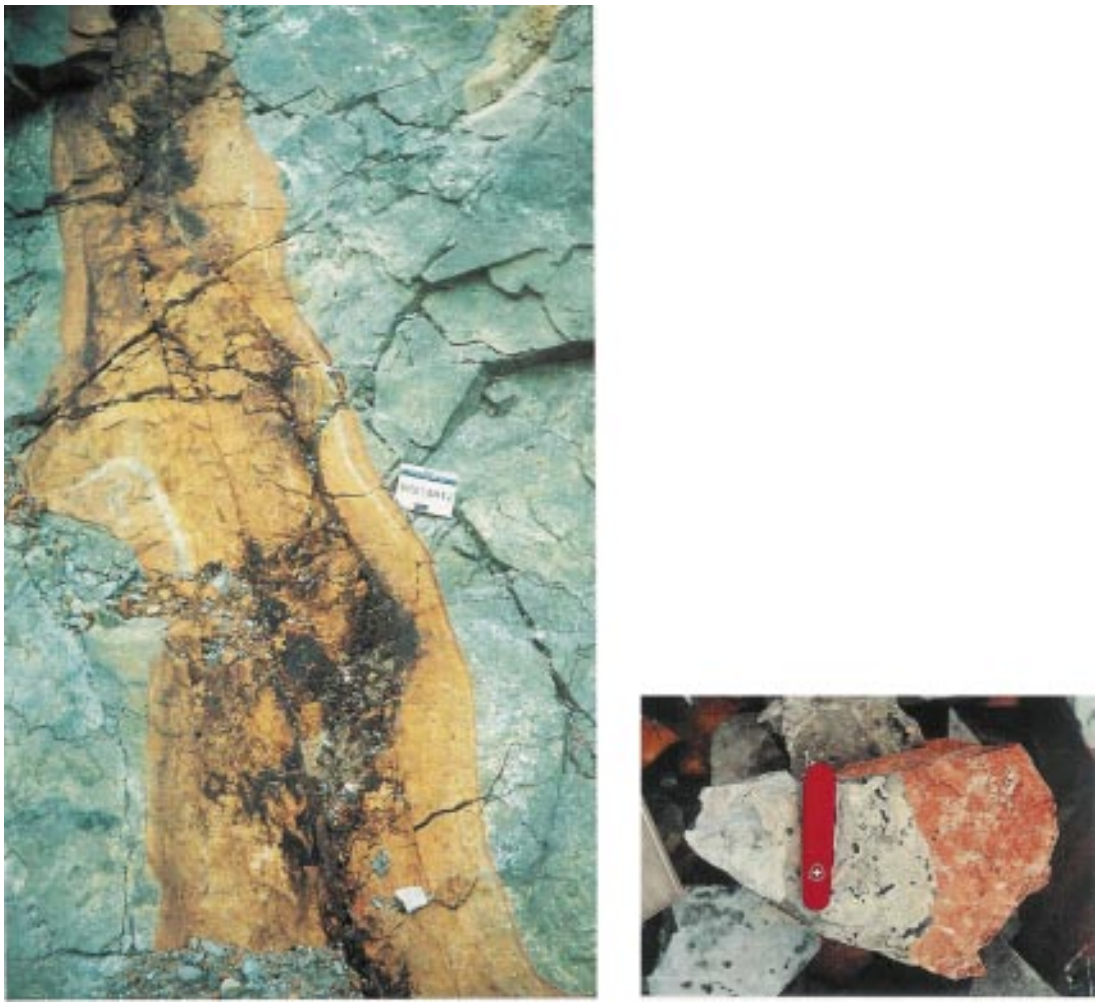

Figure 4-5. *Redox front (left picture) associated with a fracture zone showing also the outward oxidation (yellow-brown colouration) into the reduced rock matrix (blue-grey colour) by diffusion processes. Right: a small scale sample showing the sharp interface at the redox front. The black nodules in the reduced rock are pitchblende precipitated ahead of the advancing redox front from uranium mobilised from the oxidized rock.*

The formation and evolution of the redox fronts was modelled by applying chemical transport models of different complexity, addressing both advective flow in a porous medium and also fracture flow involving channelling with differing flow rates /Romero et al. 1992/. The overall oxidized zone in the Osamu Utsumi mine (~ upper 50 m) can be explained by advective transport in a porous medium. The model applied by /Romero et al. 1992/, which is essentially equivalent to the models discussed in this section /Neretnieks 1986, Sidborn and Neretnieks 2006/, was successful in showing that the deeper penetrating oxidation along individual fractures, fracture zones and fracture networks is due to fracture flow (channelling) and it indicated that matrix diffusion is an important mechanism to access the reducing capacity of the rock matrix adjacent to the fracture pathways.

Consumption of oxygen in deformation zones.

The transmissivity for deformation zones in either Forsmark or Simpevarp may be at most $T \approx 10^{-4}$ m^2/s and the quotient W/Q_{flow} (= $(T \times i)^{-1}$) in Equation (5.2) above becomes too small, indicating that the interaction with the rock matrix becomes negligible. However, oxygen consumption processes still take place within the deformation zone by dissolution of fracture filling minerals. This has been modelled among others by /Guimerà et al. 1999, 2006/. If the rate

of dissolution of fracture minerals is fast, then oxygen can only advance if the reducing capacity of the fracture is totally exhausted, and the rate of advancement of oxygen, v_{O_2}, is given by materials balancing:

$$v_{O_2}(\mathrm{m}\cdot\mathrm{yr}^{-1}) = \frac{R_{O_2}(\mathrm{mol}\cdot\mathrm{yr}^{-1})}{\frac{1}{4}c_{Fe}\frac{V}{d}} = \frac{c_{O_2}^{x=0}\cdot Q_{flow}}{\frac{1}{4}c_{Fe}\frac{W\cdot\delta\cdot d}{d}} = \frac{c_{O_2}^{x=0}\cdot v_{H_2O}\cdot W\cdot\delta}{\frac{1}{4}c_{Fe}\frac{W\cdot\delta\cdot d}{d}} = \frac{c_{O_2}^{x=0}\cdot v_{H_2O}}{\frac{1}{4}c_{Fe}}$$

where R_{O_2} is the rate of inflow of oxygen into the fracture zone; c_{Fe} is the Fe(II) available in the deformation zone (mol/L_{water}); V the groundwater volume in the channels; d the distance along the flow path where the volume V is found; $W\times\delta$ the total cross section of the flow channels in the deformation zone (width times aperture); and v_{H_2O} is the groundwater velocity.

However, it may be expected that the rate of dissolution or of oxidation of fracture filling minerals is not as fast as the inflow of O_2, resulting in a faster penetration of the oxidizing perturbation. In this case the residence time of the water controls the O_2 advance: slower water velocities allow more time for fracture minerals to dissolve or become oxidized. Important parameters are therefore not only the reducing capacity of the fracture filling minerals (amount of chlorite, biotite, etc) and the groundwater velocity, but also the rate of release of Fe(II) per unit length along the deformation zone.

The model of /Guimerà et al. 1999, 2006/ was limited to the release of Fe(II) from fracture filling minerals. The rate of this process may be expressed as follows:

$$r_{Fe}(\mathrm{mol}\cdot\mathrm{L}_{water}^{-1}\cdot\mathrm{hr}^{-1}) = S_A\cdot f(\mathrm{pH}) = S_A\left(k_0 + k_H[H^+]^{n_1} + k_{OH}[OH^-]^{n_2}\right)$$

where S_A is the available surface area for reaction (m^2/L_{water}) which is further discussed below, and f(pH) is a rate expression that describes the variation of the mineral dissolution rate as a function of pH. The rate is smallest at neutral pH, and it increases in acidic and alkaline solutions.

When the O_2-rich glacial melt water enters the deformation zone, the Fe(II) minerals begin to dissolve slowly. The groundwater advances quickly but at a certain distance, d_s, along the fracture, the overall rate of release of Fe(II) matches exactly the inflow of O_2:

$$R_{O_2}(\mathrm{mol}\cdot\mathrm{hr}^{-1}) = c_{O_2}^{x=0}\cdot Q_{flow} = c_{O_2}^{x=0}\cdot v_{H_2O}\cdot W\cdot\delta$$

$$R_{Fe}(\mathrm{mol}\cdot\mathrm{hr}^{-1}) = r_{Fe}\cdot V = S_A\cdot f(\mathrm{pH})\cdot d_s\cdot W\cdot\delta$$

$$R_{O_2} = R_{Fe} \quad\rightarrow\quad d_s = \frac{c_{O_2}^{x=0}\cdot v_{H_2O}}{\frac{1}{4}S_A\cdot f(\mathrm{pH})}$$

Once the O_2 front has reached the distance d_s it remains stationary until the available reducing capacity is exhausted, and then it continues to advance at a constant rate dictated by mass balance. It can be shown that the time needed for the oxygen front to restart advancing depends only on the reducing capacity of the system (c_{Fe}) and on the rate of dissolution of the Fe(II)-minerals ($r_{Fe}\propto S_A$).

The reactive surface area, S_A, is proportional to the available reducing capacity. In /Guimerà et al. 2006/ the deformation zone has been modelled assuming a porosity of 20%, corresponding to 4 dm^3 of fracture filling minerals in contact with each dm^3 of groundwater in the deformation zone. In this model the Fe(II) content of the fracture fillings, expressed as Fe_2O_3, is set to 2.5%. The few measurements available /Drake et al. 2006/ indicate that this is conservative, see Table 4-1. The reducing capacity in the system becomes ≈ 3.4 mol Fe(II)/L_{water}. The surface area available for the reaction is more uncertain. Measured values for crushed samples used in laboratory experiments are ≈ 2 to 5 m^2/g for biotite /Malmström and Banwart 1997, Samson et al. 2005/ and ≈ 0.5 to 7 m^2/g for chlorite /Brandt et al. 2003, Gustafsson and Puigdomenech 2003, Gustafsson et al. 2004, Lowson et al. 2005/. It may be expected that in a fracture the

available surface area is much smaller than for a crushed sample, and a conservative value of 0.015 m^2/g has been used in the modelling of /Guimerà et al. 2006/. Combined with a Fe(II)-mineral amount of ≈ 0.6 kg/L_{water} it results in $S_A \approx 8.6\ m^2/L_{water}$.

For glacial melt water interacting with calcite present in the fractures, the equilibrium pH is calculated to be ≈ 9.7, which agrees with what it is observed in infiltrated meteoric waters, for example at Grimsel. The rate of dissolution of biotite at pH ≈ 9.7 is $f(\text{pH}) \approx 10^{-7.4}$ $mol \times m^{-2} \times hr^{-1}$ /Malmström and Banwart 1997, Samson et al. 2005/, while for chlorite $f(\text{pH}) \approx 10^{-8.8}$ $mol \times m^{-2} \times hr^{-1}$ /Lowson et al. 2005/. In the modelling, the rate of dissolution of biotite was used, giving $r_{Fe} \approx 10^{-6.5}$ $mol \times L_{water}^{-1} \times hr^{-1}$, and $c_{O_2}^{x=0}$ was set to 0.25 mM.

The values of d_s calculated with the expression given above and the parameters used by /Guimerà et al. 2006/ agree well with the results of the numerical calculations presented by these authors. For example, $v_{H2O} = 10^{-5}$ m/s, corresponding to a water advection time of 1.6 years, gives $d_s = 113$ m. Equally good agreement is found for the time at which the O_2 front starts advancing again (≈ 1,200 years at any groundwater velocity) and the subsequent rate of the O_2 front advancement: $v_{O2} \approx 0.1$ m/year for $v_{H2O} = 316$ m/year.

A conclusion of the arguments and assumptions presented here is that for both **Case A** and **Case B** defined above (40 and 1,300 years of increased meltwater inflow) the oxygen front would not reach repository depth.

The parameters in this model have different levels of uncertainty. The rate of dissolution of the Fe(II)-minerals, r_{Fe}, which is proportional to the available surface area S_A, is the most important parameter and quite uncertain. On the other hand the value 0.015 m^2/g selected by /Guimerà et al. 2006/ is quite conservative. The other important parameter is the total amount of Fe(II) minerals in contact with the flowing water in a deformation zone. The data in Table 4-1 is important when estimating the available reducing capacity of this system.

Glaciation; Conclusions on Redox conditions

For single fractures, with transmissivities ≈ 10^{-7} m^2/s, the processes of matrix diffusion and dissolution of Fe(II) minerals in the rock are able to effectively neutralise the inflow of O_2 present in glacial meltwaters.

In the most transmissive deformation zones the process of matrix diffusion has very little influence. Instead the dissolution of Fe(II) minerals in contact with the flowing melt waters will oppose the advancement of O_2-rich waters for hundreds of years until the upper parts of the deformation zone have exhausted their Fe(II) content. Afterwards the dissolution of Fe(II) minerals will retard substantially the travel velocity of O_2 with respect to that of water. This sequence of events is shown to occur even for the fast water velocities required for advection times as short as a few years.

Although the model parameters assumed are believed to be cautiously selected, they do not cover the complete range of possibilities. It may be envisaged, for example, a situation where melt waters have high O_2-concentrations not observed in natural environments, or that a deformation zone is devoid of any reducing capacity, or even a groundwater channel may be envisaged that is tens of centimetres in aperture, allowing an extremely fast hydraulic transport. These possibilities have to be analysed in the realm of "what if" scenarios.

4.2.5 Glaciation: Discussion and conclusions

a) Reducing conditions; Eh limited.

The reducing conditions during the initial temperate period are expected to continue to exist throughout the reference glacial cycle. The only identified challenge to this conclusion concerns the possible penetration of oxygenated glacial meltwaters to repository depth for glacial situations with enhanced groundwater flow.

Evaluations show that this is a very unlikely phenomenon even for situations with increased flow rates driven by an ice sheet on top of the repository. It is, therefore, concluded that reducing conditions will generally prevail during the reference glacial cycle used in SR-Can.

b) Salinity; TDS limited.

For temperate domains during the reference glacial cycle, the salinity is not expected to exceed that of the initial temperate period, i.e. the salinities are well within the ranges where the buffer and backfill have favourable swelling properties.

For permafrost conditions, out-freezing of salt above the repository may increase the groundwater salinity at repository depth. A pessimistic, generic model calculation of this effect puts an upper bound of 1.6 M Cl^-, whereas realistic estimates are considerably lower.

For glacial conditions, the highest salinities are expected as a result of possible upconing of deep saline waters driven by increased flow rates under an ice front. Salinities of up to around 50 g/L (≈ 1 M Cl^-) were estimated in a study of the Oskarshamn area.

c) Ionic strength; $\sum[M^{2+}] > 1$ mM.

For temperate domains during the reference glacial cycle, the minimum groundwater concentration of divalent cations is not expected to fall below that of the initial temperate period.

For permafrost conditions, the concentrations of divalent cations are expected to increase in comparison with the conditions during temperate periods, see Section 4.1.1. Therefore, this safety function criterion is fulfilled also for permafrost conditions.

However, for glacial conditions, with intrusion of dilute glacial melt water, this cannot be claimed to be the case. This means that the extent of buffer erosion must be analysed in SR-Can for such conditions.

d) Limited concentrations of K, HS^-, Fe.

For temperate domains during the reference glacial cycle, the concentrations of these substances are expected to be similar to those occurring during the initial temperate period.

For permafrost conditions, the concentrations of potassium and iron will be similar to those found nowadays in groundwaters at the sites. For sulphide the *maximum* concentration will be 10^{-4} M, based on the precipitation of iron(II) sulphide.

For glacial conditions, the intrusion of melt waters will decrease the concentrations of potassium and iron. Even sulphide concentrations will be decreased, and the *maximum* concentration will be 10^{-4} M, based on the precipitation of iron(II) sulphide.

e) Alkalinity; pH < 11.

For temperate domains during the reference glacial cycle, the pH is expected to be similar to that of the initial temperate period, i.e. between 6.5 and 8.5.

Permafrost conditions are not expected to influence the pH values to any significant extent.

For glacial conditions, three typical groundwater types have to be considered: *a*) saline waters during upconing will have close to neutral pH values, similar to those encountered during the temperate and permafrost conditions; *b*) very dilute groundwaters from glacial melting will have relatively high pH values 9 to 10; and *c*) mixtures of these waters will have pH values intermediate between the *a* and *b* types.

In addition, leach water from grout, shotcrete and cement may exhibit pH-values of ≈ 9 for extended periods of time. The use of low-pH formulations of these materials limits pH in these situations.

5 Greenhouse variant

As one variant of the reference evolution, a case with an increased greenhouse effect has been investigated in SR-Can.

For both candidate sites, the climate during the 120,000 year glacial cycle is dominated in the greenhouse variant by an initial ~ 100,000 year long period without ice sheet coverage, a period that gets successively colder towards the end. The temperate domain is dominant in this scenario, with temperate conditions prevailing for 78,000 years at Forsmark, and for 86,000 years at Laxemar. Permafrost conditions prevail for 28,000 years at both sites, whereas glacial conditions prevail for 11,000 years at Forsmark and for 6,000 years at Laxemar.

During a large part of the initial warm period, mean annual air temperatures at the candidate sites may be as warm as, or warmer than, at present. During this long warm period, it is likely that climate within the temperate domain may vary significantly, with a range that may be largerthan that during the Holocene.

For the greenhouse variant atmospheric CO_2 levels increase, temporarily up to ≈ 1,000 ppm /IPCC 2001/, corresponding to about 4 times the pre-industrial values. The consequences of the increased acidity of superficial waters on a granitic aquifer were analysed in /Wersin et al. 1994/, where it was concluded that several tens of thousands of years would be necessary to exhaust the calcite present in fracture filling minerals. In addition, silicate weathering and ion-exchange processes also contribute to neutralise the increased inflow of carbonic acid in infiltrating waters. It may thus be concluded that the groundwater conditions will be similar to those of the reference evolution, with the difference that a longer period of exposure to groundwaters of meteoric origin is expected at repository depth. The composition of the waters is, however, not expected to vary substantially during the temperate period, as shown by the modelling results of the Forsmark and Laxemar sites discussed in Chapter 3 and the results in /Wersin et al. 1994/. Groundwater compositions from sites in temperate countries, such as Spain, may be used as examples. Samples from the granitic sites of El Berrocal /Bruno et al. 1998/ and Los Ratones /Gómez et al. 2006b/ evidence fresh groundwaters with concentrations of divalent cations (Ca^{2+} and Mg^{2+}) around 1 mM.

The conclusions are, therefore, similar to those presented in Sections 3.6. For the whole first temperate period following repository closure, anoxic groundwater conditions will prevail at repository depth, in spite of the increasing proportion of meteoric waters with time. Salinities during this period will be limited, ensuring that the swelling properties of the buffer and backfill are not negatively affected. However, calcium concentrations at repository depth will be close to 0.001 mol/L, that is, near to the limit where montmorillonite colloids start to become stable. The concentration of sulphide, which is another important parameter, is expected to be $\leq 10^{-5}$ on the average. For colloids, the levels are expected to remain at the concentrations that have been measured during the site investigations, around 50 µg/L.

6 Conclusions

According to our present understanding of the hydrogeology of the candidate sites for a spent nuclear fuel repository, the composition and evolution of the groundwaters at repository level in the rock, both in fractures and in the matrix porosity, depends on the climatic conditions and on their evolution. For example, if the site is submerged by waters more saline than the groundwaters in the rock fractures, a density turnover is expected to occur. Similarly, groundwater at repository level will be affected by meteoric waters during temperate periods when the site is above the sea level and by glacial meltwaters during periods when the site is covered by warm-based glaciers.

The geochemical evolution of groundwaters presented in this report follows therefore closely the reference climate evolution of SR-Can's main scenario, as well as the modelled hydrogeological evolution that follows from this reference climate scenario.

The processes expected during repository construction and operation have been examined within the SR-Can project and no geochemical changes that could influence negatively the long-time performance of the repository were identified.

For the temperate period following repository closure, a first attempt has been made in this work of coupling results from detailed modelling of the hydrogeological evolution of the sites with chemical mixing and mineral dissolution and precipitation. The procedure combines hydrogeological results obtained with CONNECTFLOW within the SR-Can project /Hartley et al. 2006ab/ with a chemical mixing and reaction-path simulation using PHREEQC.

The hydrogeological results reflect the progressive inflow of meteoric waters into the sites, and indicate that far-field groundwaters during the temperate period will not affect negatively the performance of the safety functions of the repository. The PHREEQC calculations show that the progressive inflow of groundwaters of meteoric origin displaces to greater depths the zone where these waters, relatively rich in HCO_3^-, mix with deeper waters with high Ca^{2+} content, resulting in calcite precipitation. This mixing zone has lower pH and higher Eh values than the surrounding rock volumes. As the mixing zone moves downwards, the zone with relatively low pH and higher Eh also is displaced to larger depths during the temperate period.

The geochemical modelling results presented offer a degree of detail for the description of the heterogeneity at the sites which is difficult to obtain from groundwater sampling in boreholes. The coupling of hydrogeological and geochemical models can therefore reduce the need for data within the vicinity of the repository volume, where the low permeability of the rock might preclude both groundwater sampling and in situ measurements of redox potentials. However, the description of the geochemical site heterogeneity is naturally dependent on the current geological and hydrogeological understanding of the sites.

The conclusions are not changed for the case of an increased greenhouse effect with an elongated temperate period, as it is expected that the hydrogeological and geochemical conditions will remain quite stable after the initial few thousand years when the Baltic shore line moves away from the repository locations.

For the permafrost and glacial periods, groundwater compositions are proposed based on the results from hydrological evaluations performed within the SR-Can project. It is concluded that for permafrost conditions groundwaters in the rock volume surrounding a repository will not affect negatively its performance since their movement will be restricted, if not totally static, depending on the vertical extent of the permafrost. However, under glacial conditions meltwaters are expected to penetrate deep into the bedrock, at least in rock domains of high permeability. If such low saline waters were to penetrate to the vicinity of the repository, designed to be hosted by low permeability rock domains, then, on the whole, the groundwaters

would affect negatively the stability of the bentonite buffer surrounding the canisters in the repository. It may be, however, that exchange mechanisms with the rock matrix pore water might increase the salinity of the penetrating groundwaters within these low permeable domains due to greater residence times.

An analysis of the possibility of penetration of O_2-rich meltwaters down to repository depths during glacial periods is made based on studies performed within the SR-Can project and elsewhere. It is concluded the inflow of oxygen in single fractures is neutralised by the process of matrix diffusion and dissolution of Fe(II) minerals in the rock matrix. For fracture zones, with water advective times down to repository depths of only a few years, advancement of O_2-rich waters to repository depth does not occur if variables are cautiously selected. For extreme situations, and given our present understanding of fracture zones, the occurrence of oxidizing conditions at repository depths within large fracture zones can not at present be completely ruled out, but at least they can be avoided in the repository design.

References

Ahokas H, Hellä P, Ahokas T, Hansen J, Koskinen K, Lehtinen A, Koskinen L, Löfman J, Mészáros F, Partamies S, Pitkänen P, Sievanen U, Marcos N, Snellman M, Vieno T, 2006. Control of water inflow and use of cement in ONKALO after penetration of fracture zone R19. POSIVA WR-2006-45, Posiva Oy, Olkiluoto, Finland.

Ahonen L, Vieno T, 1994. Effects of glacial meltwater on corrosion of copper canisters. YJT-94-13, Nuclear Waste Commission of Finnish Power Companies, Finland.

Alekseev A, Alekseeva T, Ostroumov V, Siegert C, Gradusov B, 2003. Mineral transformations in permafrost-affected soils, North Kolyma Lowland, Russia. Soil Sci. Soc. Am. J., 67: 596-605.

Appelo C A J, Postma D, 2005. Geochemistry, Groundwater & Pollution, 2nd. ed. Balkema, Rotterdam, The Netherlands.

Apps J A, van de Kamp P C, 1993. Energy gases of abiogenic origin in the Earth's crust. In: D.G. Howell (Editor), The Future of Energy Gases. U.S. Geological Survey Prof. Paper 1570; U.S. Gov. Printing Office, Washington, D.C., USA, pp. 81-132.

Ball J W, Nordstrom D K, 2001. User's manual for WATEQ4F, with revised thermodynamic data base and test cases for calculating speciation of major, trace, and redox elements in natural waters. USGS-OFR-91-183, U.S. Geological Survey, Menlo Park, California. Revised and reprinted April, 2001.

Banwart S, Gustafsson E, Laaksoharju M, Nilsson A-C, Tullborg E-L, Wallin B, 1994. Large-scale intrusion of shallow water into a vertical fracture zone in crystalline bedrock: initial hydrochemical perturbation during tunnel construction at the Äspö Hard Rock Laboratory, southeastern Sweden. Water Resour. Res., 30: 1747–1763.

Banwart S A, 1999. Reduction of iron(III) minerals by natural organic matter in groundwater. Geochim. Cosmochim. Acta, 63: 2919–2928.

Banwart S A, Gustafsson E, Laaksoharju M, 1999. Hydrological and reactive processes during rapid recharge to fracture zones. the Äspö large scale redox experiment. Appl. Geochem., 14: 873–892.

Bath A, Milodowski A, Ruotsalainen P, Tullborg E-L, Cortés Ruiz A, Aranyossy J-F, 2000. Evidence from mineralogy and geochemistry for the evolution of groundwater systems during the quaternary for use in radioactive waste repository safety assessment (EQUIP project). EUR 19613 EN, European Commission, Nuclear Science and Technology.

Bath A, 2005. Geochemical investigations of groundwater stability. SKI Report 2006:12, Swedish Nuclear Power Inspectorate, Stockholm, Sweden.

Benning L G, Wilkin R T, Barnes H L, 2000. Reaction pathways in the Fe-S system below 100°C. Chem. Geol., 167: 25–51.

Berner R A, 1967. Thermodynamic stability of sedimentary iron sulfides. Am. J. Sci., 265: 773–785.

Berner U R, 1987. Modeling porewater chemistry in hydrated Portland cement. In: J.K. Bates, W. B. Seefeldt (Editors), Scientific Basis for Nuclear Waste Management X. Mat. Res. Soc. Symp. Proc., Vol. 84. Mater. Res. Soc., Pittsburgh, Penn., Symp. held in Boston, Mass., on Dec. 1986, pp. 319–330.

Bonneville S, Van Cappellen P, Behrends T, 2004. Microbial reduction of iron(III) oxyhydroxides: effects of mineral solubility and availability. Chem. Geol., 212: 255–268.

Boulton G S, Zatsepin S, Maillot B, 2001. Analysis of groundwater flow beneath ice sheets. SKB TR-01-06, Svensk Kärnbränslehantering AB.

Brandt F, Bosbach D, Krawczyk-Bärsch E, Arnold T, Bernhard G, 2003. Chlorite dissolution in the acid pH-range: A combined microscopic and macroscopic approach. Geochim. Cosmochim. Acta, 67: 1451–1461.

Brown G H, Tranter M, Sharp M J, Davies T D, Tsiouris S, 1994. Dissolved oxygen variations in alpine glacial meltwaters. Earth Surface Processes and Landforms, 19: 247–253.

Brown G H, 2002. Glacier meltwater hydrochemistry. Appl. Geochem., 17: 855–883.

Bruno J, Duro L, de Pablo J, Casas I, Ayora C, Delgado J, Gimeno M J, Peña J, Linklater C, Pérez del Villar L, Gómez P, 1998. Estimation of the concentrations of trace metals in natural systems. The application of codissolution and coprecipitation approaches to El Berrocal (Spain) and Poços de Caldas (Brazil). Chem. Geol., 151: 277–291.

Bågander L E, Carman R, 1994. In situ determination of the apparent solubility product of amorphous iron sulphide. Appl. Geochem., 9: 379–386.

Carman R, Rahm L, 1997. Early diagenesis and chemical characteristics of interstitial water and sediments in the deep deposition bottoms of the Baltic proper. Deep-sea Res., 37: 25–47.

Casanova J, Négrel P, Blomqvist R, 2005. Boron isotope fractionation in groundwaters as an indicator of past permafrost conditions in the fractured crystalline bedrock of the Fennoscandian shield. Water Res., 39: 362–370.

Chapman N A, McKinley I G, Penna Franca E, Shea M E, Smellie J A T, 1992. The Poços de Caldas Project: an introduction and summary of its implications for radioactive waste disposal. J. Geochem. Explor., 45: 1–24.

Chen W-F, Liu T-K, 2005. Ion activity products of iron sulfides in groundwaters: implications from the Choshui fan-delta, Western Taiwan. Geochim. Cosmochim. Acta, 69: 3535–3544.

Cooper R J, Wadham J L, Tranter M, Hodgkins R, Peters N E, 2002. Groundwater hydrochemistry in the active layer of the proglacial zone, Finsterwalderbreen, Svalbard. J. Hydrol., 269: 208–223.

Cornell R M, Schwertmann U, 2003. The iron oxides, 2nd. ed. Wiley-VCH, Weinheim, Germany.

Culkin F, Cox R A, 1966. Sodium, potassium, magnesium, calcium and strontium in sea water. Deep-sea Res., 13: 789–804.

Davison W, 1991. The solubility of iron sulfides in synthetic and natural waters at ambient temperatures. Aquat. Sci., 53, 309–329. Aquat. Sci., 53: 309–329.

Davison W, Phillips N, Tabner B J, 1999. Soluble iron sulfide species in natural waters: Reappraisal of their stoichiometry and stability constants. Aquat. Sci., 61: 23–43.

Degueldre C, 1994. Colloid properties in groundwaters from crystalline formations. Nagra-TB-92-05, National Cooperative for the Disposal of Nuclear Waste (Nagra), Wettingen, Switzerland.

Degueldre C, Grauer R, Laube A, Oess A, Silby H, 1996. Colloid properties in granitic groundwater systems. II: Stability and transport study. Appl. Geochem., 11: 697–710.

Domènech C, Arcos D, Duro L, Grandia F, 2006. Effect of the mineral precipitation-dissolution at tunnel walls during the operational and post-operational phases. SKB R-06-108, Svensk Kärnbränslehantering AB.

Drake H, Sandström B, Tullborg E-L, 2006. Mineralogy and geochemistry of rocks and fracture fillings from Forsmark and Oskarshamn: Compilation of data for SR-Can. SKB R-06-109, Svensk Kärnbränslehantering AB.

Drew M C, 1983. Plant injury and adaptation to oxygen deficiency in the root environment: A review. Plant and Soil, 75: 179–199.

Engesgaard P, Kipp K L, 1992. A geochemical transport model for redox-controlled movement of mineral fronts in groundwater flow systems: A case of nitrate removal by oxidation of pyrite. Water Resour. Res., 28: 2829–2843.

Engkvist I, Albinsson Y, Johansson Engkvist W, 1996. The long-term stability of cement – Leaching tests. SKB-TR-96-09, Svensk Kärnbränslehantering AB.

Follin S, Svensson U, 2003. On the role of mesh discretisation and salinity for the occurrence of local flow cells. Results from a regional-scale groundwater flow model of Östra Götaland. SKB-R-03-23, Svensk Kärnbränslehantering AB.

Follin S, Stigsson M, Svensson U, 2005. Regional hydrogeological simulations for Forsmark – numerical modelling using DarcyTools. Preliminary site description Forsmark area – version 1.2. SKB R-05-60, Svensk Kärnbränslehantering AB.

Follin S, Stigsson M, Svensson U, 2006. Hydrogeological DFN modelling using structural and hydraulic data from KLX04. Preliminary site description. Laxemar subarea – version 1.2. SKB R-06-24, Svensk Kärnbränslehantering AB.

Frape S K, Blyth A, Blomqvist R, McNutt R H, Gascoyne M, 2005. Deep fluids in the continents: II. Crystalline Rocks. In: J.I. Drever (Editor), Surface and ground water, weathering, and soils. Treatise on Geochemistry, Vol. **5.** Elsevier, Amsterdam, The Netherlands, pp. 541–580.

Freedman V L, Ibaraki M, 2003. Coupled reactive mass transport and fluid flow: Issues in model verification. Adv. Water Res., 26: 117–127.

Gascoyne M, 1999. Long-term maintenance of reducing conditions in a spent nuclear fuel repository. SKB R-99-41, Svensk Kärnbränslehantering AB.

Gascoyne M, 2004. Hydrogeochemistry, groundwater ages and sources of salts in a granitic batholith on the Canadian Shield, southeastern Manitoba. Appl. Geochem., 19: 519–560.

Gimeno M J, Auqué L F, Gómez J B, 2004. Appendix 4: Mass balance modelling. In: Hydrogeochemical evaluation for Simpevarp model version 1.2. Preliminary site description of the Simpevarp area. SKB R-04-74, Svensk Kärnbränslehantering AB, pp. 289–336.

Gimeno M J, Auqué L F, Gómez J B, 2005. Appendix 3: PHREEQC modelling. In: Hydrogeochemical evaluation. Preliminary site description. Forsmark area – version 1.2. SKB R-05-17, Svensk Kärnbränslehantering AB, pp. 263–322.

Gómez J B, Laaksharju M, Skårman E, Gurban I, 2006a. M3 version 3.0: Concepts, methods, and mathematical formulation. SKB TR-06-27, Svensk Kärnbränslehantering AB.

Gómez P, Garralón A, Buil B, Turrero M J, Sánchez L, de la Cruz B, 2006b. Modeling of geochemical processes related to uranium mobilization in the groundwater of a uranium mine. Sci. Total Env., 366: 295–309.

Grandia F, Domènech C, Arcos D, Duro L, 2006. Assessment of the oxygen consumption in the backfill. SKB R-06-106, Svensk Kärnbränslehantering AB.

Grenthe I, Stumm W, Laaksoharju M, Nilsson A-C, Wikberg P, 1992. Redox potentials and redox reactions in deep groundwater systems. Chem. Geol., 98: 131–150.

Grimaud D, Beaucaire C, Michard G, 1990. Modelling of the evolution of ground waters in a granite system at low temperature: the Stripa ground waters, Sweden. Appl. Geochem., 5: 515–525.

Guimerà J, Duro L, Jordana S, Bruno J, 1999. Effects of ice melting and redox front migration in fractured rocks of low permeability. SKB TR-99-19, Svensk Kärnbränslehantering AB.

Guimerà J, Duro L, Delos A, 2006. Changes in groundwater composition as a consequence of deglaciation: implications for PA. SKB-R-06-105, Svensk Kärnbränslehantering AB.

Gustafsson Å B, Puigdomenech I, 2003. The effect of pH on chlorite dissolution rates at 25°C. In: R.J. Finch, D.B. Bullen (Editors), Scientific Basis for Nuclear Waste Management XXVI. Mat. Res. Soc. Symp. Proc., Vol. 757. Mater. Res. Soc., Pittsburgh, Penn., pp. 649–655.

Gustafsson Å, Molera M, Puigdomenech I, 2004. Study of Ni(II) sorption on chlorite – a fracture filling mineral in granites. In: J.M. Hanchar, S. Stroes-Gascoyne, L. Browning (Editors), Scientific Basis for Nuclear Waste Management XXVIII. Mat. Res. Soc. Symp. Proc., Vol. 824. Mater. Res. Soc., Warrendale, Penn., pp. 373–378.

Hallbeck L, Grivé M, Gaona X, Duro L, Bruno J, 2006. Main organic materials in a repository for high level radioactive waste. SKB R-06-104, Svensk Kärnbränslehantering AB.

Hartley L, Cox I, Hunter F, Jackson P, Joyce S, Swift B, Gylling B, Marsic N, 2005. Regional hydrogeological simulations for Forsmark – numerical modelling using CONNECTFLOW. Preliminary site description Forsmark area – version 1.2. SKB R-05-32, Svensk Kärnbränslehantering AB.

Hartley L, Hoch A, Jackson P, Joyce S, McCarthy R, Rodwell W, Swift B, Marsic N, 2006a. Groundwater flow and transport modelling during the temperate period for the SR-Can assessment: Forsmark area – Version 1.2. SKB R-06-98, Svensk Kärnbränslehantering AB.

Hartley L, Hoch A, Jackson P, Joyce S, McCarthy R, Swift B, Gylling B, Marsic N, 2006b. Groundwater flow and transport modelling during the temperate period for the SR-Can assessment: Laxemar area – Version 1.2. SKB R-06-99, Svensk Kärnbränslehantering AB.

Hartley L, Hunter F, Jackson P, McCarthy R, Gylling B, Marsic N, 2006c. Regional hydrogeological simulations using CONNECTFLOW. Preliminary site description Laxemar subarea – version 1.2. SKB R-06-23, Svensk Kärnbränslehantering AB.

Hoehn E, Eikenberg J, Fierz T, Drost W, Reichlmayr E, 1998. The Grimsel Migration Experiment: field injection-withdrawal experiments in fractured rock with sorbing tracers. J. Contaminant Hydrol., 34: 85–106.

Holmes D C, Pitty A E, Noy D J, 1992. Geomorphological and hydrogeological features of the Poços de Caldas caldera analogue study sites. J. Geochem. Explor., 45: 215–247.

IPCC, 2001. Climate Change 2001: Synthesis Report A. Contribution of Working Groups I, II, and III to the Third Assessment Report of the Intergovernmental Panel on Climate Change, R.T. Watson, the Core Writing Team (Editors). Cambridge University Press, Cambridge UK, 398 pp.

Jaquet O, Siegel P, 2006. Simpevarp 1.2 – Regional groundwater flow model for a glaciation scenario. SKB R-06-100, Svensk Kärnbränslehantering AB.

Jockwer N, Wieczorek K, 2003. Gas generation measurements in the FEBEX project. In: Clays in Natural and Engineered Barriers for Radioactive Waste Confinement. Experiments in Underground Laboratories. Sci. & Technol. Ser. ANDRA: Agence nationale pour la gestion des déchets radioactifs, Châtenay-Malabry, France, pp. 108–117. ISBN: 2-9510108-5-0. Proc. from the Int. Meeting held in Reims (France) 9–12 Dec.2002.

Kaija J, Blomqvist R, Ahonen L, Hakkarainen V, 1998. The hydrogeochemical database of Palmottu. 1998 version. The Palmottu Natural Analogue Project. Technical Report 98-08, Geological Survey of Finland (Nuclear Waste Disposal Research), Espoo, Finland. 4 pp. and 56 Appendices.

Kankainen T, 1986. Loviisa power station final disposal of reactor waste. On the age and origin of groundwater from the Rapakivi granite on the island of Hästholmen. YJT-86-29, Nuclear Waste Commission of Finnish Power Companies, Helsinki, Finland.

Kay R L F, Bath A H, 1982. Groundwater geochemical studies at the Altnabreac Research Site. ENPU 82-12, Environmental Protection Unit, Institute of Geological Sciences, Natural Environment Research Council, UK.

Kharaka Y, Hanor J S, 2005. Deep fluids in the continents: I. Sedimentary basins. In: J.I. Drever (Editor), Surface and ground water, weathering, and soils. Treatise on Geochemistry, Vol. 5. Elsevier, Amsterdam, The Netherlands, pp. 499–540.

Kilchmann S, Waber H N, Parriaux A, Bensimon M, 2004. Natural tracers in recent groundwaters from different Alpine aquifers. Hydrogeol. J., 12: 643–661.

King-Clayton L, Chapman N, Ericsson L O, Kautsky F, 1997. Glaciation and Hydrogeology. Workshop on the Impact of Climate Change & Glaciations on Rock Stresses, Groundwater Flow and Hydrochemistry – Past, Present and Future. Workshop Proceedings. SKI-R-97:13, Swedish Nuclear Power Inspectorate, Stockholm, Sweden.

Laaksoharju M, Smellie J, Nilsson A-C, Skårman C, 1995. Groundwater sampling and chemical characterisation of the Laxemar deep borehole KLX02. SKB TR-95-05, Svensk Kärnbränslehantering AB.

Laaksoharju M, Wallin B, 1997. Evolution of the groundwater chemistry at the Äspö Hard Rock Laboratory. Proceedings of the second Äspö International Geochemistry Workshop, June 6–7, 1995. SKB ICR-97-04, Svensk Kärnbränslehantering AB.

Laaksoharju M, Gurban I, Skårman C, 1998. Summary of hydrochemical conditions at Aberg, Beberg and Ceberg. SKB TR-98-03, Svensk Kärnbränslehantering AB.

Laaksoharju M, Skårman C, Skårman E, 1999a. Multivariate mixing and mass balance (M3) calculations, a new tool for decoding hydrogeochemical information. Appl. Geochem., 14: 861–871.

Laaksoharju M, Tullborg E-L, Wikberg P, Wallin B, Smellie J, 1999b. Hydrogeochemical conditions and evolution at the Äspö HRL, Sweden. Appl. Geochem., 14: 835–859.

Langmuir D, 1969. The Gibbs free energies of substances in the system Fe-O_2-H_2O-CO_2 at 25°C. In: Geological Survey Research 1969. U.S.G.S. Prof. Paper, Vol. 650-B, pp. B180–B184.

Langmuir D, Whittemore D O, 1971. Variations in the stability of precipitated ferric oxyhydroxides. In: J.D. Hem (Editor), Nonequilibrium Systems in Natural Water Chemistry. Advances in Chemistry Series 106. Amer. Chem. Soc., Washington, D.C., pp. 209–234. chap. 8.

Langmuir D, 1997. Aqueous Environmental Geochemistry. Prentice Hall, New York, NY, USA.

Larsen O, Postma D, 2001. Kinetics of the reductive bulk dissolution of lepidocrocite, ferrihydrite, and goethite. Geochim. Cosmochim. Acta, 65: 1367–1379.

Lazo C, Karnland O, Tullborg E-L, Puigdomenech I, 2003. Redox properties of MX-80 and Montigel bentonite-water systems. In: R.J. Finch, D.B. Bullen (Editors), Scientific Basis for Nuclear Waste Management XXVI. Mat. Res. Soc. Symp. Proc., Vol. 75**7.** Mater. Res. Soc., Pittsburgh, Penn., pp. 643–648.

Lidmar-Bergström K, 1996. Long term morphotectonic evolution in Sweden. Geomorphology, 16: 33–59.

Lindberg R D, Runnells D D, 1984. Ground water redox reactions: an analysis of equilibrium state applied to Eh measurements and geochemical modeling. Science, 225: 925–927.

Liu C W, Narasimhan T N, 1989. Redox-controlled multiple-species reactive chemical transport. 1. Model Development. Water Resour. Res., 25: 869–882.

Louvat D, Michelot J L, Aranyossy J F, 1997. Salinity origin and residence time of the Äspö groundwater system. In: M. Laaksoharju, B. Wallin (Editors), Evolution of the Groundwater Chemistry at the Äspö Hard Rock Laboratory. Proceedings of the Second Äspö International Geochemistry Workshop, June 6–7, 1995. SKB ICR-97-04. Svensk Kärnbränslehantering AB.

Louvat D, Michelot J L, Aranyossy J F, 1999. Origin and residence time of salinity in the Äspö groundwater system. Appl. Geochem., 14: 917–925.

Lowson R T, Comarmond M-C J, Rajaratnam G, Brown P L, 2005. The kinetics of the dissolution of chlorite as a function of pH and at 25°C. Geochim. Cosmochim. Acta, 69: 1687–1699.

Luna M, Arcos D, Duro L, 2006. Effects of grouting, shotcreting and concrete leachates on backfill geochemistry. SKB R-06-107, Svensk Kärnbränslehantering AB.

Macalady D L, Langmuir D, Grundl T, Elzerman A, 1990. Use of model-generated Fe^{3+} ion activities to compute Eh and ferric oxyhydroxide solubilities in anaerobic systems. In: D.C. Melchior, R.L. Basett (Editors), Chemical Modeling of Aqueous Systems II. A.C.S. Symp. Ser. 416**.** Amer. Chem. Soc., Washington, D.C., pp. 350–367.

MacKenzie A B, Scott R D, Linsalata P, Miekeley N, 1992. Natural decay series studies of the redox front system in the Poços de Caldas uranium mineralization. J. Geochem. Explor., 45: 289–322.

Majzlan J, Navrotsky A, Schwertmann U, 2004. Thermodynamics of iron oxides: Part III. Enthalpies of formation and stability of ferrihydrite ($\sim Fe(OH)_3$), schwertmannite ($\sim FeO(OH)_{3/4}(SO_4)_{1/8}$), and ε-$Fe_2O_3$. Geochim. Cosmochim. Acta, 68: 1049–1059.

Malmström M, Banwart S, 1997. Biotite dissolution at 25°C: The pH dependence of dissolution rate and stoichiometry. Geochim. Cosmochim. Acta, 61: 2779–2799.

Martinerie P, Raynaud D, Etheridge D M, Barnola J-M, Mazaudier D, 1992. Physical and climatic parameters which influence the air content in polar ice. Earth Planet. Sci. Lett., 112: 1–13.

Michard G, 1983. Recueil de données thermodynamiques concernant les équilibres eaux minéraux dans les réservoirs géothermaux. EUR 8590 FR, Commission of the European Communities, Brussels, Belgium. In French.

Michard G, 1989. Equilibres chimiques dans les eaux naturelles. Ed. Publisud, Paris, France. In French.

Milodowski A E, Tullborg E-L, Buil B, Gómez P, Turrero M-J, Haszeldine S, G E, Gillespie M R, Torres T, Ortiz J E, Zachariáš J, Silar J, Chvátal M, Strnad L, Šebek O, Bouch J E, Chenery S R, Chenery C, Shepherd T J, McKervey J A, 2005. Application of mineralogical petrological and geochemical tools for evaluating the palaeohydrogeological evolution of the PADAMOT Study sites. PADAMOT PROJECT. Technical Report WP2, UK Nirex Ltd, Harwell, UK. EU FP5 Contract nr FIKW-CT2001-20129.

Molinero-Huguet J, Samper-Calvete F J, Zhang G, Yang C, 2004. Biogeochemical reactive transport model of the Redox Zone experiment of the Äspö Hard Rock Laboratory in Sweden. Nucl. Technol., 148: 151–165.

Mäder U, Frieg B, Puigdomenech I, Decombarieu M, Yui M, 2004. Hyperalkaline cement leachate-rock interaction and radionuclide transport in a fractured host rock (HPF Project). In: V.M. Oversby, L.O. Werme (Editors), Scientific Basis for Nuclear Waste Management XXVII. Mat. Res. Soc. Symp. Proc., Vol. 807. Mater. Res. Soc., Pittsburgh, Penn., pp. 861–866.

Négrel P, Casanova J, 2005. Comparison of the Sr isotopic signatures in brines of the Canadian and Fennoscandian shields. Appl. Geochem., 20: 749–766.

Neretnieks I, 1986. Some uses for natural analogues in assessing the function of a HLW repository. Chem. Geol., 55: 175–188.

Nordstrom D K, Munoz J L, 1985. Geochemical Thermodynamics, 2nd ed. The Benjamin/ Cummings Publ. Co., Menlo Park, California, 477 pp.

Nordstrom D K, Ball J W, Donahoe R J, Whittemore D, 1989. Groundwater chemistry and water-rock interactions at Stripa. Geochim. Cosmochim. Acta, 53: 1727–1740.

Nordstrom D K, Plummer L N, Langmuir D, Busenberg E, May H M, Jones B F, Parkhurst D, 1990. Revised chemical equilibrium data for major water-mineral reactions and their limitations. In: D.C. Melchior, R.L. Basett (Editors), Chemical Modeling of Aqueous Systems II. A.C.S. Symp. Ser. 416. Amer. Chem. Soc., Washington, D.C., pp. 398–413.

Nordstrom D K, McNutt R H, Puigdomenech I, Smellie J A T, Wolf M, 1992. Ground water chemistry and geochemical modeling of water-rock interactions at the Osamu Utsumi mine and the Morro do Ferro analogue study sites, Poços de Caldas, Minas Gerais, Brazil. J. Geochem. Explor., 45: 249–287.

Parkhurst D L, Appelo C A J, 1999. User's guide to PHREEQC (Version 2) – A computer program for speciation, batch-reaction, one-dimensional transport, and inverse geochemical calculations. USGS/WRI-99-4259, U.S. Geol. Survey, Denver, Colorado. 312 p.

Pedersen K, Kennedy C, Nederfeldt K-G, Bergelin A, 2004. Äspö Hard Rock Laboratory. Prototype repository. Chemical measurements in buffer and backfill; sampling and analyses of gases. SKB IPR-04-26, Svensk Kärnbränslehantering AB.

Pedersen H D, Postma D, Jakobsen R, Larsen O, 2005. Fast transformation of iron oxyhydroxides by the catalytic action of aqueous Fe(II). Geochim. Cosmochim. Acta, 69: 3967–3977.

Pedersen K, 2006. Microbiology of transitional groundwater of the porous overburden and underlying fractured bedrock aquifers in Olkiluoto, Finland. POSIVA WR-2006-09, Posiva Oy, Olkiluoto, Finland.

Peterman Z E, Wallin B, 1999. Synopsis of strontium isotope variations in groundwater at Äspö, southern Sweden. Appl. Geochem., 14: 939–951.

Pirhonen V, Pitkänen P, 1991. Redox capacity of crystalline rocks. Laboratory studies under 100 bar oxygen gas pressure. SKB TR-91-55, Svensk Kärnbränslehantering AB.

Pitkänen P, Luukkonen A, Ruotsalainen P, Leino-Forsman H, Vuorinen U, 1999. Geochemical modelling of groundwater evolution and residence time at the Olkiluoto site. POSIVA-98-10, Posiva Oy, Helsinki, Finland.

Pitkänen P, Luukkonen A, Ruotsalainen P, Leino-Forsman H, Vuorinen U, 2001. Geochemical modelling of groundwater evolution and residence time at the Hästholmen site. POSIVA-2001-01, Posiva Oy, Helsinki, Finland.

Pitkänen P, Partamies S, Luukkonen A, 2004. Hydrogeochemical interpretation of baseline groundwater conditions at the Olkiluoto site. POSIVA 2003-07, Posiva Oy, Helsinki, Finland.

Postma D, 1993. The reactivity of iron oxides in sediments: a kinetic approach. Geochim. Cosmochim. Acta, 57: 5027–5034.

Puigdomenech I, Kotelnikova S, Pedersen K, Tullborg E-L, 2000. In-Situ determination of O2 uptake by geologic media: Field data for the redox experiment in detailed scale (REX). SKB IPR-00-23, Svensk Kärnbränslehantering AB.

Puigdomenech I, Ambrosi J-P, Eisenlohr L, Lartigue J-E, Banwart S A, Bateman K, Milodowski A E, West J M, Griffault L, Gustafsson E, Hama K, Yoshida H, Kotelnikova S, Pedersen K, Michaud V, Trotignon L, Rivas Perez J, Tullborg E-L, 2001a. O_2 depletion in granitic media: The REX project. SKB TR-01-05, Svensk Kärnbränslehantering AB.

Puigdomenech I, Gurban I, Laaksoharju M, Luukkonen A, Löfman J, Pitkänen P, Rhén I, Routsalainen P, Smellie J, Snellman M, Svensson U, Tullborg E-L, Wallin B, Vuorinen U, Wikberg P, 2001b. Hydrochemical Stability of groundwaters surrounding a spent nuclear fuel repository in a 100,000 year perspective. SKB TR-01-28, Svensk Kärnbränslehantering AB.

Rivas Perez J, Banwart S A, Puigdomenech I, 2005. The kinetics of $O_{2(aq)}$ reduction by structural ferrous iron in naturally occurring ferrous silicate minerals. Appl. Geochem., 20: 2003–2016.

Romero L, Neretnieks I, Moreno L, 1992. Movement of the redox front at the Osamu Utsumi uranium mine, Poços de Caldas, Brazil. J. Geochem. Explor., 45: 471–502.

Ruskeeniemi T, Ahonen L, Paananen M, Frape S, Stotler R, Hobbs M, Kaija J, Degnan P, Blomqvist R, Jensen M, Lehto K, Moren L, Puigdomenech I, Snellman M, 2004. Permafrost at Lupin. Report of phase II. Permafrost project GTK-SKB-POSIVA-NIREX-OPG. Report YST-119, Geological Survey of Finland, Helsinki, Finland.

Samson S D, Nagy K L, Cotton W B, III, 2005. Transient and quasi-steady-state dissolution of biotite at 22–25°C in high pH, sodium, nitrate, and aluminate solutions. Geochim. Cosmochim. Acta, 69: 399–413.

Schwertmann U, Murad E, 1983. Effect of pH on the formation of goethite and hematite from ferrihydrite. Clays Clay Min., 31: 277–284.

Sharp M, Parkes J, Cragg B, Fairchild I J, Lamb H, Tranter M, 1999. Widespread bacterial populations at glacier beds and their relationship to rock weathering and carbon cycling. Geology, 27: 107–110.

Sidborn M, Neretnieks I, 2003. Modelling of biochemical processes in rocks: Oxygen depletion by pyrite oxidation – Model development and exploratory simulations. In: R.J. Finch, D.B. Bullen (Editors), Scientific Basis for Nuclear Waste Management XXVI. Mat. Res. Soc. Symp. Proc., Vol. 757. Mater. Res. Soc., Pittsburgh, Penn., pp. 553–558.

Sidborn M, Neretnieks I, 2004. Modelling biochemical processes in rocks: Analysis and exploratory simulations of competition of different processes important for ferrous mineral oxidation and oxygen depletion. In: V.M. Oversby, L.O. Werme (Editors), Scientific Basis for Nuclear Waste Management XXVII. Mat. Res. Soc. Symp. Proc., Vol. 807. Mater. Res. Soc., Pittsburgh, Penn., pp. 829–834.

Sidborn M, Neretnieks I, 2006. Long term redox evolution in granitic rocks: Modelling the redox front propagation in the rock matrix. Appl. Geochem. (submitted).

Silver W L, Lugo A E, Keller M, 1999. Soil oxygen availability and biogeochemistry along rainfall and topographic gradients in upland wet tropical forest soils. Biogeochem., 44: 301–328.

Sjöberg L, Georgala D, Rickard D, 1984. Origin of interstitial water compositions in postglacial black clays (Northeastern Sweden). Chem. Geol., 42: 147–158.

SKB, 2004. Hydrogeochemical evaluation for Simpevarp model version 1.2. Preliminary site description of the Simpevarp area. SKB R-04-74, Svensk Kärnbränslehantering AB.

SKB, 2005a. Hydrogeochemical evaluation. Preliminary site description Forsmark area – version 1.2. SKB R-05-17, Svensk Kärnbränslehantering AB.

SKB, 2005b. Preliminary site description Forsmark area – version 1.2. SKB R-05-18, Svensk Kärnbränslehantering AB.

SKB, 2006a. Buffer and backfill process report for the safety assessment SR-Can. SKB TR-06-18, Svensk Kärnbränslehantering AB.

SKB, 2006b. Climate and climate-related issues for the safety assessment SR-Can. SKB TR-06-23, Svensk Kärnbränslehantering AB.

SKB, 2006c. Data report for the safety assessment SR-Can. SKB TR-06-25, Svensk Kärnbränslehantering AB.

SKB, 2006d. Geosphere process report for the safety assessment SR-Can. SKB TR-06-19, Svensk Kärnbränslehantering AB.

SKB, 2006e. Hydrogeochemical evaluation. Preliminary site description Laxemar subarea – version 1.2. SKB R-06-12, Svensk Kärnbränslehantering AB.

SKB, 2006f. Initial state report for the safety assessment SR-Can. SKB TR-06-21, Svensk Kärnbränslehantering AB.

SKB, 2006g. Long-term safety for KBS-3 repositories at Forsmark and Laxemar – a first evaluation. Main report of the SR-Can project. SKB TR-06-09, Svensk Kärnbränslehantering AB.

SKB, 2006h. Preliminary site description Laxemar subarea – version 1.2. SKB R-06-10, Svensk Kärnbränslehantering AB.

Smellie J, Larsson N-Å, Wikberg P, Carlsson L, 1985. Hydrochemical investigations in crystalline bedrock in relation to existing hydraulic conditions: experience from the SKB test-sites in Sweden. SKB TR-85-11, Svensk Kärnbränslehantering AB.

Smellie J, Larsson N-Å, Wikberg P, Puigdomenech I, Tullborg E-L, 1987. Hydrochemical investigations in crystalline bedrock in relation to existing hydraulic conditions: Klipperås test-site, Småland, southern Sweden. SKB TR-87-21, Svensk Kärnbränslehantering AB, 115 p.

Smellie J A T, Wikberg P, 1989. Hydrochemical investigations at the Finnsjön site, central Sweden. J. Hydrol., 126: 129–158.

Smellie J, Laaksoharju M, 1992. The Äspö Hard Rock Laboratory: Final evaluation of the hydrogeochemical pre-investigations in relation to existing geologic and hydraulic conditions. SKB TR-92-31, Svensk Kärnbränslehantering AB.

Smellie J A T, Laaksoharju M, Wikberg P, 1995. Äspö, SE Sweden: a natural groundwater flow model derived from hydrogeochemical observations. J. Hydrol., 172: 147–169.

Smellie J, Tullborg E-L, Waber N, Morales T, 2006. Appendix 1: Explorative analysis and expert judgement of major components and isotopes. In: Hydrogeochemical evaluation. Preliminary site description. Laxemar subarea – version 1.2. SKB R-06-12. Svensk Kärnbränslehantering AB, pp. 83–269.

Sohlenius G, Emeis K-C, Andrén E, Andrén T, Kohly A, 2001. Development of anoxia during the Holocene fresh-brackish water transition in the Baltic Sea. Marine Geol., 177: 221–242.

Starinsky A, Katz A, 2003. The formation of natural cryogenic brines. Geochim. Cosmochim. Acta, 67: 1475–1484.

Stefánsson A, Arnórsson S, Sveinbjörnsdóttir Á E, 2005. Redox reactions and potentials in natural waters at disequilibrium. Chem. Geol., 221: 289–311.

Stipp S L S, Hansen M, Kristensen R, Hochella J, M. F., Bennedsen L, Dideriksen K, Balic-Zunic T, Léonard D, Mathieu H J, 2002. Behaviour of Fe-oxides relevant to contaminant uptake in the environment. Chem. Geol., 190: 321–337.

Stumm W, Morgan J J, 1996. Aquatic Chemistry. Chemical Equilibria and Rates in Natural Waters, 3rd ed. John Wiley & Sons, New York, 1022 pp.

Svensson U, 1999. Subglacial groundwater flow at Äspö as governed by basal melting and ice tunnels. SKB R-99-38, Svensk Kärnbränslehantering AB.

Svensson U, 2005. The Forsmark repository – Modelling changes in the flow, pressure and salinity fields, due to a repository for spent nuclear fuel. SKB R-05-57, Svensk Kärnbränslehantering AB.

Svensson U, 2006. The Laxemar repository – Modelling changes in the flow, pressure and salinity fields, due to a repository for spent nuclear fuel. SKB R-06-57, Svensk Kärnbränslehantering AB.

Thorstenson D C, 1984. The concept of electron activity and its relation to redox potentials in aqueous geochemical systems. USGS Open-File Report 84-072, U.S. Geol. Survey, Denver, Colorado, USA.

Thury M, Gautschi A, Mazurek M, Müller W H, Naef H, Pearson F J, Vomvoris S, Wilson W, 1994. Geology and hydrology of the crystalline basement of Northern Switzerland. Synthesis of regional investigations 1981–1993 within the Nagra radioactive waste disposal program. Nagra-NTB-93-01, National Cooperative for the Disposal of Nuclear Waste (Nagra), Wettingen, Switzerland.

Torstenfelt B, Allard B, Johansson W, Ittner T, 1983. Iron content and reducing capacity of granites and bentonite. SKBF/KBS TR-83-36, Svensk Kärnbränslehantering AB.

Trotignon L, Beaucaire C, Louvat D, Aranyossy J F, 1997. Equilibrium geochemical modelling of Äspö groundwaters: a sensitivity study to model parameters. In: M. Laaksoharju, B. Wallin (Editors), Evolution of the Groundwater Chemistry at the Äspö Hard Rock Laboratory. Proceedings of the Second Äspö International Geochemistry Workshop, June 6–7, 1995. SKB ICR-97-04. Svensk Kärnbränslehantering AB.

Trotignon L, Beaucaire C, Louvat D, Aranyossy J F, 1999. Equilibrium geochemical modelling of Äspö groundwaters: a sensitivity study of thermodynamic equilibrium constants. Appl. Geochem., 14: 907–916.

Trotignon L, Michaud V, Lartigue J-E, Ambrosi J-P, Eisenlohr L, Griffault L, de Combarieu M, Daumas S, 2002. Laboratory simulation of an oxidizing perturbation in a deep granite environment. Geochim. Cosmochim. Acta, 66: 2583–2601.

Tullborg E-L, Larson S Å, 1982. Fissure fillings from Finnsjön and Studsvik, Sweden. Identification, chemistry and dating. SKBF/KBS TR-82-20, Svensk Kärnbränslehantering AB.

Tullborg E-L, 1986. Fissure fillings from the Klipperås study site. SKB TR-86-10, Svensk Kärnbränslehantering AB.

Tullborg E-L, 1997a. How do we recognize remnants of glacial meltwater in the bedrock? In: L. King-Clayton, N. Chapman, L.O. Ericsson, F. Kautsky (Editors), Glaciation and Hydrogeology. Workshop on the Impact of Climate Change & Glaciations on Rock Stresses, Groundwater Flow and Hydrochemistry – Past, Present and Future. Workshop Proceedings. SKI-R-97:13. Swedish Nuclear Power Inspectorate, Stockholm, Sweden, pp. A75–A76.

Tullborg E-L, 1997b. Recognition of low-temperature processes in the Fennoscandian shield. Ph.D. Thesis, Dept. Geol., Earth Sciences Centre, Göteborg University, Göteborg, Sweden.

Tullborg E-L, 2004. Palaeohydrogeological evidences from fracture filling minerals – Results from the Äspö/Laxemar area. In: V.M. Oversby, L.O. Werme (Editors), Scientific Basis for Nuclear Waste Management XXVII. Mat. Res. Soc. Symp. Proc., Vol. 807. Mater. Res. Soc., Pittsburgh, Penn., pp. 873–878.

Tung H C, Bramall N E, Price P B, 2005. Microbial origin of excess methane in glacial ice and implications for life on Mars. PNAS, 102: 18292–18296.

Wallin B, 1995. Palaeohydrological implications in the Baltic area and its relation to the groundwater at Äspö, south-eastern Sweden – A literature study. SKB TR-95-06, Svensk Kärnbränslehantering AB.

Washington J W, Endale D M, Samarkina L P, Chappell K E, 2004. Kinetic control of oxidation state at thermodynamically buffered potentials in subsurface waters. Geochim. Cosmochim. Acta, 68: 4831–4842.

Wersin P, Bruno J, Laaksoharju M, 1994. The implications of soil acidification on a future HLW repository. Part II: Influence on deep granitic groundwater. The Klipperås study site as test case. SKB TR 94-31, Svensk Kärnbränslehantering AB.

Westman P, Wastegård S, Schoning K, Gustafsson B, Omstedt A, 1999. Salinity change in the Baltic Sea during the last 8,500 years: evidence, causes and models. SKB TR-99-38, Svensk Kärnbränslehantering AB.

Vidstrand P, Svensson U, Follin S, 2006. Simulation of hydrodynamic effects of salt rejection due to permafrost. Hydrogeological numerical model of density-driven mixing, at a regional scale, due to a high salinity pulse. SKB R-06-101, Svensk Kärnbränslehantering AB.

Vieno T, Nordman H, 1999. Safety assessment of spent fuel disposal in Hästholmen, Kivetty, Olkiluoto and Romuvaara: TILA-99. POSIVA 99-07, Posiva Oy, Helsinki, Finland.

Wikberg P, Laaksoharju M, Bruno J, Sandino A, 1988. Site characterization and validation – Hydrochemical investigations in stage I. Stripa Project Internal Report 88-09, Svensk Kärnbränslehantering AB.

Wilkin R T, Barnes H L, 1997. Pyrite formation by reactions of iron monosulfides with dissolved inorganic and organic sulfur species. Geochim. Cosmochim. Acta, 60: 4167–4179.

Wolthers M, van der Gaast S J, Rickard D, 2003. The structure of disordered mackinawite. Am. Mineral., 88: 2007–2015.

Wolthers M, Charlet L, van der Linde P R, Rickard D, van der Weidjen C H, 2005. Surface chemistry of disordered mackinawite (FeS). Geochim. Cosmochim. Acta, 69: 3469–3481.

Appendix A

Changes in the WATEQ4F thermodynamic database for SR-Can geochemical calculations

A.1 Introduction

To carry out the mixing and reaction simulations with PhreeqC code /Parkhurst and Appelo 1999/ in SR-Can, a few modifications have been introduced to the WATEQ4F.dat database that is distributed with PhreeqC (version 2.12.5.669, released November 16, 2005). The modifications affect the solubility (equilibrium constants) of several phases, quite problematical but very important in the groundwater system under study. The affected phases are:

a) *Iron oxy-hydroxides and amorphous or crypto-crystalline iron monosulphides*. Both groups of phases are involved in the redox processes that control the Eh of the groundwaters, and their solubility is highly dependent on the degree of crystallinity, specific surface area, and re-crystallization or ripening.

b) *Aluminosilicate phases*. They are present as rock forming minerals and as fracture filling minerals in most granitic systems. Due to extensive solid-solution between end-member phases, their thermodynamic properties are not well known.

The next sections contain a brief discussion of the main difficulties encountered when working with these type of phases, the range of proposed solubility values, and the selected solubility values for the granitic groundwater systems under study.

A.2 Iron oxy-hydroxides

The iron oxy-hydroxides is a group of minerals whose main specimens range from amorphous or poorly crystalline (ferrihydrite or hydrous ferric oxides, $Fe(OH)_3$, see Section 12.1.3 in /Langmuir 1997/), to intermediate phases like lepidocrocite (FeOOH), to more stable and crystalline phases like haematite (Fe_2O_3) or goethite (FeOOH). The stability, solubility and reactivity of this complex group of phases are controlled by their mineralogy, crystallinity, degree of hydration, impurities and particle size, see e.g. /Langmuir and Whittemore 1971, Postma 1993/.

From all the factors affecting the solubility, particle size and specific surface area are among the most important /Macalady et al. 1990, Nordstrom et al. 1990, Langmuir 1997/. These properties have a wide range of variation, complicated by temporal changes in each phase as the interaction time with groundwaters increases. All the above ferric phases are thus linked by re-crystallization processes (ripening) by which less crystalline phases are converted with time into more crystalline ones (haematite and goethite), decreasing this way their solubility and increasing their particle size and decreasing specific surface area /Larsen and Postma 2001, Pedersen et al. 2005/.

The fractured granitic groundwater systems of the Scandinavian Shield have an ample variety of oxy-hydroxides, ranging in crystallinity from amorphous (ferrihydrites) in the near surface groundwaters /Banwart et al. 1994, Banwart 1999/, to fully crystalline (haematite and goethite), found as fracture filling minerals of hydrothermal origin /Drake et al. 2006/ in contact with deep, long-residence time reducing groundwaters /Grenthe et al. 1992/. Besides in groundwater systems with a variable redox potential iron oxy-hydroxides are not static phases of fixed composition, but dynamic entities that evolve as the surrounding groundwater change /Pedersen et al. 2005/.

Obviously, all these variable factors complicate the selection of specific thermodynamic values and justify the revision of the WATEQ4F database. It is important to bear in mind that the inherent difficulty in selecting appropriate solubility values for the oxy-hydroxides sets a limit on the accuracy of the geochemical computations.

Solubility of oxy-hydroxides: literature review

Table A-1 summarises the solubility values of the iron oxy-hydroxides found in the literature according to the following reaction:

$$Fe(OH)_3(s) \rightleftharpoons Fe^{3+} + 3\ OH^- \quad (A.1)$$

From the lowest to the highest, the solubility values span seven orders of magnitude, and those of individual phases have a spread of two to four orders of magnitude.

The less crystalline phases ("ferrihydrites") show only a limited overlap in solubility with other iron oxy-hydroxides. Most authors agree on their solubility, but even so the range of values spans two orders of magnitude. This solubility variability is a major concern when performing geochemical calculations /Majzlan et al. 2004/.

The most stable phases, haematite and goethite, are affected by variations of solubility of four orders of magnitude. The solubility product of the low specific surface area varieties of these crystalline phases is around $pK = 44$ (44.15 for goethite and 44.0 for haematite /Macalady et al. 1990, Langmuir 1997/), but can vary with surface area. For example, /Bonneville et al. 2004/ give for low-surface area (LSA) haematite (12 m^2g^{-1}) an experimentally derived pK of 42.8, whereas for nano-crystalline haematite (specific surface area of 125 m^2g^{-1}) the value given is $pK = 41.5$.

For the most crystalline phases, studies carried out in the Scandinavian Shield by /Grenthe et al. 1992/ can help narrowing the range of solubilities. This study on the factors controlling the reducing redox state of several Swedish groundwaters of long residence time allowed the indirect determination of the solubility of the iron oxy-hydroxides involved in the redox control. The deduced equilibrium constant for the reaction:

$$Fe(OH)_3(s) + 3\ H^+ \rightleftharpoons Fe^{3+} + 3\ H_2O(l) \quad (A.2)$$

was $\log K = -(1.1 \pm 1.1)$. Expressed in terms of reaction (A.1), that is, $pK = -\log K = -\log([Fe^{3+}]\times[OH^-]^3)$ this value is $pK = (43.1 \pm 1.1)$, inside the range shown in Table A-1 for haematite and goethite, and also in agreement with the type of oxy-hydroxide found in these groundwater systems as fracture filling mineral (mostly haematite, with minor goethite). Furthermore, haematite is the expected iron oxy-hydroxide in long residence time groundwaters, where less stable phases have disappeared or re-crystallised to more stable varieties. The re-crystallization is exceptionally fast, of the order of days to years, when the groundwaters are alkaline and reducing /Schwertmann and Murad 1983, Stipp et al. 2002, Pedersen et al. 2005/. Thus, the solubility value found by /Grenthe et al. 1992/ is particularly important when dealing with long residence time waters. For this reason, the value has been incorporated in the WATEQ4F database.

Table A-1. Solubility ranges of the main iron oxy-hydroxides. The solubility values as expressed as $pK = -\log K = -\log([Fe^{3+}]\times[OH^-]^3)$ corresponding to reaction (A.1).

	/Langmuir 1969, 1997/	/Cornell and Schwertmann 2003, Appelo and Postma 2005/	/Bonneville et al. 2004/	/Nordstrom et al. 1990/
Ferrihydrite [(1)]	37–39.4	37.5–39.5	37.7–39.5	37–39
Lepidocrocite	38.7–≥ 40.6	39–41	39.3–42.5	–
Haematite	41–43.9	40.3–43	40.3–43.9	–
Goethite	39.9–44.1	40–42	–	42.2–43.8

[(1)] Hydrous ferric oxide (HFO), amorphous to microcrystalline, in the terminology of /Nordstrom et al. 1990/. For the other authors cited, "ferrihydrite" includes from 2-lines ferrihydrite to 6-lines ferrihydrite, e.g. /Majzlan et al. 2004/.

The situation is much more complex when water-rock interaction occurs in the shallowest part of the groundwater system, where active circulation of oxic or sub-oxic meteoric waters is important. Here, several iron oxy-hydroxides can be present at the same time, with variable crystallinity and surface area, dynamically transforming into phases of higher stability as interaction time increases.

The maximum depth of the shallow groundwaters with meteoric imprint changes spatially. This transition depth is the place of complex interactions between different types of iron oxy-hydroxides, from amorphous to phases of intermediate crystallinity, as identified in field studies by /Banwart et al. 1994, Banwart 1999/ and in laboratory experiments by /Trotignon et al. 2002/.

A.2.1 Modifications to the WATEQ4F database

In the WATEQ4F.dat database distributed with PhreeqC /Parkhurst and Appelo 1999/, the less crystalline iron oxy-hydroxides are grouped under the name "$Fe(OH)_3(a)$", with a single log K of 4.891 for reaction (A.2) above. This value is very close to the value usually assigned to the less crystalline ferrihydrite (2-lines ferrihydrite) of log $K = 5$ for reaction (A.2) ($pK = 37$ in Table A-1 for reaction (A.1)). In addition a log $K \approx 3.2$ is given for maghemite in the original database.

However, because of the wide range of solubilities assigned to the phases collectively labelled as "ferrihydrite", this single entry has been supplemented by an entry for a less amorphous (microcrystalline) ferrihydrite, "$Fe(OH)_3(micro)$", following the terminology of /Nordstrom et al. 1990/. The corresponding entry in the database is:

Fe(OH)3(micro)

Fe(OH)3 + 3 H+ = Fe+3 + 3 H2O

log_k 3.00

Also, another mineral phase has been included, called "Fe(OH)3(hematite_Grenthe)", with the equilibrium constant proposed by /Grenthe et al. 1992/ for this type of systems:

Fe(OH)3(hematite_Grenthe)

Fe(OH)3 + 3 H+ = Fe+3 + 3 H2O

log_k –1.1

These new value complements the log K values in the original database of −2 for haematite and −1 for goethite. Its inclusion facilitates the calculation of redox potentials according to the correlations observed in the Swedish sites /Grenthe et al. 1992/.

A.3 Iron monosulphides

Under the "iron mono-sulphides" term the amorphous mono-sulphide (FeS(am), also named disordered mackinawite /Wolthers et al. 2003, 2005/, the ordered or crystalline mackinawite (tetragonal FeS) and greigite (Fe_3S_4) are included. All of them can be involved in the transformation to pyrite (FeS_2). Although there are different reaction pathways to explain this transformation /Wilkin and Barnes 1997, Benning et al. 2000/, all of them start with the precipitation of an initially amorphous iron monosulphide and its successive transformation through ordered mackinawite, greigite and, finally, pyrite.

During the site investigation program at Laxemar /SKB 2006e/ several mistakes have been detected in the solubility constants of amorphous iron monosulphides and mackinawite in the PHREEQC.dat and WATEQ4F.dat databases distributed with PhreeqC /Parkhurst and Appelo 1999/ and included in the Wateq4F code /Ball and Nordstrom 2001/.

The dissolution reaction for the two phases included in these databases is:

$$FeS(s) + H^+ \rightleftharpoons Fe^{2+} + HS^- \quad (A.3)$$

with an equilibrium constant value of log $K = -3.91$ for FeS(am) and a value of log $K = -4.648$ for mackinawite. In the Wateq4F user's manual /Ball and Nordstrom 2001/ it is indicated that these values come from /Berner 1967/. However, /Chen and Liu 2005/ have shown that the value included in these databases is the consequence of a mistake in the conversion of the reactions and thermodynamic data from /Berner 1967/ to the format that the databases accept (reaction (A.3)). The correct value as deduced from Berner's data for FeS(am) is log $K = -2.98$, i.e. almost an order of magnitude larger.

A similar case affects the equilibrium constant of mackinawite /SKB 2006e/. Manipulating the reactions and thermodynamic values proposed by /Berner 1967/ to obtain the equilibrium constant of reaction (A.3), the resulting value is log $K = -3.6$ for mackinawite.

This mistake is also found in the MINTEQ.dat database distributed with PhreeqC /Parkhurst and Appelo 1999/. However, the newest version of this database, MINTEQ.v4.dat, has the correct values for FeS(ppt) and mackinawite (log $K = -2.95$ and log $K = -3.6$ respectively). Note, however, that along with MINTEQ.v4.dat, the older version of the database, including the mistakes mentioned above, is also distributed with PhreeqC.

A.3.1 Review of the solubility of iron monosulphides

Besides the experimental solubility values of iron monosulphides obtained by /Berner 1967/, there are more recent determinations, both by experiment and based on natural systems. For amorphous monosulphides /Davison et al. 1999/ found a value of $-(3.00 \pm 0.12)$ at 20°C; pH = 3 to 7.9; and $p_{H_2S} = 10^{-1}$ to 10^{-5} MPa, very similar to the value proposed in a previous review /Davison 1991/: log $K = -(2.946 \pm 0.2)$ for reaction (A.3).

A value of log $K = -3.15$ was obtained for the amorphous FeS at temperatures 12.8 to 18.8°C in a study of in situ sediments from the Baltic Sea /Bågander and Carman 1994/; and $-(3.07 \pm 0.34)$ was reported in a study of the groundwaters from the Chosui delta (Taiwan) /Chen and Liu 2005/. Using additional data of sulphidic waters in different bedrocks (limestones, coastal plain sediments, wetlands, fractured limestones, etc) these authors obtained an average of log $K = -2.98$. Finally, a value of log $K = -(2.98 \pm 0.36)$ was obtained for the sulphidic groundwaters in the Laxemar area /SKB 2006e/.

For mackinawite, the proposed solubility value by /Davison 1991/ is log $K = -(3.6 \pm 0.2)$ at 25°C, almost identical to the experimental value obtained later by /Davison et al. 1999/. More recently, /Benning et al. 2000/ found experimentally a value of log $K = -3.77$ at 25°C, inside the uncertainty of previous values. A log $K = -3.6$ for this phase has given consistent results in different groundwater systems /Chen and Liu 2005, SKB 2006e/.

A.3.2 Modifications to the WATEQ4F database

The original solubility value of FeS(ppt) in the WATEQ4F.dat database has been changed from −3.915 to the following value:

FeS(ppt)

FeS + H+ = Fe+2 + HS–

log_k –3.00

A.4 Aluminosilicates

Chlorite is the most common aluminosilicate in fracture fillings in Forsmark, Simpevarp, Äspö and Laxemar areas /Drake et al. 2006/. It occurs as several different varieties and is present in most open fractures. Other common aluminosilicates are epidote, prehnite, laumontite, adularia (low-temperature K-feldspar), albite, and several clay minerals. In the Forsmark area, prehnite and epidote are relatively rare or appear only in some fractures, whereas harmotome (Ba-zeolite) is accidental /Drake et al. 2006/.

As a group, aluminosilicates dominate the fracture filling mineralogy, showing variations with depth and also from area to area. Fe-Mg chlorites, smectites, and interstratified clay minerals (illite-smectite, smectite-vermiculite and corrensite /Drake et al. 2006/) are abundant and, together with zeolites (laumontite, prehnite, harmotome) are the most active due to their high specific surface area. At the same time, they are the most difficult to treat quantitatively because of extensive solid-solution and extreme variations in crystallinity, e.g. /Nordstrom et al. 1990, Trotignon et al. 1999/.

Several mineral dissolution-precipitation calculations for SR-Can have been run with albite, potassium feldspar (adularia) and kaolinite as the only aluminosilicates. Albite and potassium feldspar are common fracture filling and rock-forming minerals, and kaolinite has been used as a "simplified" fracture-filling clay mineral. However, the thermodynamic data for these phases are not devoid of uncertainties, and their solubility and equilibrium constants should be evaluated on a case by case basis /Nordstrom et al. 1990/.

A.4.1 Review of solubility values for albite, potassium feldspar and kaolinite

Only solubility values deduced, and/or successfully used, in studies of low temperature granitic groundwater systems have been considered in the evaluation. Although in the Scandinavian Shield water-rock interactions involving aluminosilicates have been poorly studied, a few key studies exist that have been used in the selection of revised values.

Grimaud et al. gave a set of equilibrium constants for albite, K-feldspar and kaolinite at 15°C (Table A-2) valid for groundwaters in the Stripa area /Grimaud et al. 1990/. These authors were able to successfully reproduce the geochemical evolution of the waters assuming successive partial equilibrium conditions triggered by the irreversible addition of chlorine.

Following a similar procedure for the Äspö groundwater system, /Trotignon et al. 1997, 1999/ arrived at a different set of equilibrium constants (Table A-2) based on thermodynamic data by /Michard 1989/. They performed a sensitivity analysis by propagating the thermodynamic uncertainties into the geochemical calculations.

Both groups of researchers used the thermodynamic data of /Michard 1983, 1989/ for the three aluminosilicates: /Trotignon et al. 1997/ as a direct input for their geochemical simulations; and /Grimaud et al. 1990/ to estimate solubility values for the Stripa groundwaters.

Table A-2. Solubility values of albite, potassium feldspar and kaolinite proposed by several authors in granitic groundwater systems. The solubility is expressed as the log K of the corresponding dissolution reaction using the species $H_4SiO_4(aq)$, $Al(OH)_4^-$, Na^+, K^+ and H^+.

	/Grimaud et al. 1990/ (15°C)	/Trotignon et al. 1997/ (15°C) [1]	/Michard 1983/	/Michard 1989/ 25°C	/Michard 1989/ 15°C
Albite (low)	–20.3	–20.7 (–19.52 to –21.52)	–19.98	–19.98	–20.65
K-Feld. (adularia)	–22.8	–23.4 (–22.52 to –24.52)	–22.12	–22.62	–23.41
Kaolinite	–37.3	–40.41 (–37.04 to –41.04)	–39.2	–39.16	–40.42

[1] Values between brackets are the uncertainty limits given by the authors from a sensitivity analysis.

The selected solubility values for albite and potassium feldspar in the SR-Can calculations are those of /Michard 1989/. For kaolinite, the solubility calculated by /Grimaud et al. 1990/ for Stripa groundwaters has also been selected due to the similarities between that system and the Forsmark and Laxemar sites.

A.4.2 Modifications to WATEQ4F database

The stability of albite and potassium feldspar proposed by /Michard 1989/ have been added to Wateq4F database in the form of a $K(T)$ fit. The values at 25, 50, 100, 150 and 250°C from /Michard 1989/ have been fitted to the $K(T)$ expression used in PhreeqC /Parkhurst and Appelo 1999/:

$$\log K = A_1 + A_2 T + \frac{A_3}{T} + A_4 \log T + \frac{A_5}{T^2}, \qquad \text{(A.4)}$$

where T is absolute temperature. The values of the parameters A_1–A_5 are listed in Table A-3, and have been fitted by a non-linear least-squares method.

The stability of kaolinite as calculated by /Grimaud et al. 1990/ at 15°C has been added to the database under the label "Caolinita_Grimaud" with a log K = −37.3 (Table A-2 and Table A-3). The PhreeqC database values should correspond instead to 25°C, but because the simulations designed for SR-Can have been performed for 15°C, this value should be more appropriate.

The original values in the Wateq4F database included in the PhreeqC distribution have bee kept. These values are −18.00 for albite, −20.57 for adularia, −37.97 for kaolinite.

Table A-3. Chemical reactions and thermodynamic data for albite, potassium feldspar and kaolinite added to the WATEQ4F.dat database. The values of log K are given at 25°C. Under the heading "analytic" are listed the fitting parameters A_1 to A_5 to Equation (A.4).

```
Albita
NaAlSi3O8 + 8H2O = Al(OH)4– + 3H4SiO4 + Na+
log_k     –19.98
–analytic –5429.59545 –0.81939 293813.48663 1966.59164 –17577933.12184
Feldespato_K
KAlSi3O8 + 8H2O = Al(OH)4– + 3H4SiO4 + K+
log_k     –22.62
–analytic –5701.00975 –0.87173 304836.7864 2069.03705 –18119139.36096
Caolinita_Grimaud
Al2Si2O5(OH)4 + 7H2O = 2Al(OH)4- + 2H+ + 2H4SiO4
log_k     –37.3
```

Appendix B

Dilute waters and their importance to repository performance and safety

B.1 Background

From a repository performance and safety viewpoint the potential interaction of dilute or fresh groundwaters with the buffer material (bentonite) may be detrimental in that colloids may be formed; these particles can act as carriers for radionuclides. Colloid formation can be avoided if the groundwater contains a minimum of dissolved salts, in particular the presence of divalent cations such as Ca^{2+} where a lower cut-off of ≈ 40 mg/L is normally used. Under undisturbed conditions it is unlikely that dilute waters will penetrate to repository depths as mixing and rock interaction will change the chemistry resulting in a more mineralised (i.e. > 40 mg/L Ca) mature groundwater. However under disturbed conditions, such as during the excavation and construction of a repository installation, hydraulic drawdowns will occur around the excavated repository area eventually resulting in saturation by a large component of upper bedrock-derived meteoric groundwater. This will be particularly evident in the high transmissive rock volumes. In the low transmissive rock volumes where the repository will be constructed, the effects may be diminished but cannot be excluded. There remains, therefore, the possibility that dilute waters may come in contact with the buffer material, both during repository construction and for tens to hundreds of years after closure.

Well beyond the post-closure stage of the repository, when hydraulic and hydrochemical conditions have re-equilibrated and groundwaters at repository depth have regained their 'undisturbed' mineralization, a further dilute water scenario is possible. This involves the rapid ingress of glacial melt water to depth during future climatic change. Although this will be mainly recharged through higher transmissive rock volumes, some contact with the repository buffer material after sufficient time cannot be excluded.

Both meteoric water and glacial melt water scenarios must therefore be addressed. What is important to know is the present recharge evolution, spatial extent and chemistry of dilute meteoric water in the upper 200–300 m of bedrock and, what evidence is there that past climatic events have resulted in the ingress of dilute glacial melt water to repository depths and beyond, and what was the chemistry of these waters.

B.2 Dilute meteoric-derived waters

Dilute or fresh waters originating from modern precipitation recharge (i.e. introduced during the last 100 years), tend to be present mostly in the upper 50–150 m of the bedrock although local hydraulic conditions (e.g. higher topography) may result in their presence at greater depths. Hydrochemically they are characterised by a near-neutral pH and a low ionic content dominated by Na^+ and HCO_3^-, with minor amounts of Ca^{2+}, Cl^- and SO_4^{2-}. To provide a regional picture of the chemistry and distribution of these waters in fractured crystalline rock environments under similar climatic conditions both past and present, groundwater data have been extracted from several investigated sites in Sweden, Finland, Canada, Scotland and Switzerland, all representing fractured crystalline bedrock environments. These data are presented as calcium content versus depth plots, the objective being to highlight the extent of available sources of fresh (dilute) meteoric-derived waters which if they came in contact with the engineered barrier system, namely the clay buffer material, would be detrimental to the long-term stability of the repository. Any groundwater with less than 30–40 mg/L Ca is considered unsuitable from a safety assessment viewpoint.

The locations of the Swedish sites cited in this evaluation are included in Figure B-1 with reference to data in /Smellie and Wikberg 1989, Smellie and Laaksoharju 1992, Laaksoharju et al. 1995/. The URL Whiteshell site is located in Manitoba, Canada with reference to data in

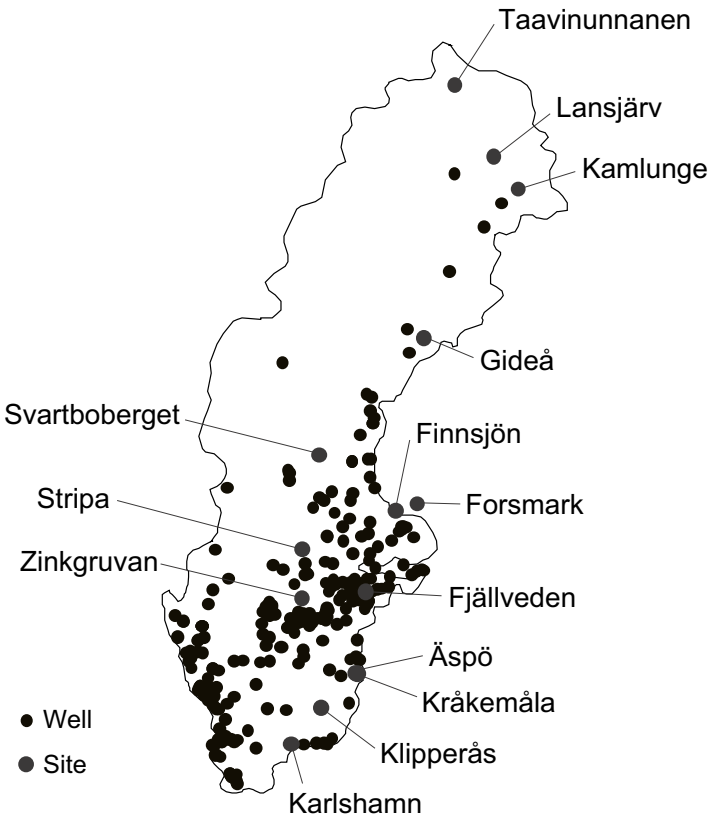

Figure B-1. *The locations of investigated Swedish sites including those cited in this evaluation.*

/Gascoyne 2004/, Altnabreac is located in the extreme NE Scotland with reference to data in /Kay and Bath 1982/, and the Swiss sites are located in the Mont Blanc Massif, SW Switzerland with reference to data in /Kilchmann et al. 2004/, and the Finnish sites located in southern Finland with reference to data in /Kaija et al. 1998, Pitkänen et al. 1999, 2001, 2004/.

Many of the KBS-3 investigation sites shown in Figure B-1 (Taavinunnanen, Kamlunge, Gideå, Svartboberget, Fjällveden, Kråkemåla and Klipperås) with reference to data in /Smellie et al. 1985, 1987/, have not been included because of widespread contamination resulting from drilling, hydraulic testing and sampling procedures. This has allowed fresh to low saline groundwaters from the upper bedrock to penetrate and mix to greater depths in the boreholes. These groundwaters have subsequently penetrated along intersected fractures or fracture zones which have been the focus of the sampling campaigns

B.3 Results

The results are shown in Figure B-2 to Figure B-19 and have been categorised generally under the headings: a) hydraulically active inland sites, and b) low relief, less hydraulically active coastal sites. As far as possible selected values were chosen, i.e. screened values deemed to be most representative. All data are from drilled boreholes with the exception of the Swiss sites which are from springs and tunnel seepages. Although some of the tunnel values have been influenced by hydraulic drawdowns, most are considered typical of young meteoric recharge waters within the upper 300–400 m of bedrock.

B.3.1 Hydraulically active inland sites

These include data from the Laxemar, Palmottu, Altnabreac, Swiss mountains and the URL Whiteshell. The plots show:

- The Laxemar subarea data show low values down to approx. 800 m (Figure B-2); further resolution from 0–600 m depth (Figure B-3) show that several values are under 50 mg/L Ca with around 40% under 30 mg/L Ca.
- Palmottu (Figure B-4) shows that down to 350 m depth all data show less than 40 mg/L Ca with 67% less than 30 mg/L Ca.
- Altnabreac granite (Figure B-5) shows a variable distribution of values irrespective of depth ranging from 3–69 mg/L Ca; some 64% lie below 40 mg/L Ca.
- Trient and Finhaut granites and gneisses (Figure B-6) show that all values lie under 40 mg/L Ca with 74% under 20 mg/L Ca.
- Mont Blanc granite (Figure B-7) shows that with one exception all values lie at or under 14 mg/L Ca.
- URL Whiteshell granite (Figure B-8) indicates an overall increase in calcium with depth but many low content samples are concentrated between 0–400 m. Figure B-9 for 0–200 m indicates that the majority of waters (~ 70%) are below the 40 mg/L Ca cut-off.

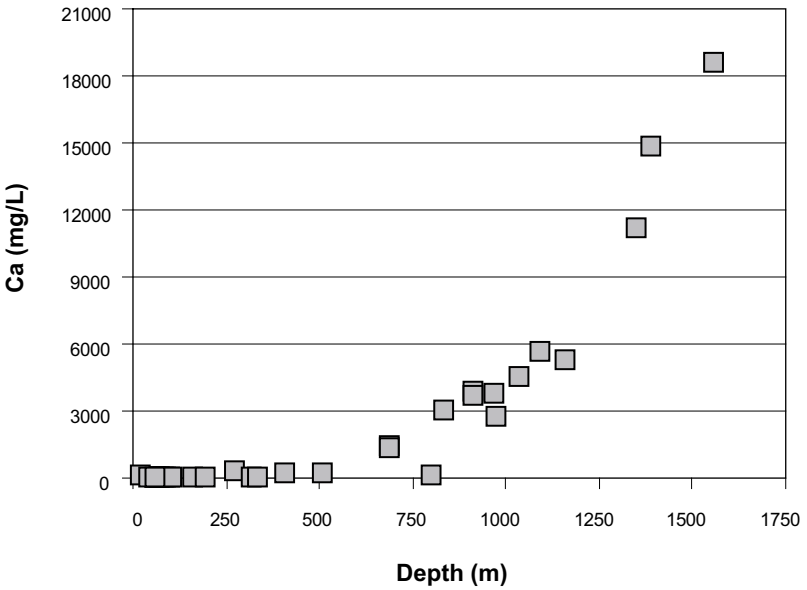

Figure B-2. *Calcium groundwater concentrations as a function of depth for Laxemar.*

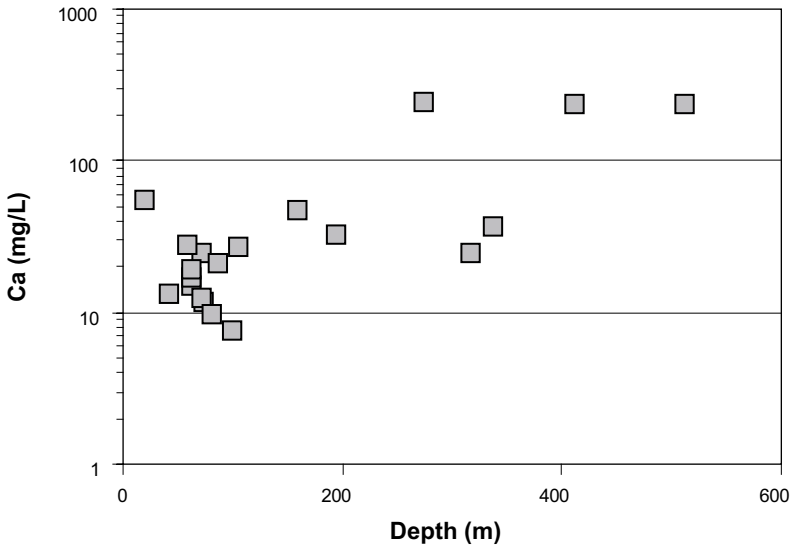

Figure B-3. *Calcium groundwater concentrations for Laxemar (log_{10}-scale) at depths less than 600 m.*

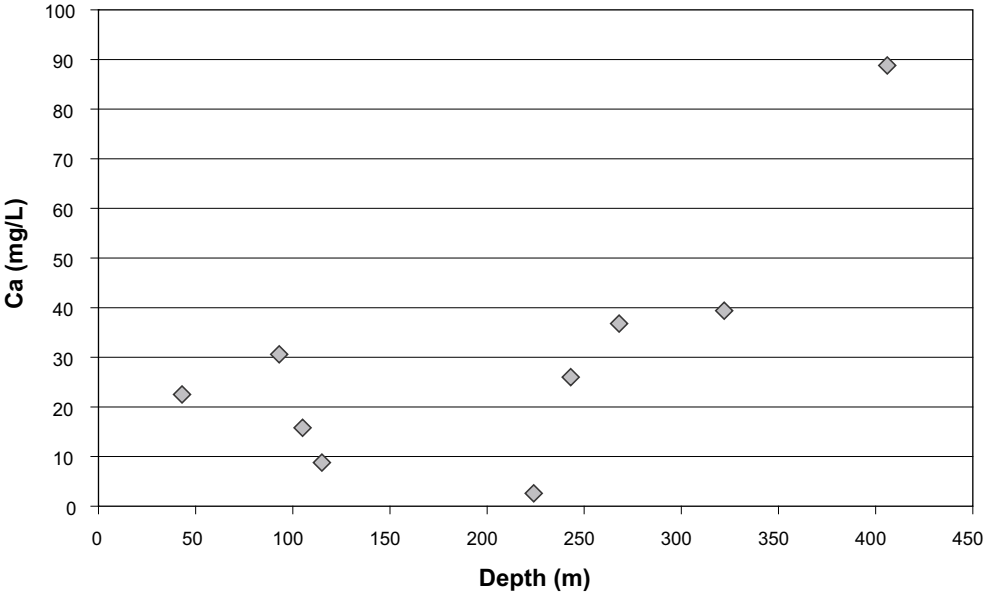

Figure B-4. *Calcium groundwater concentrations as a function of depth for Palmottu (Finland).*

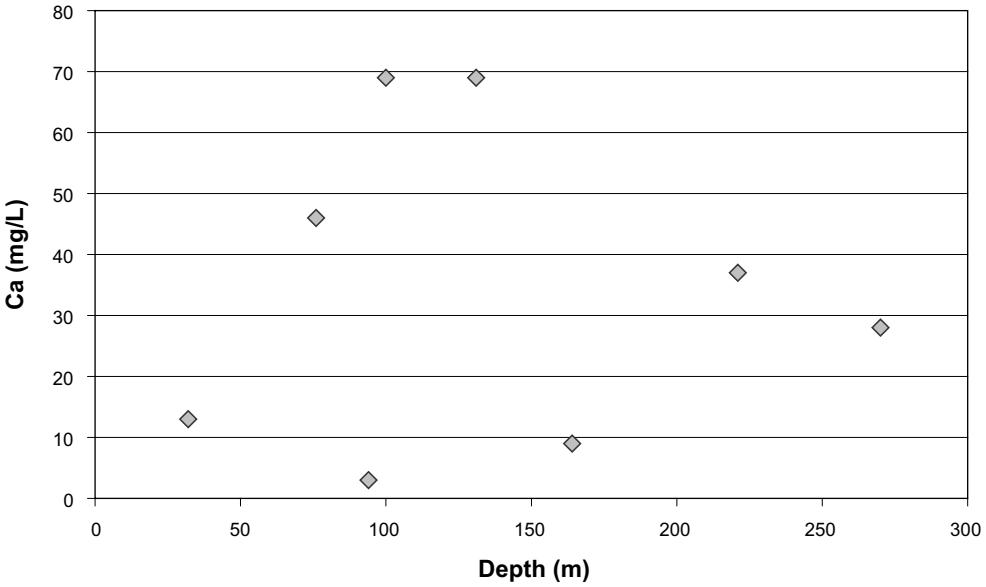

Figure B-5. *Calcium groundwater concentrations as a function of depth at Altnabreac (Scotland).*

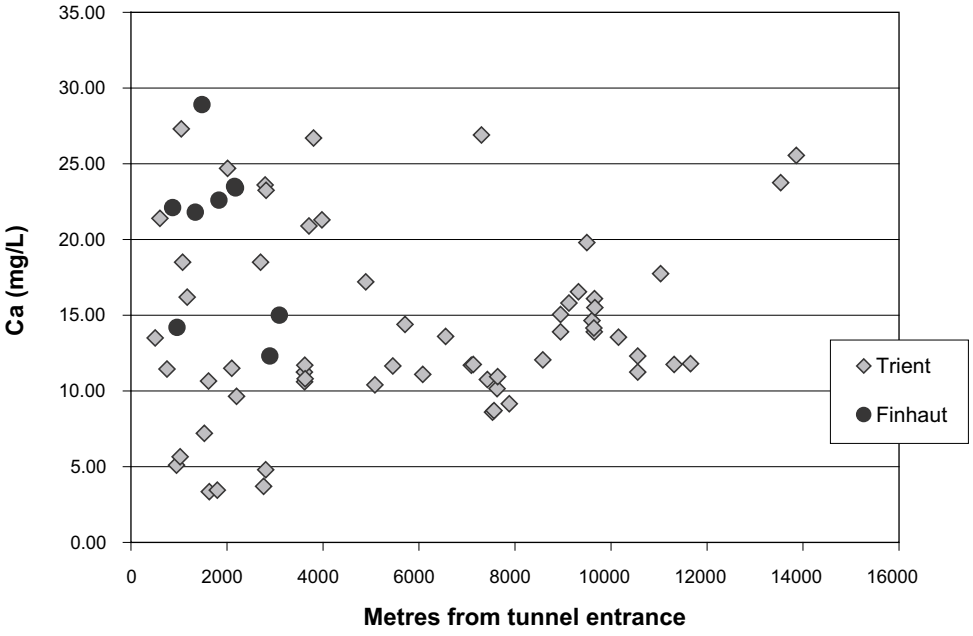

Figure B-6. *Calcium concentrations in Swiss Mountain Springs and Tunnel Seepages.*

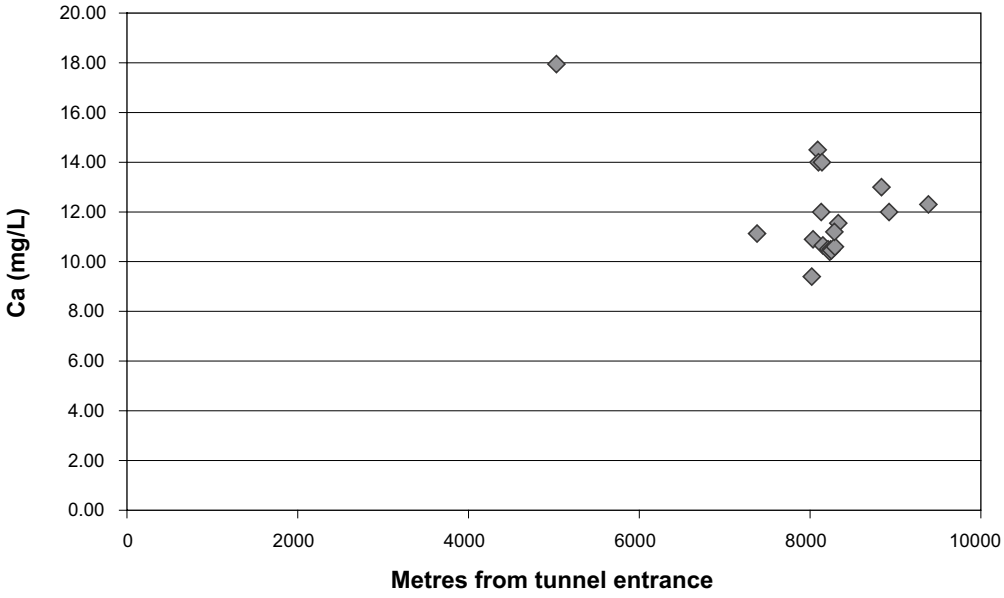

Figure B-7. *Calcium concentrations in seepages in the Mont Blanc Tunnel (Switzerland).*

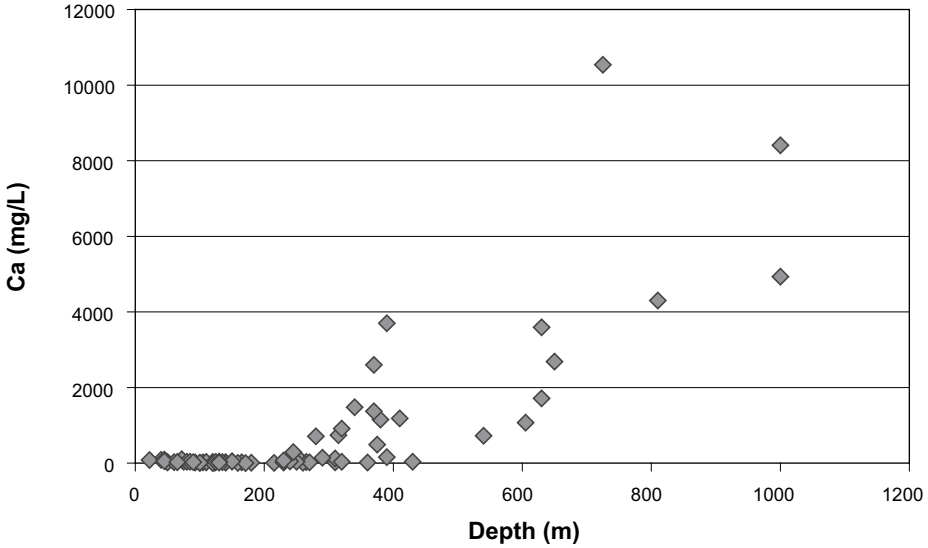

Figure B-8. *Calcium concentrations versus depth at the underground research laboratory (URL) in Whiteshell, Canada.*

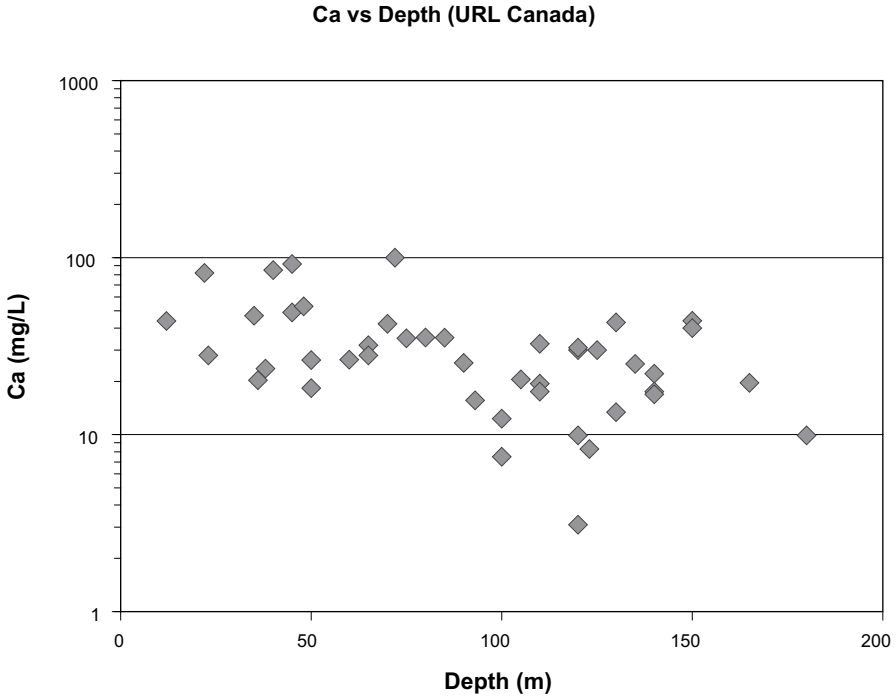

Figure B-9. *Calcium concentrations (log_{10}-scale) at depths less than 200 m for the underground research laboratory (URL) in Whiteshell, Canada.*

B.3.2 Low relief, less hydraulically active coastal sites

These include data from the Swedish and Finnish coastal sites: Äspö, Ävrö, Simpevarp, Forsmark Finnsjön, Olkiluoto and Hästholmen. The plots show:

- Äspö island shows generally high calcium values and an overall increase of calcium with depth (Figure B-10). Between 0–300 m depth the groundwaters vary between 0–1,000 mg/L Ca; greater resolution (Figure B-11) shows only one sample (at 25 mg/L Ca) below the 40 mg/L Ca cut-off level.
- A comparison of the Äspö-Ävrö data (also Figure B-10 and Figure B-11) shows that Ävrö appears to have lower Ca at shallower depths (~ 0–100 m). The reason for this is not clear, but the higher Ca at Äspö may be an artefact of excessive pumping which preceded much of the pre-investigation hydrochemical sampling at that time.
- Forsmark (Figure B-12) indicates an irregular but consistent increase in calcium with depth; between 0–200 m a large cluster of lower calcium content (< 1,000 mg/L) is indicated. Greater resolution of this cluster (Figure B-13) shows that all samples but four contain more than 40 mg/L Ca.
- Finnsjön (Figure B-14), further inland from Forsmark and with a little higher topography, shows a slightly greater percentage of lower calcium contents. The figure shows some 23% of the samples with 20–40 mg/L Ca.
- Olkiluoto (Figure B-15 and Figure B-16), representing a similar coastal site to Forsmark, shows the same major trends as those from Forsmark (cf Figure B-12 and Figure B-13).
- Hästholmen (Figure B-17 and Figure B-18), also a coastal site, shows similar trends to Forsmark and Olkiluoto; it is only at very shallow depths (0–60 m) that calcium falls below 40 mg/L (8.3–35 mg/L).

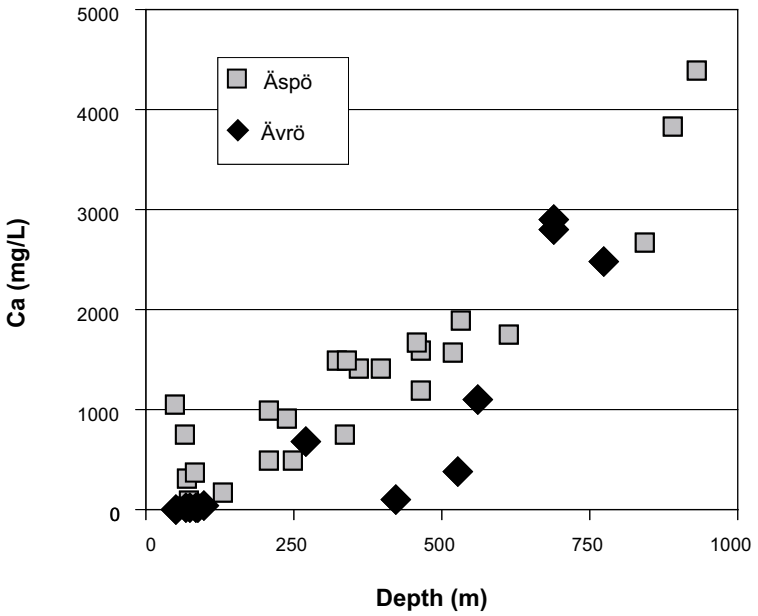

Figure B-10. *Calcium concentrations versus depth at Äspö and Ävrö, Sweden (selected pre-investigation samples).*

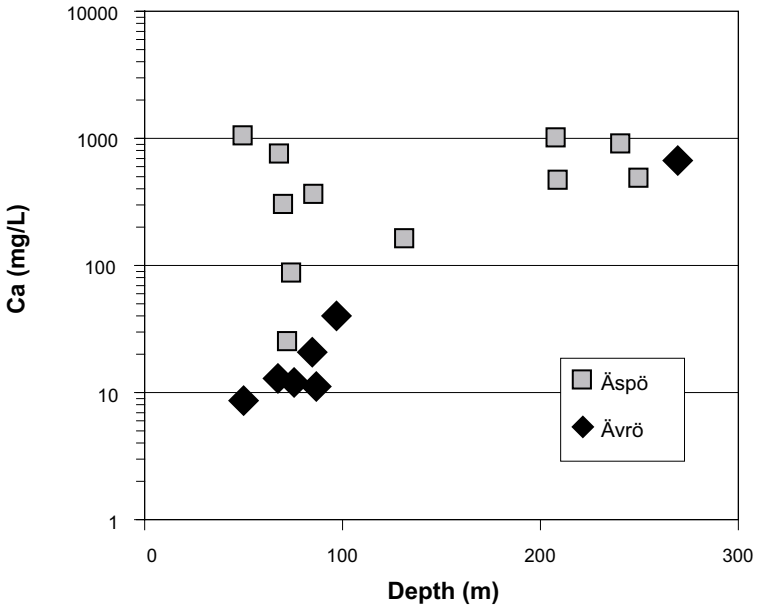

Figure B-11. *Calcium concentrations (log_{10}-scale) at depths less than 300 m for groundwaters from Äspö and Ävrö, Sweden (selected pre-investigation samples).*

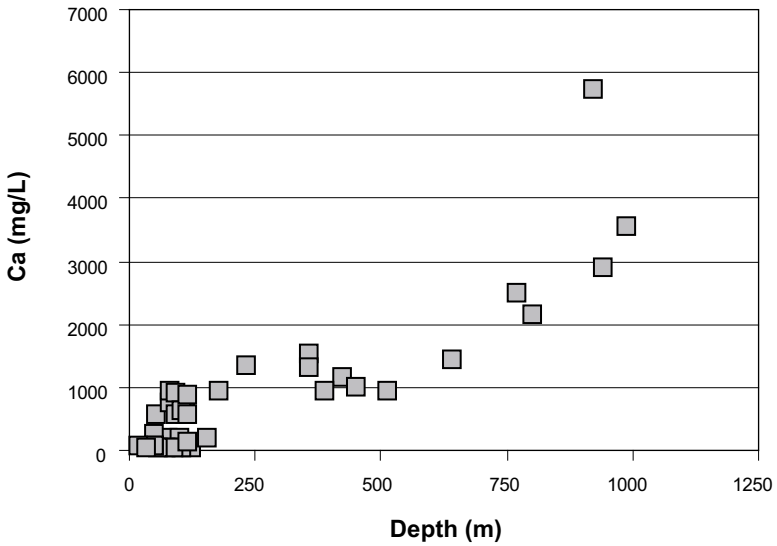

Figure B-12. *Calcium concentrations versus depth for Forsmark, Sweden (selected samples).*

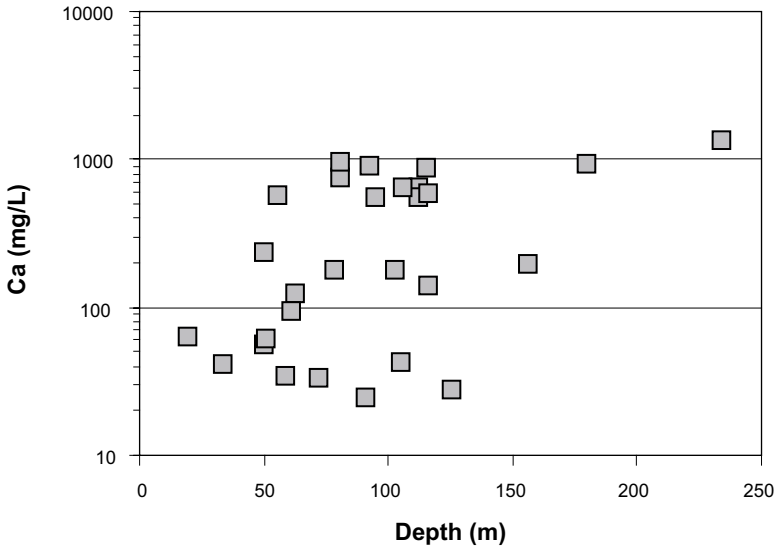

Figure B-13. *Calcium concentrations (log_{10}-scale) at depths less than 250 m for groundwaters from Forsmark, Sweden (selected samples).*

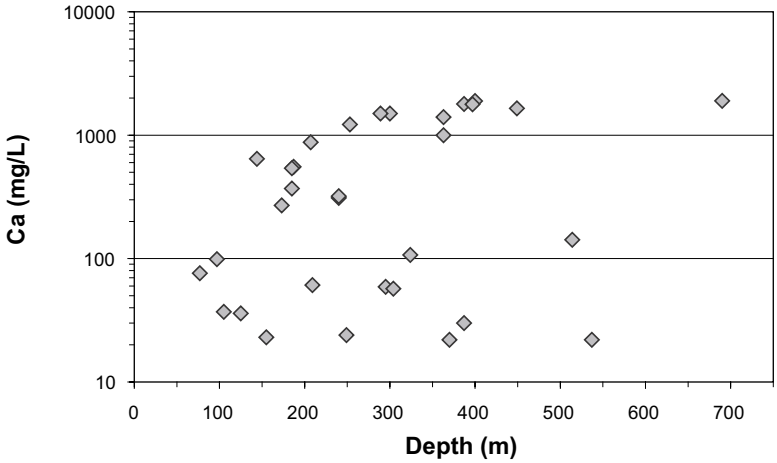

Figure B-14. *Calcium concentrations (log_{10}-scale) versus depth for groundwaters from Finnsjön, Sweden (selected samples).*

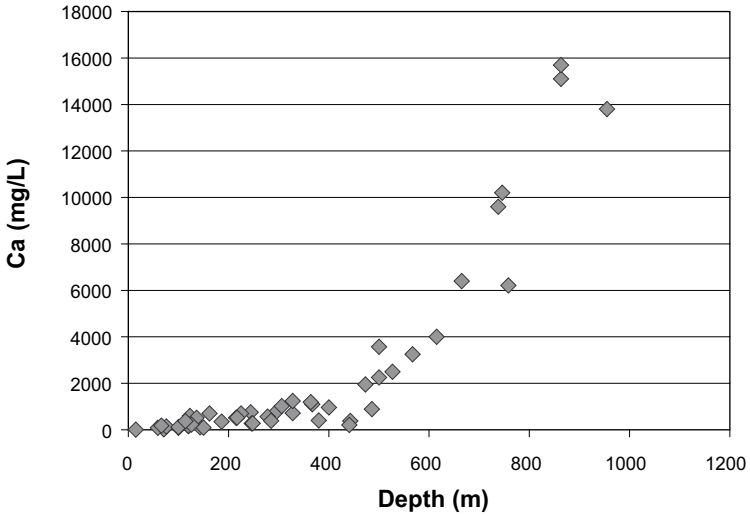

Figure B-15. *Calcium concentrations versus depth for groundwaters from Olkiluoto, Finland (selected samples).*

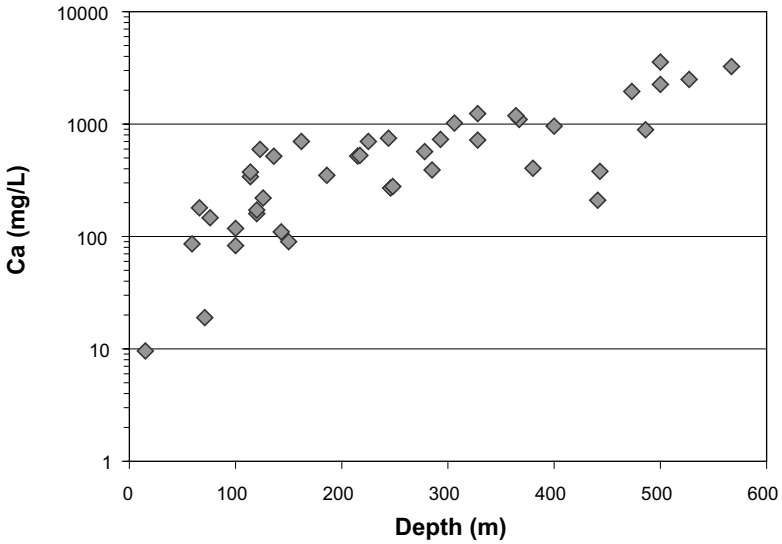

Figure B-16. *Calcium concentrations (log_{10}-scale) for depths less than 600 m for groundwaters from Olkiluoto, Finland (selected samples).*

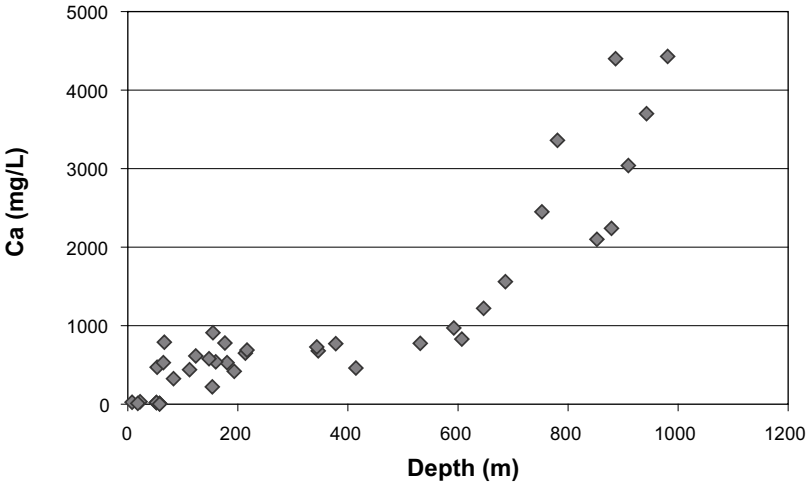

Figure B-17. *Calcium concentrations versus depth for groundwaters from Hästholmen, Finland* ***(selected samples).***

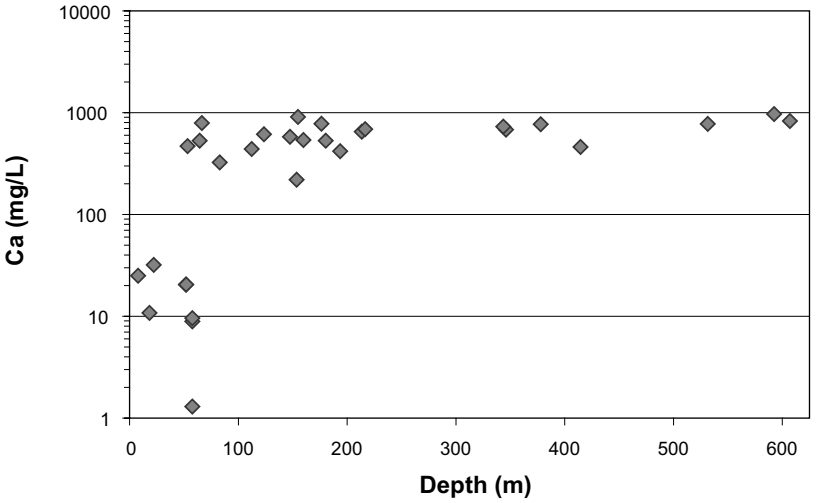

Figure B-18. *Calcium concentrations (log_{10}-scale) for depths less than 600 m for groundwaters from Hästholmen, Finland (selected samples).*

B.3.3 Combined inland-coastal profile

This profile combines the Laxemar (inland) site with the Äspö, Simpevarp and Ävrö sites (coastal). Figure B-19 shows that at depths from 0–400 m a large group of values at shallow depths (0–100 m) occurs where calcium is under 30 mg/L; for Laxemar this trend can extend down to about 350 m (Figure B-3) which reflects greater hydraulic gradients driven by higher topography.

B.3.4 Conclusions

At all sites there exist fresh, low calcium groundwaters (i.e. below the 40 mg/L cut-off) in the upper approx. 50–100 m of the bedrock irrespective of site location. Such fresh waters obviously extend to greater depths in more hydraulically active recharge systems associated with the inland sites, and will tend to be restricted to shallower levels in coastal sites mainly characterised by discharge systems and where the Baltic sea has only recently been displaced by the isostatic rebound. A good example to illustrate these differences is the Simpevarp area plot (Figure B-19) where Laxemar is compared with Äspö, Simpevarp and Ävrö.

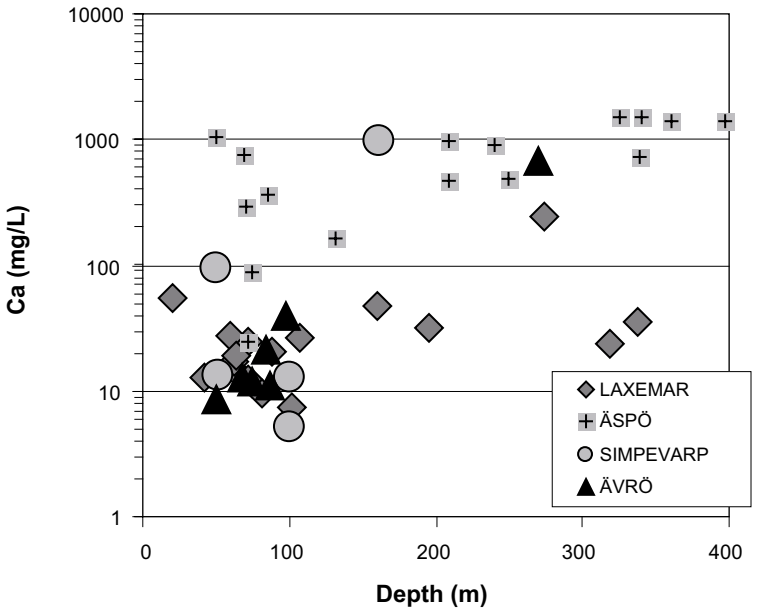

Figure B-19. *Calcium concentrations (log_{10}-scale) for depths less than 400 m for groundwaters from Simpevarp area, Sweden (inland-coastal section).*

From a repository construction viewpoint, open conditions at an inland site will be saturated quickly by low calcium groundwaters since under undisturbed conditions these groundwaters already exist almost to repository depths. At coastal sites saturation by low calcium groundwaters eventually will occur also, but over greater timescales when isostatic rebound moves the Baltic shoreline away from the site.

B.4 Dilute glacial melt-derived waters

Dilute waters originating from glacial melt water recharge have been introduced under high hydraulic gradients during previous glacial events (i.e. minimum of 10,000 years ago) such that traces have been found at repository depth (400–600 m). Obviously access to fracture zones of higher transmissivity will result in greater depth penetration and there is evidence of a glacial water component to at least approximately 1,000 m in some of the investigated sites (e.g. Forsmark: borehole KFM03A at 930.5 m depth, see Figure 4-11, in p.172 of /SKB 2005a/). Hydrochemically these melt waters are expected to be dilute, perhaps oxygenated and aggressive (i.e. low pH due to a high CO_2 contents). However, whether they can persist in this form to repository depths is probably unrealistic since: a) they will become quickly reducing because of the buffering capacity of the bedrock and fracture mineralogy, and b) they will undergo mixing with increasingly saline (i.e. Ca-rich) groundwaters with increasing depth of penetration.

Appendix C

Accessible calcite in the fractures of crystalline rock and its stability

C.1 Introduction

The occurrence of calcite along possible flow paths in crystalline bedrock is of importance for safety assessment in that; 1) it provides a source of Ca^{2+} and 2) it constitutes a pH buffer ensuring that acid precipitation will be neutralised in the near surface bedrock.

Calcite stability in crystalline rocks requires, expressed in a very simple way that Ca^{2+} and HCO_3^- are present in the groundwater in concentrations high enough to maintain calcite saturation. Bicarbonate enters the system via uptake of CO_2 in the overburden, and also through microbial production of CO_2 in the bedrock aquifer. Ca^{2+} is leached from Ca-Al-silicates like plagioclase, hornblende and epidote present in the overburden or in the bedrock or by dissolution of calcite, gypsum and hydrothermal Ca-Al silicate that may be present as fracture coatings. Production of calcite (super saturation) is in most cases the results of mixing of different groundwater types: This may occur when meteoric water loaded with bicarbonate comes into contact with saline groundwater with very high Ca^{2+} e.g. out washing of saline water by fresh water recharge as a result of the present land rise. Another possibility is mixing of water caused by opening of fractures due to changes in stress regimes (e.g. during glaciations).

Figure C-1 and Figure C-2 show saturation index for calcite for groundwaters going from the near surface (overburden) to shallow bedrock (percussion boreholes) and over to cored boreholes reaching down to 1,000 m depth or more. The figures show values from the Laxemar (Figure C-1) and Forsmark sites (Figure C-2). Both areas show close to equilibrium conditions for the cored boreholes whereas the percussion boreholes and some of the near surface groundwaters (sampled in soil pipes) at Forsmark show super saturation, mainly due to high bicarbonate production. In the Simpevarp area in contrast, the near surface groundwaters (soil pipes) are generally unsaturated in respect of calcite whilst the groundwaters sampled in the depth interval between 0–100 metres in the bedrock show saturation.

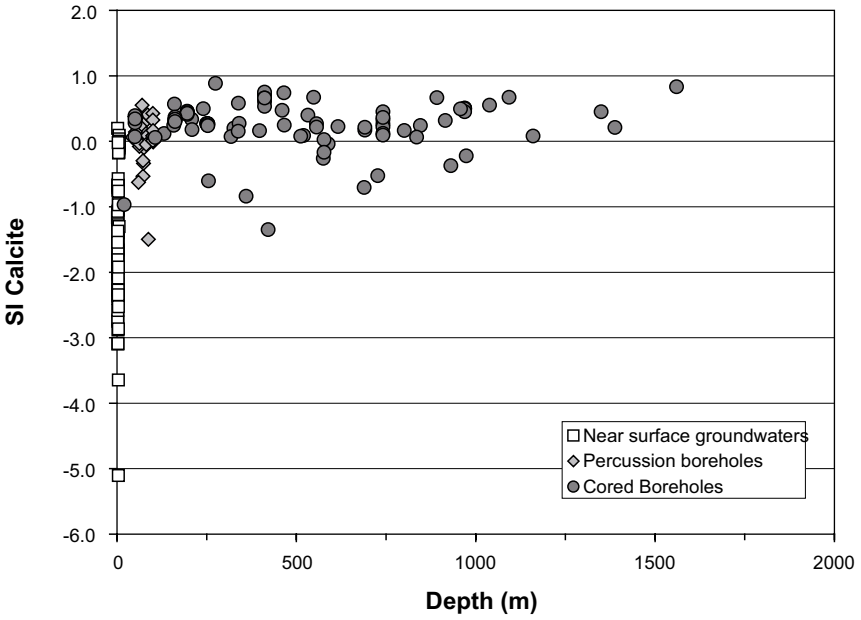

Figure C-1. *Saturation index (SI) for calcite in groundwaters from the Laxemar site.*

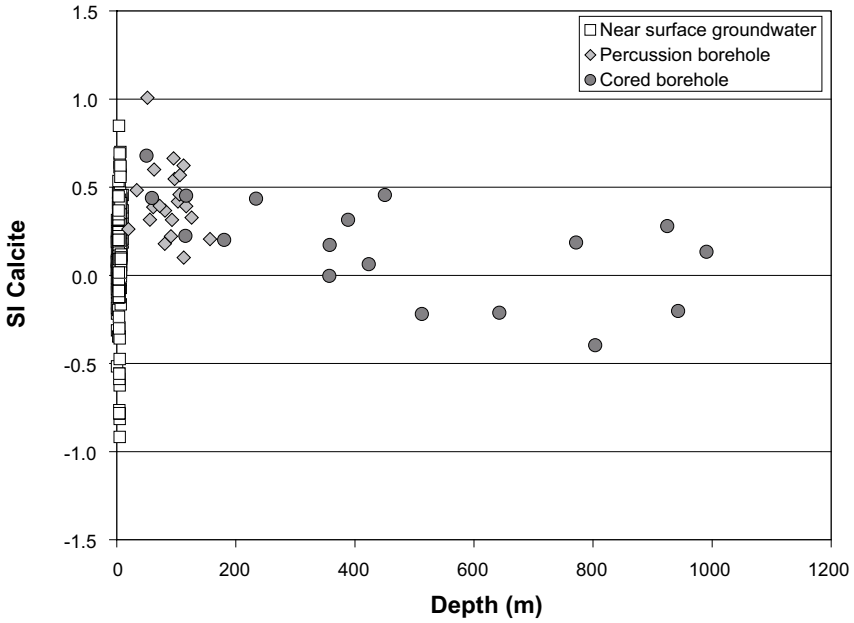

Figure C-2. *Saturation index (SI) for calcite in groundwaters from the Forsmark site.*

C.2 General information on fracture coatings in crystalline rock

Fracture fillings in crystalline rocks have been mapped in all site investigations carried out within the SKB program since the early 80´s and onwards comprising about ten sites. Inland (e.g. Taavinunnanen and Klipperås) as well as coastal sites (e.g. Forsmark and Simpevarp) have been studied. Several cored boreholes between 700 and 1,000 metres long have been drilled in each site and the core mappings show that calcite and chlorite are the most common fracture minerals in all the sites investigated. The presence of calcite is easily to prove by adding a few drops of HCl on the fracture surface and the mapping of calcite can therefore be regarding as confident. However, conventional drilling (single barrel) used within the earlier site investigations have caused damage of calcite crystals due to rotation and grinding. Moreover the relation between mapped open and sealed fractures is different in the core mappings of these drill cores; larger part of the fractures has been opened during the drilling and these fractures can be very difficult to separate from originally open ones.

Calcite found in fractures in crystalline rocks may have different origins as has been demonstrated in more detailed investigations e.g. summarised in /Tullborg 1997b/ and also shown in results from the now ongoing site investigations in Forsmark and Oskarshamn /Drake et al. 2006/. Several generations have been possible to identify at all sites where detailed studies have been undertaken (Finnsjön, Gideå, Taavinunnannen, Klipperås, Äspö, Forsmark and Simpevarp). Methods used have been, in addition to microscopy of thin sections; stable isotope analyses (O, C), trace elements chemistry and in a few cases Sr isotope ratios. Fluid inclusion studies have also been carried out on a smaller number of calcites from Finnsjön /Tullborg and Larson 1982/ and Äspö-Laxemar /Bath et al. 2000, Milodowski et al. 2005/.

Most of the fractures are initiated early in the bedrock history and repeatedly reactivated. This means that the ages of the fracture fillings spans over thousands of million years, and fractures with hydrothermal mineral infillings may have been reactivated and can contain very young fillings. Water rock interaction processes during quite different physico-chemical conditions may thus have left imprints on the fracture walls. For the calcites, largely three different origins can be traced (cf Figure C-3), although further subdivisions into six or more generations have been possible at some sites.

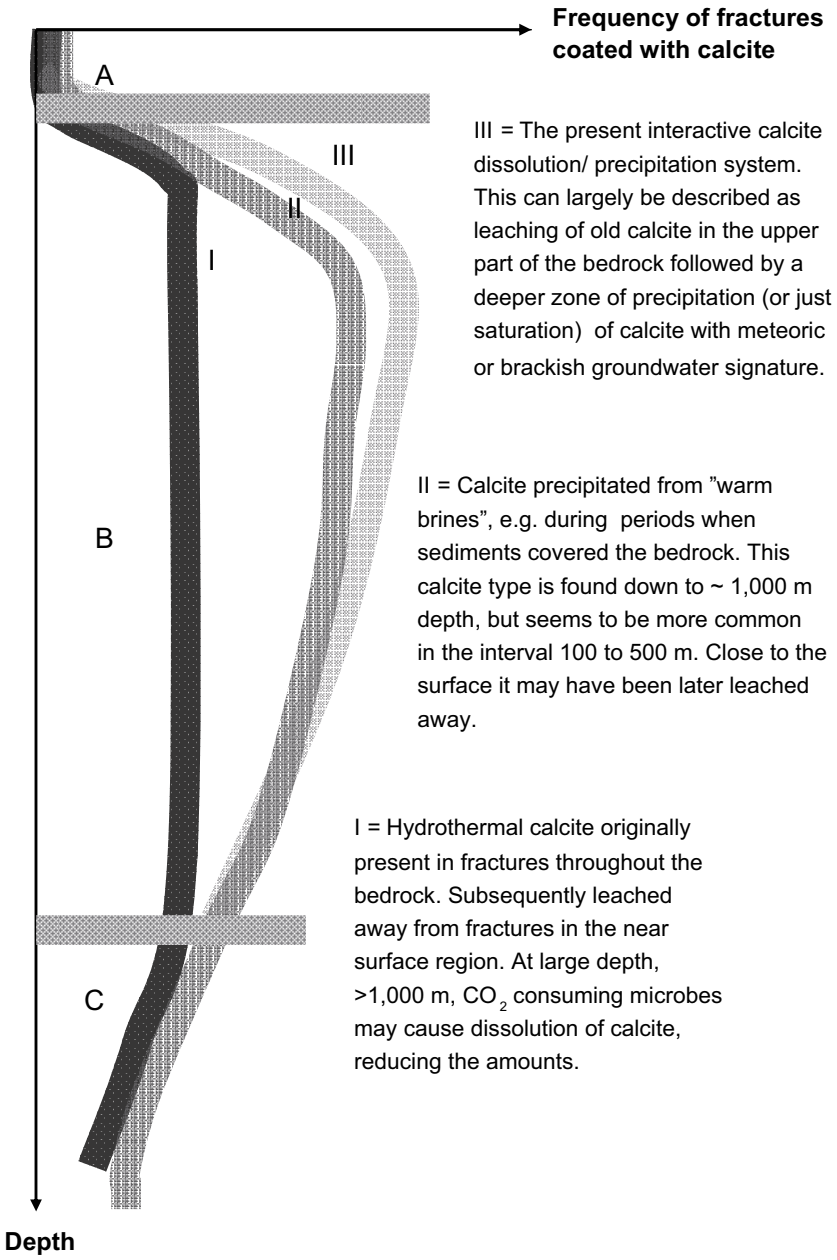

Figure C-3. *Simplified sketch showing the general view of calcites present in crystalline bedrock based on experiences from Swedish sites. See text for explanation of intervals A, B and C and for references.*

I. The oldest calcite generation (or generations) is of hydrothermal origin and precipitated together with minerals like epidote, prehnite or laumontite The carbon isotopes values in hydrothermal calcite is usually restricted to atmospheric values (−2 to −7‰ PDB) and the $\delta^{18}O$ values are usually low (−15 to −25‰ PDB) in accordance with precipitation at elevated temperatures (200 to 400°C) from a fluid with relatively high $\delta^{18}O$ values. This type of calcite is common in sealed fractures but also in reactivated fractures often with a rim of younger calcite grown on top of the older more massive calcite. In the Swedish crystalline bedrock, hydrothermal conditions corresponding to the above outlined temperature interval are with a few exceptions restricted to the Precambrian era. The generations described are however not formed during one single event in all the areas, instead several hydrothermal periods have produced calcite and in some cases even several hydrothermal generations have been possible to identify within one single area.

II. Calcites precipitated during lower temperature conditions (< 150°C) but still at temperatures higher than the present 5–20°C have been identified in several areas. This calcite generation is related to increased influence of carbon with biogenic signature; usually in the $\delta^{13}C$ interval of −20 to −7‰ PDB and some of them show even more extreme negative $\delta^{13}C$ values. Sr isotopes ratios show less radiogenic values than today's groundwater, cf results from Forsmark and Äspö-Laxemar-Simpevarp /Bath et al. 2000, Milodowski et al. 2005/. These calcites are referred to as "Warm brine precipitates" /Bath et al. 2000, Milodowski et al. 2005/ and they are supposed to have been produced in the crystalline aquifer beneath a sedimentary cover. The present bedrock surface has been covered with sediments ranging from Cambro-Silurian marine sandstone and limestone over to Late Silurian to Devonian terrestrial sediments of molasse type. This sedimentary cover lasted until the Mesozoic and in places until the Tertiary /Lidmar-Bergström 1996/.

III. Calcites precipitated as a result of the present (Quaternary) hydrogeochemical and hydrogeological situation are the latest calcites and found on the outermost fracture surfaces. This means that the identification of them is highly dependent on the drill core quality and also on the possibilities of studying overgrowth of younger calcite on earlier calcite generations. The Quaternary scenario includes a number of glaciations and the global sea level changes. This in addition to the glacio-isostatic changes during the same period has changed the hydrogeological and hydrochemical conditions significantly in the coastal areas, especially in the Baltic Sea region where the co-variation of $\delta^{18}O$ and salinity is obvious. It is therefore reasonable to assume that the low temperature calcites may have been precipitated from very different groundwaters including glacial and temperate climate meteoric, and brackish or even marine waters. It is especially the mixing of waters with different compositions that may have caused dissolution or precipitation of calcite. But also microbial activity plays an important role.

The observed calcite distribution pattern is the net effect of calcite-fluid interactions (and also of subsurface microbiological activity during long periods) during the entire geological history of the sites. A tentative description based on the depth distribution of different types of calcites as outlines in Figure C-3, gives that at least three different zones can be distinguished (mainly based on studies from the Oskarshamn area and from Finnsjön-Forsmark):

A. The upper 0 to ~ 50–100 metres are characterised by a dynamic situation including dissolution/precipitation of calcite. During some time periods, biogenic activity has been significant, producing reducing conditions, whereas during other periods oxidizing conditions may have prevailed. The depth of this zone is dependent on the thickness of the soil cover, hydrogeological regime and the fracturing of the bedrock. This means that in some areas the dissolution zone is found in the soil cover whereas in others it reaches down to 50 m in the bedrock and in fracture zones even deeper; e.g. 120 m in Klipperås /Tullborg 1986/.

B. At depth below ~ 100 m down to ~ 500–600 m, mainly precipitation (or re-crystallisation) of calcite is detected. Several generations (zoning) are common at these depths. Redox conditions have probably been stable and reducing, at least during the Phanerozoic, and contributions of biogenic carbonate are detected in terms of low carbon isotope values and high contents of Mn, La and Ba. Between 600 m and 1,000 m the biogenic influence decreases drastically but precipitates of low temperature calcites of possible fresh meteoric water can be traced down to 1,000 m, see /Tullborg 2004/.

C. At even larger depth (> 1,000 m) recent calcite precipitation is rare and the biogenic input seems to be insignificant due to relatively stagnant conditions.

The dissolution and replacement of the hydrothermal calcite in the upper part of the bedrock may have occurred during two different periods; when the sub Cambrian peneplain was exposed and secondly during Tertiary to present Quaternary. The depth distribution of different calcite types indicates stability in the large-scale groundwater circulation, but in detail large variations in depth may have occurred. For example, attempts to correlate calcite-groundwater pairs from specific borehole locations indicate that there is no equilibrium with the present groundwater /Bath et al. 2000/.

The largest volumes of calcite are very old and have survived for hundreds of millions of years, which mean that it will most probably do so for the future of interest for a spent fuel disposal. The present depth of calcite leaching probably corresponds to the actual conditions at site although annual variations are expected. It is reasonable that the calcite leaching front is relatively stable or is slowly moving downwards due to acid precipitation and the ongoing glacial rebound facilitating recharge of fresh meteoric water. However, the rate of land rise is decreasing and the organic buffer (the soil cover) is stable or partly growing. In conclusion this means that large variations in the present depth of the calcite leaching zone are not to be expected.

ISSN 1404-0344
CM Digitaltryck AB, Bromma, 2007